THE IDENTIFICATION OF INCREASED DYRK1A PROTEIN LEVELS IN TS65DN MICE GUIDES THE TARGETED ADMINSTRATION OF THE NOVEL DYRK1A INHIBITOR CX-4945

by

Megan Stringer

A Dissertation

Submitted to the Faculty of Purdue University

In Partial Fulfillment of the Requirements for the degree of

Doctor of Philosophy

Department of Psychology

Indianapolis, Indiana

May 2018

THE PURDUE UNIVERSITY GRADUATE SCHOOL
STATEMENT OF COMMITTEE APPROVAL

Dr. Charles Goodlett, Chair
Department of Psychology
Dr. Randall Roper
Department of Biology
Dr. Stephen Boehm
Department of Psychology
Dr. Bethany Neal-Beliveau
Department of Psychology

Approved by:
Dr. Nicholas Grahame
Head of the Graduate Program

For my parents and their unwavering support throughout the years;
Even while chasing my dreams far from home, I have never once felt alone

ACKNOWLEDGMENTS

None of my success in my graduate career would have been possible without a great team behind me. Over the past five years I have had an ever changing team behind me, and I want to thank Irushi Abeysekera, Jonathan LaCombe, Laura Hawley and Jared Thomas for their willingness to teach me everything Biology-related. I also want to thank the dozens of undergraduates who have helped me along the way. A special thank you goes to Jake Whiteside and Drew Folz who were instrumental in helping me run western blots, immunohistochemistry and behavioral tasks for my dissertation project. Thanks to my dissertation committee including Dr. Neal-Beliveau and Dr. Boehm for all of their constructive feedback and mentoring support throughout the years. Thank you to my co-advisors, Dr. Goodlett and Dr. Roper, for teaching me several invaluable lessons over the past years that have allowed me to become an excellent scientist.

For my family; Chris, Katie, Ben, Hallie, Joey, Alex, Kristin, Genny Rose, Mary Elizabeth, Rose, Cecilia and Henry. You have all supported me from day 1, and you were always there with a phone call, funny picture, a weekend visit, or a cold brewski to make everything okay. Thank you to Christa Houck for being my therapist over this past year. Even on my darkest days you reiterated your unwavering support that I could do anything. You were the friend I never knew I needed, and I couldn't have finished my last year without your friendship. To Mike, Dan, Sheila, Brandon, Mitch, Lauren, Claire, Maribel, Shelby and Sean; you guys were the best part of graduate school and I will miss saving birds with you and doing impersonations of professors. I can't wait to cheer you guys on during you last few years of graduate school, but please never forget that you all are more than "just" graduate students.

Last, but certainly not least, I would like to thank my fiancé Aaron. Approximately 70,000 miles, 1,000 slices of pizza, and 180 dreaded Sunday Scaries later- we did it.

TABLE OF CONTENTS

LIST OF TABLES

LIST OF FIGURES

ABSTRACT

Author: Stringer, Megan. PhD
Institution: Purdue University
Degree Received: May 2018
Title: The Identification of Increased Dyrk1a Protein Levels in Ts65Dn Mice Guides the Targeted Administration of a Novel Dyrk1a Inhibitor CX-4945
Major Professor: Charles Goodlett and Randall Roper

Down syndrome (DS) is caused by three copies of human chromosome 21 (Hsa21) and results in phenotypes including intellectual disability. Ts65Dn mice, the most extensively studied DS model, have three copies of ~50% of the genes on Hsa21 and display many phenotypes associated with DS, including cognitive deficits. *DYRK1A* is a dosage-sensitive gene found in three copies in humans with Trisomy 21 and in Ts65Dn mice and is involved in CNS development. Overexpression of *DYRK1A* is hypothesized to cause many of the cognitive and developmental deficits observed in DS and has been touted as a target for drug development in DS. Definitive evidence that excessive expression/activity of Dyrk1a directly contributes to specific phenotypes in DS mouse models is limited, and there is no direct evidence that verified pharmacological inhibition of Dyrk1a *in vivo* causes enduring improvement in DS cognitive phenotypes. In part, this reflects the remarkably limited knowledge of the temporal regulation of Dyrk1a expression and activity in different brain regions across development in DS mouse models. To establish the therapeutic potential of Dyrk1a inhibitors, the first aim of this study was to determine when and in what brain regions excessive Dyrk1a is evident and to identify developmental periods when elevated expression of Dyrk1a may be contributing to enduring aberrant functional development. This aim provided systematic quantification of Dyrk1a protein level at key postnatal (P) ages (P12, P15, P18, P24 P30, P42) in Ts65Dn mice, at ages of translational relevance to clinical applications in humans (birth, early adolescence, late

adolescence, young adult). Western blot analysis showed that significant elevation of Dyrk1a with the largest effect sizes occurred in trisomic mice on P15. The second aim of this study was to test whether treating Ts65Dn with a novel Dyrk1a inhibitor (CX-4945) during the time of Dyrk1a elevation would rescue the behavioral and structural abnormalities observed. From P14-P18, Ts65Dn and euploid mice were treated with 75mg/kg CX-4945 or DMSO (vehicle) and tested on a homing task and locomotor activity in a novel arena on P17-P18, counterbalanced for order. At the cessation of treatment, hippocampal cell proliferation was assessed. While there was a lack of statistically significant improvements with CX-4945 treatment, there were modest effect sizes. In addition, several of the behavioral studies were significantly underpowered, making it difficult to conclusively ascertain the efficacy of CX-4945 on specific phenotypes. Nevertheless, this study demonstrates that Dyrk1a is dynamically expressed across development in mice, and suggests that consideration of the spatial and temporal expression of Dyrk1a may well be critical in the development of therapeutics for DS.

CHAPTER 1. INTRODUCTION

1.1 Down syndrome

Down syndrome (DS) occurs in approximately 1 in every 700 live births and results from the triplication of Hsa21 (Parker et al., 2010). The genetic basis of DS was discovered in 1958 by Jerome Lejeune who observed an extra copy of Hsa21 in human tissue samples (Lejeune et al., 1959). The most common cause of DS is a maternal non-disjunction of Hsa21 during meiosis, where Hsa21 does not separate (three copies of long arm Hsa21) (Epstein, 2001). Hsa21 was one of the first chromosomes to be sequenced and contains 218 protein coding and 280 non-protein coding genes (Hattori et al., 2000; Gupta et al., 2016). Currently, the only known risk factor of DS is advanced maternal age (Yoon et al., 1996; Allen et al., 2009).

DS results in an array of phenotypes that affect the cardiovascular, skeletal and central nervous systems. Heart defects affect 40-50% of children with DS (Freeman et al., 2008; Freeman et al., 1998; Tubman et al., 1991). Bone deficits, including a reduction in bone mineral density, an increased incidence of osteoporosis, and altered craniofacial development are also observed (Guijarro et al., 2008; Center et al., 1998; Richtsmeier et al., 2000). Individuals with DS have significantly higher body mass index (BMI) levels and an increased predisposition to obesity than the general population (Artioli et al., 2017). Other phenotypes such as hearing loss (75%), obstructive sleep apnea (50%-80%) and eye disease (60%) (Bull, 2011; Källén et al., 1996; Marcus et al., 1991; Netzer et al., 2010; Shott et al., 2001; Zigman et al., 2007; Leverenz et al., 1998) are also observed in individuals with DS. Adults with DS are at a high risk of developing Alzheimer-disease (AD) pathology, including accumulation of amyloid-β (Aβ) plaques in the brain and the presence of neurofibrillary tangles (Hartley et al., 2015; Zigman, 2013; Zigman et al., 2007). A

significantly lower intelligence quotient (IQ) is present in nearly all individuals with DS, although there is a range of IQs reported (Carr et al., 2018; Silverman, 2007). These phenotypes are common among individuals with DS but there is variability in the incidence and severity of the various phenotypes (Roubertoux et al., 2006).

1.2 Structural and histological phenotypes observed in DS

The intellectual disability phenotype observed in nearly all individuals with DS is hypothesized to be caused by developmental deficits in brain structures such as the hippocampus, cerebral cortex and cerebellum. Deficits in these brain structures are observed in fetuses with DS beginning at ~17-21 weeks gestation, with a reduction in brain size and the volume and number of proliferating cells in the hippocampus, dentate gyrus (DG) and parahippocampal gyrus, as well as a smaller population of neuronal cells versus controls (Guidi et al., 2008; Contestabile et al., 2007; Larsen et al., 2008; Sylvester, 1983). Delays in myelin formation, decreased density of myelinated axons in the hilus of the DG, decreased neuronal and synaptic density, and synaptic length in the DG have been observed at ~20 weeks (Ábrahám et al., 2012).

These histological deficits extend into postnatal development, as 3-5 months old infants with DS display a smaller brain stem and cerebellum, as well as a lower brain weight. These infants also display deficits in myelination within the brain stem, cerebellum, spinal cord and posterior horn (Wisniewski, 1989). Post mortem analysis of fetuses at birth through childhood show fewer neurons, lower neuronal density, decreased synaptic density and synaptic length (Schmidt-Sidor et al., 1990). Children and young adults with DS exhibit reductions in hippocampal, cerebellar and cerebral volume, as well as increases in subcortical gray matter volumes versus controls (Jernigan et al., 1993; Pinter et al., 2001; Pinter et al., 2001).

Adults with DS exhibit a lower brain weight, as well as deficits in hippocampal, cerebellar, cerebral cortex, corpus callosum, and white matter volumes versus age matched controls (Teipel et al., 2003). Individuals with DS have been shown to develop Alzheimer-like pathology, including plaques and neurofibrillary tangles before the age of 40. These phenotypes occur in multiple areas of the brain, including the cerebral cortex and the DG of the hippocampal formation (Motte et al., 1989; Hof et al., 1995).

1.3 Cognitive and behavioral phenotypes in individuals with DS

Accompanying the reduced IQ, individuals with DS display deficits on a range of cognitive function [for extensive review see (Godfrey et al., 2018)]. Infants with DS display developmental learning delays in tasks such as the object-concept task and recognition memory tasks (Miranda et al., 1974; Nygaard et al., 2001; Milojevich et al., 2016), although these deficits may be dependent on the memory retention interval (Roberts et al., 2015). Visuospatial memory may be preserved in children with DS, as there were no reported deficits on a computer version of the Corsi block-tapping task versus controls (Jarrold et al., 1997; Vicari et al., 1995; Numminen et al., 2001; Laws, 2002). However, deficits are apparent when these tasks are utilized in a "real-world" space, requiring the integration of environmental cues to learn the task (Mangan, 1992). Young adults with DS display impairments on verbal working memory, verbal and non-verbal long-term memory tasks, as well as associative memory and spatial long-term memory tasks (Carlesimo et al., 1997; Pennington et al., 2003; Munir et al., 2000). These deficits are observed in adults with DS with impairments on both explicit and implicit verbal, non-verbal and working memory tasks (Jarrold et al., 2002; Lavenex et al., 2015; Jarrold et al., 2002; Vicari et al., 2005). Individuals with DS also display performance deficits on tasks such as the virtual Morris water maze (MWM), CANTAB Pattern Recognition Memory Test, and the NEPSY List-Learning Test (Carlesimo et

al., 1997; Pennington et al., 2003). These laboratory tasks are commonly used to assess several facets of memory function (recognition and declarative memory) because individuals with hippocampal damage show impairments on these tasks (Koehler et al., 1998; Goodrich-Hunsaker et al., 2010; Broadbent et al., 2004). Thus, the poorer performance on these tasks by individuals with DS may be due to hippocampal dysfunction.

Linking these memory deficits to a specific anatomical deficit has yielded mixed results. A negative correlation between parahippocampal gyrus size (measured via MRI) and cognitive ability has been suggested, as well as a positive correlation between corpus callosum size and cognitive ability (Teipel et al., 2003). However, the same study reported no correlations between cerebral size, cerebellar hemisphere size, or hippocampal size and cognitive ability (Teipel et al., 2003). While individuals with DS display brain-region specific abnormalities across development, future studies should aim to link structural and function impairments in specific neural circuits to specific memory or cognitive phenotypes.

There are limitations in studies assessing neurocognition in individuals with DS, including a lack of longitudinal studies, the inclusion of appropriate age-matched (chronological and/or mental) controls, and the utilization of neurocognitive assessments that can engage and challenge an individual with DS and an age-matched control in the same study (Godfrey and Lee, 2018). To address this problem, the Arizona Cognitive Test Battery (ACTB) was developed to specifically assess neurocognition in individuals with DS (Edgin et al., 2010). The ACTB has demonstrated strong test-retest reliability, was designed to be applicable to a wide range of ages and skills, and have specific correlates to brain regions that are likely to be targeted with therapeutics (Edgin et al., 2010; Edgin et al., 2017). Parallel to the development of the ACTB, the National Institutes of Health (NIH) formed a group that included DS researchers and pharmaceutical companies to create

a standard set of outcome measures for clinical trials in DS (Esbensen et al., 2017). The ACTB has also been adapted to characterize neurobehavioral deficits in the Ts65Dn mouse model of DS in order to mimic phenotypes that are observed in the clinical setting (Hunsaker et al., 2016). The development and utilization of these standard assessments will allow pre-clinical and clinical DS researchers to strengthen the evaluation and interpretation of new therapeutics for DS.

1.4 The Ts65Dn mouse model of DS

The development of DS mouse models has been instrumental for correlating the direct effects of trisomic gene expression on development and function. These models are based on the orthologous genes between Hsa21 and mouse chromosomes 16 (Mmu16), Mmu17 and Mmu10 (Pletcher et al., 2001). Early development of these models largely focused on Mmu16, as this chromosome carries the majority of the homologs found on Hsa21 (Antonarakis et al., 2004). However, mice with a full triplication of Mmu16 do not survive postnatally, and carried three copies of hundreds of genes not homologous to Hsa21. Thus, a better model would be a mouse with segmental trisomy for just the distal region of Mmu16 that is homologous to Hsa21 (Epstein et al., 1985). In order to produce offspring that contained a translocated chromosome containing the distal end of Mmu16, the testes of DBA/2J (D2) mice were irradiated and crossed with C57BL/6J (B6) females. While several translocations were identified, T65 offspring contained a translocation that resulted in an extra chromosome that contained genes from the distal end of Mmu16 attached to the centromeric end of Mmu17 (Davisson et al., 1990). These offspring were later renamed Ts (17^{16}) 65Dn and were maintained by crossing to C57BL/6J x B6C3HF1 hybrid mice (Davisson et al., 1993; Davisson et al., 1990). This model carries an extra segment of Mmu16, containing ~90 protein-coding Hsa21 gene homologs (Gupta et al., 2016). This model also carries an extra centromeric region of Mmu17, resulting in three copies of non-DS related

genes including ~35 protein-coding genes, 15 non-protein-coding genes and 10 pseudogenes (Duchon et al., 2011).

In addition to the Ts65Dn model, over 30 different mouse models of DS have been developed containing specific genetic segments of Mmu16, Mmu17 or Mmu10 including the Ts1Cje, Dp1Yey, Ts1Rhr, Ts1Yah [extensively reviewed in (Herault et al., 2017; Gardiner et al., 2010)]. Recent advances in engineering DS mouse models also include the generation of the Tc(Hsa21)1TybEmcf, or Tc1 mouse model. The Tc1 mouse was the first transchromosomic mouse line, and this model contained a freely segregating copy of Hsa21 (O'Doherty et al., 2005). However, there were several unexpected duplications and deletions observed, and these mice lose a copy of Hsa21 in certain cells, resulting in mosaicism (Gribble et al., 2013; O'Doherty et al., 2005). A triple trisomic mouse has also been created, providing a model that is trisomic for the Mmu10, Mmu16 and Mmu17 chromosome regions that contain Hsa21 homologs (Yu et al., 2010). However, the generation of these models is difficult and can be extremely time consuming to produce (Chen et al., 2013). While these and other mouse models are valuable in comparative research on genotype-phenotype correlations observed in DS, the Ts65Dn mouse model is the most extensively studied and widely used animal model of DS because it recapitulates most of the DS phenotypes, including craniofacial and skeletal abnormalities, developmental delays, low body weight, cognitive and behavioral impairments, and brain abnormalities (Baxter et al., 2000; Belichenko et al., 2004; Cooper et al., 2001; Reeves et al., 1995). The developmental, behavioral and histological deficits exhibited by Ts65Dn mice have been extensively reviewed elsewhere (Gupta et al., 2016; Rueda et al., 2012). Importantly, the Ts65Dn mouse is the model most often used to test treatments to improve the various deficits observed in DS (Gardiner, 2015).

1.5 Treatments for DS

To date, there have been over 30 different therapeutics administered to mouse models of DS, with a handful administered to individuals with DS in a clinical setting. The majority of these therapeutics focus on targeting specific neurotransmitter systems or aberrant neural pathways such as antagonists of $GABA_A$, or NMDA receptors (memantine), serotonin reuptake inhibitors (fluoxetine), anti-inflammatories (minocycline), and free radical scavengers (melatonin) (Extensively reviewed by (Gardiner, 2015; Stagni et al., 2015; Costa et al., 2013). Despite individuals with DS and Ts65Dn mice displaying neurodevelopmental deficits at fetal and neonatal stages, there is a significant imbalance in the number of studies administering treatments during these critical developmental ages. A recent review evaluated 55 studies that administered a therapeutic to Ts65Dn mice and found that almost 70% of these studies were conducted in adult mice. Therapeutics administered to adult Ts65Dn mice may modulate existing brain circuitry and rescue cognitive and behavioral deficits (Stagni et al., 2015). Developing therapeutics for adult Ts65Dn mice is critical, considering the high co-morbidity of DS and AD (Choong et al., 2015). However, interventions during key periods of Ts65Dn brain development during prenatal or neonatal ages are likely to have long-lasting impact on developmental trajectories and subsequent phenotypes, and provide an alternative means for intervening in the aberrant brain development associated with the Ts65Dn phenotype. For example, a single treatment injection with the Sonic hedgehog pathway activator SAG at birth significantly rescued granule cell precursor populations in the cerebellum at P6 and normalized cerebellar morphology when mice were aged to 4 months (Roper et al., 2006; Das et al., 2013; Gutierrez-Castellanos et al., 2013). Two separate studies examined the effects of a daily (P3-P15) fluoxetine or epigallocatechin-3-gallate (EGCG) injection in Ts65Dn mice. Both fluoxetine and EGCG rescued deficits in hippocampal neurogenesis in P15

Ts65Dn mice (Bianchi et al., 2010; Stagni et al., 2016). In both studies, a separate group of mice were aged to ~P45 after the cessation of treatment at P15 in order to determine any long-term effects on behavior. However, only fluoxetine restored hippocampal neurogenesis and hippocampal-dependent task deficits in adult (~P45) Ts65Dn mice (Bianchi et al., 2010; Guidi et al., 2013; Stagni et al., 2016). The success of these studies during neonatal or perinatal ages highlight the existence of potentially critical time points for therapeutic intervention in DS and offer new opportunities for investigators.

The majority of therapeutics to date administered to Ts65Dn mice across ages have targeted specific neurotransmitter systems or aberrant neural pathways, based on their contribution to cognitive and behavioral phenotypes. An alternate treatment approach would be to target a gene or set of genes hypothesized to have a major influence on a phenotype due to its developmental overexpression in DS (Korbel et al., 2009; Lyle et al., 2009). The goal of this approach is to target trisomic DS genes by identifying contributions of that gene's overexpression to the emergence of primary phenotypes and correcting these phenotypes, rather than secondary phenotypes that can be caused downstream of an elevated gene (Roper et al., 2006). However, the presence of a triplicated gene does not mean that it will alter development and function in every cell across development. Thus, it is critical to identify the spatial and temporal expression of a trisomic gene in conjunction with specific phenotypes, in order to understand when the trisomic gene(s) cause(s) divergence from normal patterns of development (Roper and Reeves, 2006).

1.6 What is *DYRK1A*?

Dual-specificity tyrosine phosphorylation-regulated kinases (DYRKs) are a family of protein kinases that phosphorylate serine and threonine residues in a number of substrates (Becker et al., 2011). *Dual specificity tyrosine kinase 1A (DYRK1A)* is the only DYRK located on Hsa21,

and is found in three copies in individuals with DS (Becker et al., 1999). DYRK1A is a protein kinase that contains a catalytic kinase domain, two nuclear localization signals, a PEST motif containing amino acids (proline, glutamate, serine and threonine), histidine repeats, and serine and threonine residues (Alvarez et al., 2003). DYRK1A is defined as a dual-specificity kinase because of its ability to phosphorylate on both serine/threonine residues, and it undergoes autophosphorylation on tyrosine residues in its activation loop (Alvarez et al., 2007). DYRK1A autophosphorylates independently of upstream regulators, and this autophosphorylation is crucial for DYRK1A to switch from active to inactive states (Himpel et al., 2001; Becker et al., 1998; Becker et al., 2011). *DYRK1A* phosphorylates a multitude of substrates such as splicing proteins, transcription factors, and cell cycle proteins (for extensive review see (Park et al., 2009; Wiseman et al., 2009; Tejedor et al., 2011; Becker et al., 2014).

The interest in DYRK1A started in *Drosophila* research when it was observed that flies with a mutant Minibrain (*mnb)* gene developed an abnormal spacing of neuroblasts within the brain and produced fewer neurons than controls (Tejedor et al., 1995). It was hypothesized that the altered expression or activity of this *mnb* gene played a crucial role in normal *Drosophila* brain development. Homologous genes to Mnb, renamed DYRK1A, were identified with very high degrees of conservation across species (mice, rat and human DYRK1A), allowing subsequent studies to determine the role of DYRK1A during neurodevelopment (Kentrup et al., 1996; Guimerâ et al., 1996; Shindoh et al., 1996). Alternative splicing of Dyrk1a results in five known isoforms (OMIM: 60085).

The causative role of *DYRK1A* overexpression in DS phenotypes originated from early genotype-phenotype mapping studies in individuals with segmental trisomy of Hsa21. People with segmental trisomies containing *DYRK1A* exhibited developmental and cognitive phenotypes like

individuals with DS who carried a full triplication of Hsa21 gene (Korbel et al., 2009; Lyle et al., 2009). This genotype-phenotype correlation is supported by the high levels of expression of *Dyrk1a* in the CNS during development and the deleterious phenotypes that occur when *DYRK1A* levels are either elevated or decreased in mouse models (for review see (Stringer et al., 2017)). This dosage sensitivity is also observed in humans with a deletion of *DYRK1A*, who exhibit microcephaly, intellectual disability and epilepsy (Bon et al., 2011; Courcet et al., 2012; Møller et al., 2008). The mechanism by which *DYRK1A* causes or influences these deleterious phenotypes is not well known. However, its wide range of cellular substrates, combined with the presence of *DYRK1A* in three copies in individuals with DS and mouse models of DS has fueled the publication of over 68 studies on *Dyrk1a* and its involvement in DS-related processes and phenotypes (search was conducted in PubMed on 4-19-18 using terms: [title] Down syndrome AND Dyrk1a). In parallel, there has been a steady production of Dyrk1a kinase inhibitors within the past 5 years (Becker et al., 2014; Smith et al., 2012; Nguyen et al., 2017). However, there is growing evidence that triplicated genes in DS and Ts65Dn mouse models like *DYRK1A,* are not always significantly elevated versus controls (Cheon et al., 2003; Ahmed et al., 2015; Stringer et al., 2017). Despite evidence that Dyrk1a is not significantly elevated in all tissues at all times, Dyrk1a inhibitors continue to be tested in mouse models of DS without regard for the tissue-specific temporal or spatial expression profile of Dyrk1a. This approach makes it difficult to ascertain the link between pharmacological actions and any phenotypic therapeutic effects mediated effects on Dyrk1a expression/activity.

A recent review published by Stringer et al (2017) discusses the current implications of *Dyrk1a* overexpression in DS-related phenotypes, and highlights the large gap in knowledge about the spatial and temporal patterns of expression and tissue-specific levels of Dyrk1a protein over development in various mouse models of DS. This review constructively addresses these gaps by detailing a framework for future studies assessing the effectiveness of a Dyrk1a inhibitor to target Dyrk1a activity in a mouse model of DS. The framework articulated in that review helps advance our knowledge and development of targeted therapeutics with the hopes of improving the lives of individuals with DS.

1.7 Targeting trisomic treatments: optimizing Dyrk1a inhibition to improve Down syndrome deficits

This chapter includes the publication [Targeting trisomic treatments: optimizing Dyrk1a inhibition to improve Down syndrome deficits/Stringer, Megan, Charles R. Goodlett, Randall J. Roper/*Molecular Genetics & Genomic Medicine*/ Sep; 5(5):451-465. Copyright © [2017] [Randall J. Roper]
Link: http://onlinelibrary.wiley.com/doi/10.1002/mgg3.334/full

1.8 Current status of Dyrk1a inhibitors

Several small molecule inhibitors have been developed to inhibit Dyrk1a activity. One of the most selective Dyrk1a inhibitors available is the plant alkaloid harmine; however, it also is a potent inhibitor of monoamine oxidase A (MAO-A), which greatly limits its *in vivo* application (Kim et al., 1997; Adayev et al., 2011). There has been a significant emphasis on developing other inhibitors as effective as harmine that lack inhibition of MAO-A. The molecule (1Z)-1-(3-ethyl-5-hydroxy-2(3H)-benzothiazoylidene)-2-propanone (INDY), inhibits Dyrk1a activity *in vitro* at similar concentrations as harmine and does not have inhibitory effects on MAO-A (Ogawa et al., 2010). When an additional acetyl group was added to INDY to increase its cell membrane

permeability (proINDY), this molecule was able to normalize developmental deformities in *Xenopus laevis* embryos that overexpressed *Dyrk1a* (Ogawa et al., 2010). Another potent inhibitor of Dyrk1a activity *in vitro* is Leucettine 41 (L41) which is derived from the marine sponge alkaloid Leucettamine B (Tahtouh et al., 2012; Debdab et al., 2011). L41 administered to mouse models of Alzheimer's disease rescues Aβ-induced cognitive impairments (Naert et al., 2015). However, the efficacy of L41 on Dyrk1a activity *in vivo* has not been reported. Folding intermediate-selective inhibitor of Dyrk1a (FINDY) inhibits Dyrk1a activity *in vitro* by suppressing the autophosphorylation of Dyrk1a, thereby inhibiting its catalytic activity. FINDY rescues DYRK1A-induced developmental deformities in *Xenopus laevis* embryos (Kii et al., 2016). Recently, two studies have administered novel Dyrk1a inhibitors to DS mouse models *in vivo* and reported significant improvements. An ~3 week treatment with the compound 3-(4-fluorophenyl)-5-(3,4-dihydroxyphenyl)-1H-pyrrolo[2,3-b]pyridine, 5a) (F-DANDY) via a 20mg/kg daily IP injection significantly improved MWM performance in adult Ts65Dn mice (age not specified), although trisomic (Ts) mice treated with this molecule were still significantly impaired versus euploid (Eu) controls. This study could not directly say if F-DANDY was directly inhibiting Dyrk1a activity, but quantifiable levels of F-DANDY were observed in the brain, suggesting that it is able to cross the blood-brain barrier (Neumann et al., 2018).

Another study administered the molecule ALGERNON (alternate generation of neurons) both pre-and postnatally to Ts1Cje mice, a mouse model of DS that triplicates fewer Mmu16 genes than Ts65Dn mice but still includes three copies of *Dyrk1a* (Nakano-Kobayashi et al., 2017). Normalization of the number of BrdU+ and BrdU+/DCX labeled cells in the DG was achieved when 9-week-old Ts1Cje were administered ALGERNON via SC for 12 consecutive days, as well as when mice were administered 10mg/kg SC for 10 consecutive days. Next, the study

administered ALGERNON to pregnant dams from E10-E15 and found that treatment normalized cortical layer thickness in E15.5 embryos. Mice treated with ALGERNON prenatally showed improvements in several hippocampal–dependent tasks including the Barnes maze and contextual fear conditioning when tested as adults. However, this prenatal treatment did not significantly improve BrdU+ cell proliferation observed in adult Ts1Cje mice. ALGERNON does not inhibit MAO-A activity and its rescuing effects at both embryonic and adult ages warrant further investigation.

Despite the promising preclinical studies using new Dyrk1a inhibitors like ALGERNON and F-DANDY, there is a lack of Dyrk1a inhibitors that have been administered in a clinical setting. Because a common goal is to effectively translate therapeutics to individuals with DS, it is critical that novel Dyrk1a inhibitors pass safety and efficacy studies in both preclinical and clinical settings. The development and screening of small molecule kinase inhibitors is not unique to DS, as a number of diseases, such as cancer, are linked to alterations in protein kinase signaling (Noble et al., 2004). For example, casein kinase II (CK2) is a serine/threonine kinase that plays an important role in controlling cell growth, proliferation and survival (Trembley et al., 2010; Ruzzene et al., 2010). The overexpression of CK2 is seen in several types of cancers, including breast, kidney and lung, and the inhibition of CK2 kinase activity is a target for cancer drug therapy (Ferguson et al., 2011). Many CK2 inhibitors inhibit other kinases, including proto-oncogene serine/threonine-protein kinases (PIMs) and dual-specificity tyrosine-regulated kinases (DYRKs), due to their phylogenetic similarity (Aranda et al., 2011; Pagano et al., 2008) (Debdab et al., 2011). Similar to Dyrk1a, CK2 is constitutively active and does not require phosphorylation by other kinases for activation. The recent overlap in CK2 and Dyrk1a inhibition by several small molecule

inhibitors opens the possibility for using these kinase inhibitors as targeted Dyrk1a inhibitors to improve DS-related deficits.

1.9 Justification of using CX-4945

The current study utilized the CK2 and Dyrk1a inhibitor CX-4945, [5-(3-chlorophenylamino)benzo[c][2,6]naphthyridine-8-carboxylic acid] (Pierre et al., 2011; Siddiqui-Jain et al., 2010) for several reasons. Docking studies show that CX-4945 inhibits DYRK1A activity by binding to the ATP-binding pocket with a high degree of potency and with significantly higher half maximal inhibitory concentration values (IC_{50}) than well-known Dyrk1a inhibitors including harmine, INDY, and proINDY (Kim et al., 2016; Ferguson et al., 2011). CX-4945 exhibits a half-life of ~10 hours and an oral bioavailability of ~79% in rats following a single 10mg/kg oral gavage (CX-4945 dissolved in a mixture of DMSO/PEG400/distilled water, 0.5: 4: 5.5) (Son et al., 2013). These findings are in stark contrast to EGCG, which degrades in solution, is rapidly metabolized upon ingestion, is rapidly excreted once metabolized, and is almost undetectable in human serum 8 hours after a 200mg dose (Chow et al., 2003; Lee et al., 2002; Chen et al., 1997; Chow et al., 2001). However, CX-4945 has only recently been administered with the goal of rescuing Dyrk1a-mediated tau hyperphosphorylation (Stringer et al., 2017).

Dyrk1a is hypothesized to mediate the hyperphosphorylation of Tau at the Thr-212 residue in the hippocampus and frontal cortex of transgenic *Dyrk1a* (TgDyrk1a) mice (Ryoo et al., 2007). This phenotype is also seen in 293T cells that overexpress DYRK1A, and when CX-4945 was administered *in vitro,* a significant reduction in Tau hyperphosphorylation at T212 was observed (Kim et al., 2016). The administration of CX-4945 was also shown to reverse Dyrk1a-mediated deficits in the translocation of NFAT-C, a critical transcription factor that mediates signaling pathways critical for vertebrae development (Nguyen et al., 2008). The shuttling of NFAT-C

inside the nucleus (where it can carry out transcriptional activity) has been shown to be dependent on levels of DYRK1A (Arron et al., 2006; Kurabayashi et al., 2013). *In vivo,* a single dose of 75mg/kg CX-4945 (dissolved in phosphate-buffered saline (PBS) and DMSO, amounts not described) to BACTgDyrk1a mice significantly decreased the Tau T212 hyperphosphorylation levels in the hippocampus at 30 minutes and 1 hour post administration (Kim et al., 2016).

A second factor in selecting CX-4945 is its expanding *in vivo* use beyond the recent transgenic DYRK1A mouse model study (Kim et al., 2016). The application of CX-4945 has primarily focused on animal models of cancer as an effective inhibitor of CK2, which is significantly elevated in cancerous tumors. However, the administration of CX-4945 across several studies helps establish its safety if it were to be repurposed in another mouse model. For example, CX-4945 (25mM dissolved in NaH_2PO_4 buffer) administered via oral gavage at 25, 50 and 75mg/kg twice a day for 35 consecutive days to ~8 week old nu/nu mice had no significant effect on body weight (Pierre et al., 2011). A separate study also reported no significant weight changes in 5-7 week old female CrTac:Ncr-Foxn1^{nu} mice who received 25mg/kg or 75mg/kg CX-4945 (5mM dissolved in unknown amount of DMSO) twice a day for 30 consecutive days. (Siddiqui-Jain et al., 2010). While weight was not directly reported, ~3-4 month old NRGS (NOD-Rag1^{null} IL2Rgamma^{null}) mice were treated with 75mg/kg CX-4945 via oral gavage twice daily for 18 consecutive days (Ribeiro et al., 2017). In addition, 7 week old C57BL/6NTac mice received a twice daily IP injection of 25mg/kg CX-4945 (5mM dissolved in an unknown amount of DMSO) for 6 consecutive days (Rossi et al., 2015). The safety and efficacy of CX-4945 administration in cancerous mouse models has led CX-4945 to undergo testing in Phase1b and Phase 2 clinical trials (Marschke et al., 2011)(ClinicalTrials ID: NCT02128282). The demonstration of safety and efficacy of CX-4945 administration across various mouse models, its

long half-life, and its effect on Dyrk1a-mediated deficits *in vitro* warrant further investigation in mouse models of DS.

With the exception of the two previously mentioned studies published in the last six months (ALGERNON and F-DANDY), there is a lack of studies administering novel Dyrk1a inhibitors to mouse models of DS. Along with the Dyrk1a inhibitors mentioned here, there have been over a dozen novel Dyrk1a inhibitors that have been patented in recent years (Nguyen et al., 2017). However, there seems to be a high level of disconnect between the establishment of a Dyrk1a inhibitor *in vitro* and its application and efficacy in DS mouse models *in vivo*. Despite its established safety in humans and efficacy in the previously mentioned mouse models, CX-4945 has not been administered to Ts65Dn mice. Furthermore, developmental, behavioral and histological phenotypes post-CX-4945 treatment have not been reported in any mouse model. Therefore, the administration of a novel Dyrk1a inhibitor to Ts65Dn mice during a time of elevated Dyrk1a expression would significantly contribute to the DS research field.

1.10 Introduction of specific aims

To date, the majority of therapeutics tested in DS mouse models have been administered at adult ages. However, several studies that have administered therapeutics during embryonic, neonatal or perinatal ages, have reported significant improvements in developmental, behavioral and histological deficits [for review see (Stagni et al., 2015)]. In parallel with these findings, there is a significant push from DS researchers and clinicians to start interventions/therapeutics earlier in development (Stagni et al., 2015; Edgin et al., 2015). Alterations in the transcriptome of a developing DS brain have been observed in tissue as early as 14 weeks post conception and there are significant levels of variation in gene expression between ages and brain regions (Olmos-Serrano et al., 2016). For example, the number of differentially expressed genes in the dorsal

frontal cortex appears to increase with age, but the number of differentially expressed genes in the cerebellar cortex appear to remain stable over the life span of an individual with DS (Olmos-Serrano et al., 2016). If the goal is to target Dyrk1a and its corresponding phenotypes, identifying its temporal and spatial expression patterns in brain regions that influence specific phenotypes is an important first step.

Thus, the first goal of this study was to bridge this gap by first establishing the temporal and spatial expression levels of Dyrk1a protein in regions critical for behavioral and anatomical phenotypes in perinatal and adolescent Ts65Dn mice.

1. *Specific Aim 1 (SA1): Measure Dyrk1a protein levels in the cerebellum, hippocampus and cerebral cortex of euploid (control) and Ts65Dn (3 copies of Dyrk1a) male mice at five distinct postnatal ages.* Based on previous evidence suggesting the *Dyrk1a* expression is elevated during neo- and perinatal ages, it was hypothesized that Dyrk1a protein levels would be elevated at perinatal ages (PD12, PD15, PD18) in trisomic mice, but not at late adolescence (P24, P30) and early adulthood (P42).

Once the temporal and spatial profile of elevated Dyrk1a protein levels were established in Ts65Dn mice, the second goal of the study was to administer CX-4945 during the identified period of elevation, and to determine the efficacy of CX-4945 treatment on developmental, behavioral and histological deficits in preweaning Ts65Dn mice.

2. *Specific Aim 2 (SA2) Administer 75mg/kg of CX-4945 and/or 10% DMSO vehicle at a time when Dyrk1a protein is elevated, in order to assess its effects on neurodevelopmental behavior and dentate gyrus cell proliferation in Ts65Dn and euploid mice.* It was hypothesized that treating trisomic mice with a Dyrk1a inhibitor at a specific age when Dyrk1a protein is elevated would result in improvements in locomotor

activity and the homing task. In addition, it was hypothesized that the targeting inhibition of Dyrk1a with CX-4945 would significantly improve the deficits in cell proliferation in the dentate gyrus of the hippocampal formation in trisomic mice.

CHAPTER 2. METHODS

2.1 Mating schemes

There were mating schemes used to generate mice used for both SA1 and SA2. At the start of this project, efforts were currently underway to generate Ts65Dn mice that carried a floxed allele of Dyrk1a for use in a future study (designated Ts65Dn.Dyrk1a$^{fl/+}$). These mice had very similar breeding backgrounds to the traditional Ts65Dn mice that have been extensively used in our laboratory (Stringer et al., 2015; Stringer et al., 2017). Presumably, the only significant difference between Ts65Dn.Dyrk1a$^{fl/+}$ and the Ts65Dn mice was the presence of a single floxed Dyrk1a allele. The allele containing the lox-P sites was presumably active, and without the presence of Cre-recombinase it was assumed that the offspring of both (Ts65Dn x B6C3F1) and (Ts65Dn x B6C3.Dyrk1a$^{fl/fl}$) matings would yield identical outcomes. In addition, Ts65Dn mice are difficult to breed (Roper et al., 2006) and it was hypothesized that the use of offspring from (Ts65Dn x B6C3.Dyrk1a$^{fl/fl}$) matings would allow for an adequate production of mice.

Trisomic and euploid mice were obtained from two mating schemes. Ts65Dn and euploid mice were created by crossing Ts65Dn females (approximately 50% B6 and 50% C3H background with small trisomic marker chromosome) with B6C3F1 males. Ts65Dn and B6C3F1 mice are kept in the lab for approximately 10 months. New Ts65Dn, B6C3F1, B6 AND C3H mice are purchased from the Jackson Laboratory (Bar Harbor, ME) every six months and these new mice, as well as the mice generated within our colony, are used to generate Ts65Dn mice. Ts65Dn females were used as breeders for colony maintenance, as male Ts65Dn mice are sub-fertile. Thus, in both SA1 and SA2 only male Ts65Dn and euploid mice were used.

The second breeding scheme used to produce trisomic and euploid mice involved crossing female Ts65Dn with male B6C3.Dyrk1a $^{fl/fl}$ (F6-F8) mice. As part of a developing study, our laboratory received B6.Dyrk1a$^{fl/fl+}$ mice from Northwestern University, which contained one floxed Dyrk1a allele (Thompson et al., 2015). A schematic detailing the production and mating of these mice is seen in Figure 1. These B6.Dyrk1a$^{fl/fl}$ mice were backcrossed to C3H/HeJ mice, producing B6C3.Dyrk1a $^{fl/+}$ mice that had a ~50% B6 and ~50% C3H background. These B6C3.Dyrk1a $^{fl/+}$ mice were intercrossed with B6C3.Dyrk1a $^{fl/+}$ siblings, resulting in B6C3.Dyrk1a mice that were either floxed at both Dyrk1a alleles (B6C3.Dyrk1a $^{fl/fl}$), one allele (B6C3.Dyrk1a $^{fl/+}$) or neither allele (B6C3.Dyrk1a $^{+/+}$). Mice that were floxed at both Dyrk1a alleles (B6C3.Dyrk1a $^{fl/fl}$) were intercrossed with other B6C3.Dyrk1a $^{fl/fl}$ siblings until the sixth-eighth filial (F6-F8) generation was reached. Once this generation was reached (F7 in Figure 1), B6C3.Dyrk1a$^{fl/fl}$ males were bred with female Ts65Dn mice. From this mating, the current study utilized the male euploid and trisomic mice that had one floxed Dyrk1a allele, from here on after referred to as euploid or trisomic Dyrk1a $^{fl/+}$ mice (bolded in Figure 1).

Near the end of SA2, it became obvious that the offspring from the two breeding schemes were in fact yielding different outcomes. However, the majority of mice used for both SA1 and SA2 were from (Ts65Dn x B6C3.Dyrk1a$^{fl/fl}$) matings, and there were too few mice from (Ts65Dn x B6C3F1) matings for meaningful statistical conclusions to be drawn. Therefore, the primary data reported in this study are from euploid and trisomic mice from (Ts65Dn x B6C3.Dyrk1a$^{fl/fl}$) matings, whereas data from the euploid and trisomic mice from (Ts65Dn x B6C3F1) matings are located in the appendix.

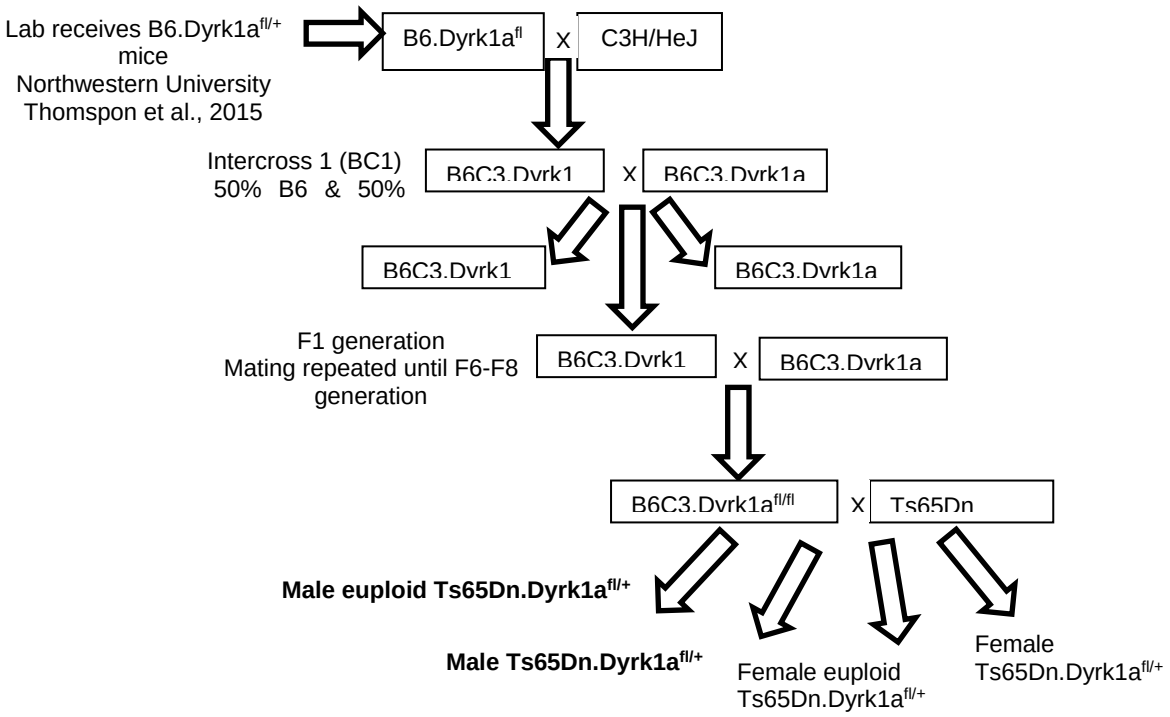

Figure 1. Breeding schematic for the offspring from (Ts65Dn x B6C3.Dyrk1a$^{fl/fl+}$) matings.

2.2 Ts65Dn PCR

Offspring from both (Ts65Dn x B6C3F1) and (Ts65Dn x B6C3F1.Dyrk1a$^{fl/fl}$) matings used in this study were genotyped using the breakpoint PCR (Reinholdt et al., 2011). For euploid and trisomic Ts65Dn mice, the breakpoint PCR makes use of a forward (Chromosome 17) (GTGGCAAGAGACTCAAATTCAAC) and a reverse (Chromosome 16) primer (TGGCTTATTATTATCAGGGCATTT) set to amplify a ~275 bp product at the translocation point on 17^{16} murine chromosome and a positive control primer set of IMR1781 (TGTCTGAAGGGCAATGACTG) and IMR1782 (GCTGATCCGTGGCATCTATT) that amplifies a 544bp product (primers from Invitrogen). The final PCR mix contained MyTaq reaction buffer (1x final), MyTaq polymerase (2.5U/µl final) (Bioline Taunton, MA), water, the

two sets of primers (0.4μM final) (Bioline), and DNA (100ng/rxn). The PCR cycling conditions were set to 94°C for 2 minutes to initialize the reaction, followed immediately by 45 seconds at 94°C to melt the template DNA in a denaturation step that yields single stranded DNA molecules. The template DNA was then cooled to 55°C for 45 seconds to allow annealing of the primers to the template, and strand elongation to occur through the action of Taq polymerase at 72°C for 1 minute. The denaturation, annealing and elongation steps were repeated for 34 cycles and were followed by a final elongation step for 7 minutes at 72°C. To verify the PCR products, the samples were separated on a 1.5% agarose gel made by dissolving 0.75 g of agarose (Fisher Scientific, Geel, Belgium) in 50 mL 1X TAE buffer (40mM tris, 20mM acetic acid, 1mM EDTA). The size(s) of PCR products were determined by comparison with a DNA ladder, which contained DNA fragments of known size, run alongside the products on the gel. This is a crucial step in our studies as it is important to positively distinguish trisomic Ts65Dn mice from the euploid mice.

2.3 PCR on offspring from (Ts65Dn x B6C3.Dyrk1a$^{fl/fl}$) matings

Both euploid and trisomic offspring from (Ts65Dn x B6C3.Dyrk1a$^{fl/fl}$) matings underwent a separate PCR protocol as previously described (Thompson et al., 2015). Briefly, each 25μL reaction contained 2.5U/μL MyTaq, 1x MyTaq buffer (Bioline), 0.4μM primers forward 5'-ATTACCTGGAGAAGAGGGCAAG-3' and reverse 5'-TTCTTATGACTGGAATCGTCCC-3' (Invitrogen), and 16.75μL H_2O. Both the forward and reverse primers were used to identify and amplify the presence of loxP sites flanking (floxed) located just before exon 5 and spanning exon 6 on Dyrk1a alleles. The PCR cycling conditions were as follows: 95°C for 3 min, 35 cycles of 95°C for 20 s, 60°C for 15 s, and 72°C for 15s, followed by a final 1 minute extension at 72°C and 4° for 5 minutes. PCR products were

separated on a 1.5% agarose gel. WT amplicons are 503bp and floxed amplicons are 603bp as seen in Figure 2.

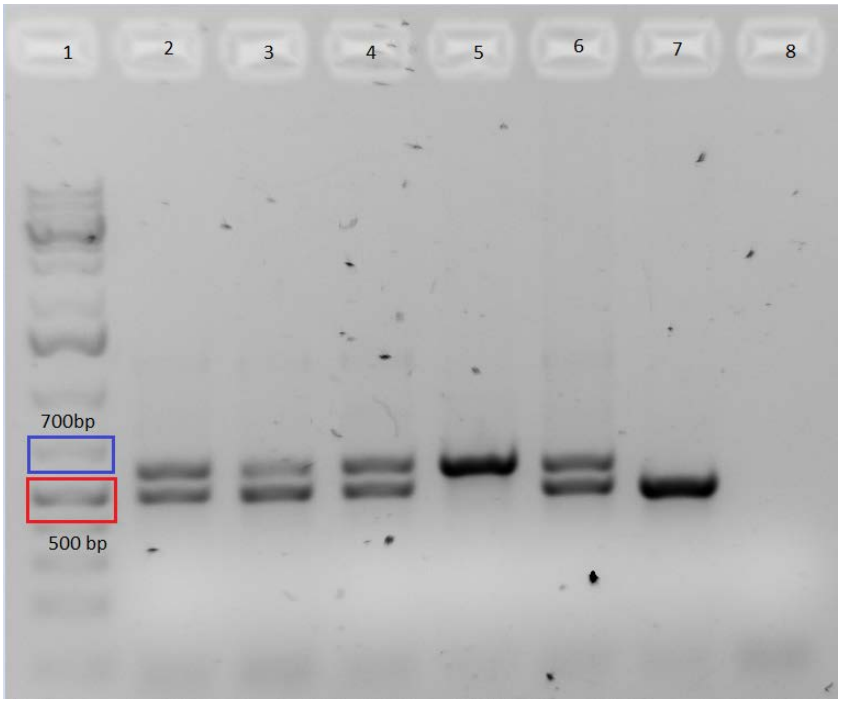

Figure 2. PCR Gel image from offspring of (Ts65Dn x B6C3.Dyrk1a$^{fl/+}$) matings.
The ladder in lane 1 contains the weight marker for 500bp (outlined in red) and 700bp (outlined in blue). Lanes 2, 3, 4 and 6 contain mice heterozygous for one floxed Dyrk1a allele. The animal in lane 5 has both Dyrk1a alleles floxed (band seen at ~603bp) and in lane 7 the animal has neither Dyrk1a allele floxed (band seen at ~503bp). Lane 8 contains water as a control.

2.4 Determination of genotypic sex by PCR

Sex was genetically determined by PCR on offspring from (Ts65Dn x B6C3F1) and (Ts65Dn x B6C3.Dyrk1a$^{fl/fl}$) matings used in this study (McFarlane et al., 2013). Amplification of *Sly* and *Xly* genes, which reside on the Y and X chromosome, respectively, was accomplished using the following primer pairs: forward 5'-GATGATTTGAGTGGAAATGTGAGGTA-3'; reverse 5'-CTTATGTTTATAGGCATGCACCATGTA-3'. Reactions were performed with a final

volume of 25µL containing 1x KCl buffer, 1.5mM $MgCl_2$, 0.2mM dNTPs, 0.2µM primers, 19.05 µL H_20, 1 unit Taq polymerase (Bioline) and 100ng DNA using the following PCR specifications: denaturation at 94°C for 2 min, followed by 35 cycles at 94°C for 30 s, 57°C for 30 s, 55°C for 30 s, and 72°C for 30 s, ending with a 72°C final elongation step for 5 min and 4°C for 5 min. Products were visualized via electrophoresis on a 2% agarose gel. Amplification using the aforementioned primers resulted in a single 280-bp amplicon for males, while female DNA yielded three amplicons of 685-, 660-, and 440-bp.

2.5 Animal care

All animals were housed in the secure AAALAC-accredited Science Animal Resource Center facility in the IUPUI School of Science. Mice were housed in rooms with a standard 12:12 light:dark cycle. Experiments with animals were carried out in accordance with the NIH Guide for the Care and Use of Laboratory Animals and received prior approval from the IACUC committee at IUPUI.

2.6 Timeline for SA1

On postnatal days 12, 15, 18 and 24, male mice were removed from their home cages and euthanized using isoflurane followed by cervical dislocation. Mice used for the late adolescent/early adult age groups (P30, P42) were weaned at P21, group-housed in standard mouse cages and were euthanized in the same manner at their respective ages. Following cervical dislocation, tissue from the cerebellum, cerebral cortex and hippocampus was rapidly dissected, snap frozen, and stored at -80º C.

2.7 Isolation of protein from brain tissue and quantification

Tissue samples were removed from a -80º C freezer and homogenized in RIPA buffer (10mM Phosphate Buffer (pH 7.4), [10% Glycerol (Fisher Scientific, Fair Lawn, NJ), 1% NP-40 (United States Biological, Swampscott, MA) 0.1% SDS (Fisher Scientific, Fair Lawn, NJ), 4mM EDTA (Fisher Scientific, Fair lawn, NJ), 0.15M NaCl (Fisher Scientific, Fair Lawn, NJ), 1x Protease inhibitor cocktail (Roche Diagnostics, Mannheim, Germany)]. The sample was then vortexed at 10,000 rpm for 10 minutes at 4º C. After the sample was vortexed, the supernatant was slowly extracted (to ensure no part of the protein pellet was extracted) and transferred to a new centrifuge tube, which was stored at -80º C. The isolated protein was then quantified using a Bradford assay (Bradford, 1976).

2.8 Western blot to quantify Dyrk1a protein

Protein levels were first quantified for P30 and P42 male animals, and normalized to actin. Isolated protein lysates (20µg) from the three brain regions were resolved electrophoretically on polyacrylamide gels (Bolt 4-12% Bis Tris Plus Gels), and then transferred to PVDF membranes. Membranes were blocked in 5% milk in Tris Buffered Saline with 0.1% Tween 20 (TBS-T), incubated overnight at 4°C in primary antibodies diluted in 5% milk-TBS-T as follows: rabbit anti-DYRK1A antibody, 1:500 (A303-802A, Bethyl Laboratories); mouse anti-beta-actin, 1:5000 (A2228, Sigma Aldrich), and labeled with donkey anti-rabbit IgG AlexaFluor 790 and donkey anti-mouse IgG AlexaFluor 680 secondary antibodies (1:10,000, Jackson Immunoresearch). Fluorescence was detected using a LI-COR CLx Imager, and both Dyrk1a and actin bands were quantified using Image Studio.

Dyrk1a protein levels were then quantified in the adolescent and perinatal male mice (P24, P18, P15 and P12) and normalized to total protein from Coomassie blue stain. Using the same

primary and secondary antibodies as the P30 and P42 mice, it was observed that multiple bands were observed at ~90 kDa, the approximate weight of Dyrk1a. The first band directly below ~90kDa is likely the first and second isoforms of Dyrk1a, which are reported to have a weight of ~86 and ~84kDa. Subsequent isoforms of Dyrk1a weigh ~66, 60, 59kDa. The remaining observable faint bands do not appear to match the weights of the Dyrk1a isoforms, thus, these residual faint are likely due to several methodological variables, including the type of gels and membranes used (Abnova, personal communication). The multiple bands were more pronounced at these younger ages, and at the suggestion of a fellow researcher who had encountered a similar problem, an alternate primary antibody was used to quantify Dyrk1a protein levels and total protein was used as a standard. With the new antibody, multiple bands were still observed. It was determined that quantifying just the top band or all of the multiple bands produced very similar normalized values (correlation >0.8). The multiple bands were very close to each other, so in order to ensure a consistent measurement, all of the bands were boxed together and a single fluorescence level from that box was used (see Figure 3a). The Western blot procedure remained the same as previously mentioned, but the antibodies were; mouse anti-DYRK1A antibody, 1:500 (MO1 Clone 7D10A Abnova), and labeled donkey anti-mouse IgG AlexaFluor 790 secondary antibodies (1:10,000, Jackson Immunoresearch). Fluorescence was detected using a LI-COR CLx Imager, and Dyrk1a was quantified using Image Studio. After the membrane was scanned, it was stained with Coomassie blue dye (Coomassie Brilliant Blue R-250 [Thermo Fisher] 0.5mg, 250mL 100% ethanol, 50mL acetic acid, 200mL H_2O) for 2 minutes with gentle agitation. The dye was then drained, and the membrane was gently agitated in a destain solution (500mL 100% ethanol, 400mL H_20, 100mL acetic acid) for ~20 minutes. Then, the destain was drained and the membrane sat in

water overnight. After 24 hours, the membrane was scanned using a HP Scanner, and the total protein (measured from ~90kDa to ~40kDa) was quantified in Image J.

For P30 and P42 animals, Dyrk1a fluorescent levels were normalized to fluorescent actin levels. For P12, P15, P18 and P24 animals, fluorescent Dyrk1a levels were normalized to total protein levels. Across all ages, each membrane contained two controls (Euploid) and two Ts65Dn mice (Trisomic), with all three brain regions from each mouse (total of 12 samples ran on each gel). Each normalized value was expressed as a ratio relative to the mean intensity value of the same region for the two controls that were run in the same blot (see Figure 3a).

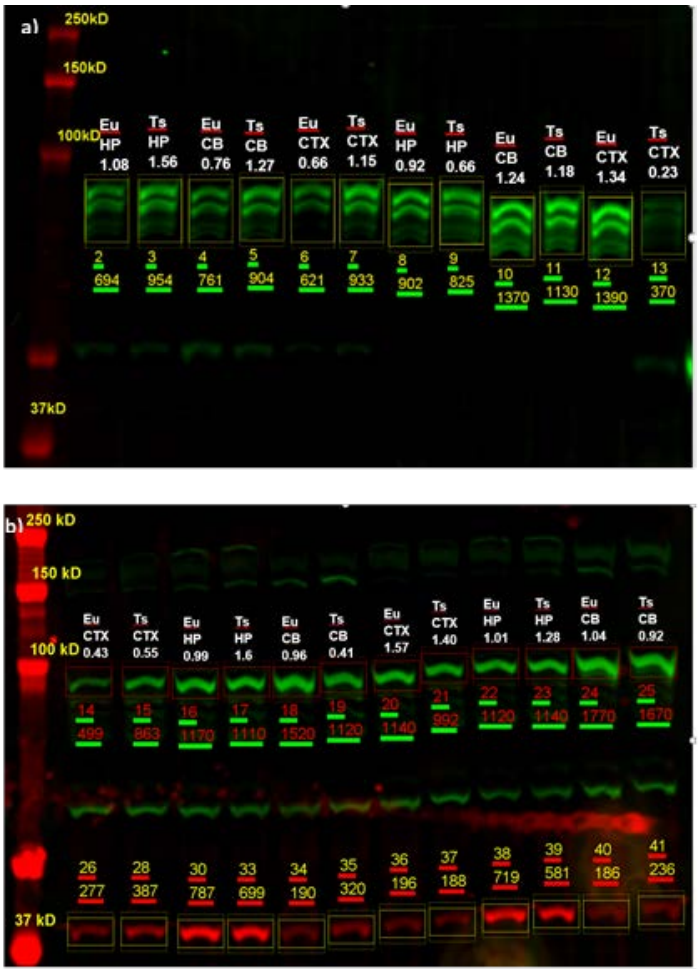

Figure 3. Representative Western blot from P12 and P30 male mice from (Ts65Dn x B6C3.Dyrk1a$^{fl/fl}$) matings

On the far left on both 3a and 3b is the protein ladder (red lines) to assess the weight of specific protein bands. The values in yellow text below the multiple green bands is the measure of Dyrk1a fluorescence. The values in white text above the green bands represent the ratio of Dyrk1a fluorescence: total protein loaded, normalized to the euploids within each brain region. Figure 3a represents two euploid (Eu) and two trisomic (Ts) mice. Figure 3b represents a Western blot with P30 males. The P30 and P42 Western blots also included a quantification of Dyrk1a fluorescence bands. However, in these scans Dyrk1a fluorescence levels were normalized to actin levels (seen at ~42kD).

2.9 Statistical analysis

For the Western blot analysis at a specific age, the normalized ratio from each brain region was analyzed using a mixed ANOVA with brain region as a within subjects measure and genotype

as a between-group factor. Fisher's LSD tests were used for *post hoc* comparisons to follow up significant ANOVA main effects or interactions. At each age, effect sizes were calculated using the standardized mean difference of the normalized ratios of a specific brain region between euploid and trisomic mice.

2.10 Identifying appropriate phenotypes to assess in P14-P18 euploid and Ts65Dn mice

The goal of this study was to determine if treatment with a Dyrk1a inhibitor during a specific period of Dyrk1a elevation would significantly improve deficits in trisomic phenotypes. For behavioral evaluation, ~P14-P18 mice have fully developed neurodevelopmental reflexes (i.e. prehensile reflex, negative geotaxis, righting reflex, startle response, etc.) (Fox, 1965). Although there are few studies that have characterized behaviors and anatomical phenotypes at this age in transgenic *Dyrk1a* (TgDyrk1a) or mouse models of DS, the studies provided the rationale for selecting appropriate behaviors to assess. At P14, TgDyrk1a mice exhibit significant deficits on a single homing test, wire suspension test and coat hanger test (Altafaj et al., 2001). Ts1Cje mice exhibited deficits on a two-trial homing test at P12, and Ts65Dn mice exhibited similar homing deficits at P12 and hyperactive behavior at P21 (Guedj et al., 2015; Holtzman et al., 1996). Ts65Dn mice exhibit significant decreases in DG cell proliferation at P15 and P18 (Bianchi et al., 2010; Contestabile et al., 2007). In the cerebellum, P14 Ts65Dn mice have significantly decreased cerebellar area, internal granule layer thickness, and granule cell density (Roper et al., 2006).

With a five-day treatment span during a pre-weaning age, special consideration was made to select behavioral tests that minimized stress and the length of time mice were removed from the home cage. In addition to daily growth, mice were assessed for motor coordination (locomotor activity), exploratory behavior (modified homing test), and hippocampal neurogenesis.

2.11 Timeline for SA2

Each (Ts65Dn x B6C3F1) or (Ts65Dn x B6C3.Dyrk1a$^{fl/fl}$) litter was randomly assigned to receive either CX-4945 or vehicle treatment. In (Ts65Dn x B6C3.Dyrk1a$^{fl/fl}$) litters, all mice (both males and females) received the same treatment. One reason for administering the same treatment to the entire litter was that the genotypes and sexes of the mice was not always known at the time of treatment. By treating the entire litter, this helped ensure that group sizes remained balanced across treatment groups. The exception to this was in offspring from (Ts65Dn x B6C3F1) litters, as only the males received treatment. The females were necessary for colony growth as they are an integral part of the breeding colony. However, all mice (both males and females) from (Ts65Dn x B6C3F1) or (Ts65Dn x B6C3.Dyrk1a$^{fl/fl}$) litters were weighed daily, even females from (Ts65Dn x B6C3F1) matings. Both males and females from (Ts65Dn x B6C3.Dyrk1a$^{fl/fl}$) matings were treated and underwent behavioral testing, however, on data on the male mice are reported here. A schematic of the treatment and behavioral timeline is seen in Figure 4. In SA1, an elevation in Dyrk1a protein at P15 was observed in male Ts65Dn.Dyrk1a$^{fl/+}$ mice. Therefore, the treatment began just before the onset of significant elevation, P14, and ended when the elevation was no longer significant, at P18. On P14-15, mice received the single daily subcutaneous (SC) injection of their litter-assigned treatment. There were two behavioral tasks used in this behavioral paradigm; the homing and locomotor activity task. Each of these tasks was administered once to an entire litter, and the order of these tasks (P16 or P17) was counterbalanced across litters. On P16, mice received the treatment injection, and approximately 30 minutes later, underwent behavioral testing in either the locomotor activity or homing test. This procedure was repeated on P17, with the second behavioral task (either homing or locomotor activity, depending on

counterbalanced order). On P18 mice received their final treatment injection along with a single BrdU injection (100mg/kg) and were sacrificed two hours later.

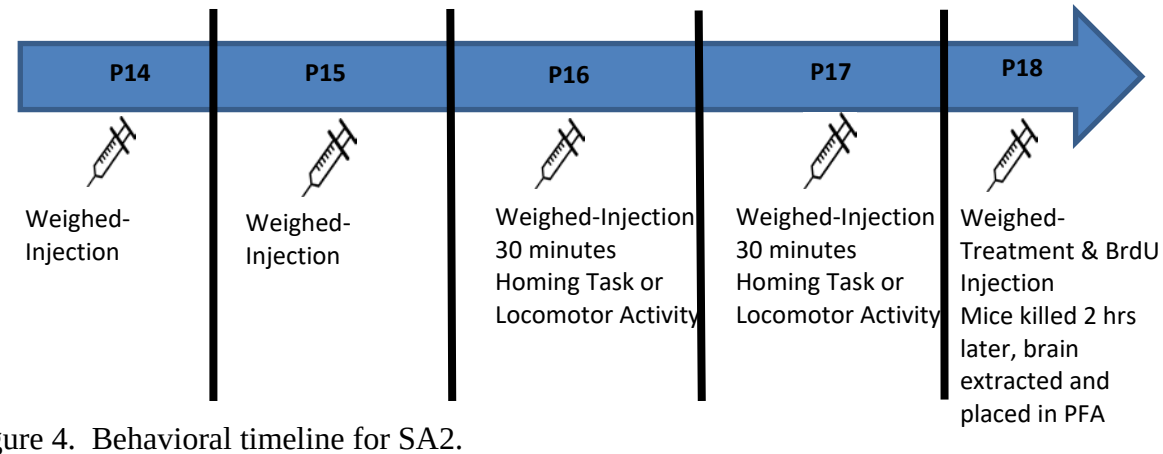

Figure 4. Behavioral timeline for SA2.

2.12 Treatment preparation and delivery

CX-4945 was obtained from SignalChem (400mg of CX-4945, received 10/31/17; MW: 349.77g/mol). A 250mM solution was made by vigorously vortexing 24.5mg CX-4945 with 280µL DMSO in a 1.5mL microcentrifuge tube at room temperature. The treatment suspension was prepared by combining 60µL 250mM CX-4945 with 540µL PBS in a separate 1.5mL microcentrifuge tube. The suspension was vortexed vigorously and stored at -20°C. The 10% DMSO was also aliquoted into microcentrifuge tubes and stored at -20°C. On the day of treatment, tubes were removed from the freezer, warmed to 37° C, and vortexed. Starting on PD14, litters were randomly assigned to one of two treatments; 75mg/kg CX-4945 or volume-matched 10% DMSO. Each animal due to receive treatment was removed from its cage and weighed. The appropriate amount of treatment was delivered SC using a new 28-gauge disposable needle for each mouse. After the injection, the animal was placed in a holding cage while the other mice in

the same cage were weighed and treated, if necessary. After all mice had been treated, they were transferred from the holding cage to their home cage.

2.13 Locomotor activity

Approximately 30 minutes post-injection, the entire cage (including parents and any untreated mice) was removed from the colony room, covered with a navy cloth and transferred to the Open Field testing room. Mice acclimated to the room for ~5 minutes while the experimenter started the computer and set up the test chambers for testing. Each mouse was placed in a Versamax Animal Activity Monitor (Accuscan Instruments, Columbus, OH) for 10 minutes. Activity was recorded by intersecting infrared photocell beams (2 cm above the chamber floor) evenly spaced along the walls of the 40×40 cm test chamber. Sound attenuating box chambers (inside dimensions, 53 cm across × 58 cm deep × 43 cm high) equipped with a house light and fan for ventilation and background noise encased the test chamber. For this study, the house light was turned on. The chambers are attached to a Dell computer which recorded accumulated activity counts every minute. Following the end of the session, the chambers were cleaned with 20% ethanol and animals were returned to their home cage in the colony room.

2.14 Homing task

The homing task is based on a mouse's development to orientate itself towards their home cage once removed. The task was first utilized by Altman and Sudarshan who demonstrated that rats would orientate themselves and begin crawling toward their home cage and littermates when removed from the home cage (Altman et al., 1975). A common homing task design is to remove pups from their home cage and mother for approximately 30 minutes. They are then placed in a new cage, opposite of the end in which home cage bedding covers 1/3 of the floor. The time it

takes the mouse to reach the home bedding is recorded. Depending on the task procedure and the age of the animal, this task can assess locomotion, olfaction and/or exploratory behavior. This task has been extensively used in animal models of prenatal malnutrition, drug exposure, and neurodevelopmental disorders to assess postnatal sensorimotor development (Pometlová et al., 2009; Lim et al., 2008; Tonkiss et al., 1996; Holtzman et al., 1996; Mikulecká et al., 2014). The current study used a modified homing task (Tonkiss et al., 1996) in order to assess pre-weaning locomotion and exploratory behavior in Ts65Dn mice.

Approximately 15 minutes post injection, all pups in the litter were transferred to a clean cage containing fresh bedding and a cardboard igloo. The cage was covered with a navy cloth and brought to the homing test testing room. The cloth was removed, and the animals were left to habituate to the testing room for approximately 20 minutes undisturbed. The lighting for the testing room was approximately 60 lux. The homing test apparatus was a standard clean mouse cage (25.4 x 16.5 x 12 cm) containing two plastic lids (7cm in diameter) placed in opposite corners 3cm from the wall. The lids contained bedding from the home cage, or new bedding. The location of the lids was counterbalanced across animals. Trials were recorded with video tracking using ANYMAZE Software (Stoelting Co., Wood Dale, IL). A mouse was removed from the transfer cage and placed in a new holding cage that was placed next to the homing apparatus. The lids were placed in their respective pre-determined location, and the mouse was removed from the holding cage and placed next to the apparatus wall, facing towards the center. The mouse was allowed to explore for 60 seconds, then it was removed and placed in the adjacent holding cage. The lids were removed, wiped with 20% ethanol and their locations were reversed. The entire apparatus was cleaned with 20% ethanol. The inter-trial interval was approximately 60 seconds. Once cleaned, the mouse was returned to the apparatus for the second trial and allowed to explore

for 60 seconds. Once the second trial ended, the mouse was removed and placed back in the transfer cage with the other pups. The lids were removed, and the bedding used for the previous animal was discarded. The lids and apparatus were wiped with 20% ethanol, the lids were once again filled with home cage bedding or new bedding and were placed in the respective location for the next mouse.

2.15 Bromo-2-hydroxyuridine preparation and brain extraction

5-Bromo-2-hydroxyuridine (BrdU; B5002 Sigma) was stored at -20° C until the day of treatment. BrdU was removed from the freezer, weighed on analytical scale, added to a 2ml tube, and heated (50° C) 0.9% sterile saline solution was slowly added via syringe to yield a final concentration of 10mg/mL. The solution was gently vortexed and was used immediately for injections. On PD18, the animal received a single IP injection of 100 mg/kg of BrdU (10mg/ml concentration in 0.9% sterile saline, approximately 10mg/kg injection volume). This injection was given immediately after the final treatment injection was delivered.

Two hours later, mice were euthanized using isoflurane followed by cervical dislocation. Brains were carefully removed from the skull and placed in 4% paraformaldehyde for 24 hours. The next day brains were embedded in gelatin block and fixed with 4% paraformaldehyde (PFA) for at least 72 hours 40-µm-thick coronal sections were cut on a free floating vibratome (Leica Microsystems VT1000) for immunohistochemistry procedures. Each brain was sectioned throughout the extent of the hippocampal formation. Each brain produced approximately 60 coronal sections throughout the hippocampal formation, and all of these slices were stored at -80° C in a cryoprotectant solution containing glycerol and ethylene glycol in Tris-buffer solution for 48 hours.

2.16 Immunohistochemistry

A one in five random sampling ratio was used to select slices for peroxidase immunohistochemistry to label BrdU+ cells. For each brain, this sampling ratio yielded 10-12 sections that underwent immunohistochemical processing. For the peroxidase immunohistochemistry, sections were washed in TBS (0.15 M NaCl and 0.1M Trizma HCl) and treated with 3% H_2O_2 in water for 10 minutes to block endogenous peroxidases. Then, the slices were washed 5x2 min in TBS, and underwent a 30-minute incubation in 2N HCl at 37ºC. Sections were then washed in 0.1M Boric acid (pH=8.6) in TBS, in TBS alone, incubated for 1 hour in blocking solution (0.5% Triton X-100 and 3% normal goat serum in TBS), and then incubated with the primary antibody solution (rat anti-BrdU, 1:500; Accurate Chemical, OBT0030) for 48 hours at 4ºC. Following primary antibody incubation, sections were washed in the blocking solution, followed by a 1-hour incubation in the blocking solution. The slices were then washed 3 times in TBS and were incubated in the secondary antibody (biotinylated anti-rat made in goat, 1:250; Vector Laboratories, BA-9400), then for 1 hour in avidin-biotin-peroxidase complex solution (ABC Elite Kit; Vector Laboratories, PK-4000) with nickel-enhanced diaminobenzidine as the chromagen. Slices were mounted to chrome-alum subbed slides and allowed to dry for 48 hours.

2.17 Tissue staining and counting

Slides were briefly dipped in milli-q water, and then placed in a 0.5% Methyl green solution (Sigma-Aldrich) for 2 minutes. This was followed by 5 slow dips in water. Slides were then placed in 70% ethanol for approximately 2 minutes, with slices being monitored for differentiation. This was followed by a 5 second dip in 95% ethanol, then a 1-minute dip in 100% ethanol. Finally, slides were left in xylene for 5 minutes, and then the counterstained slides were coverslipped with

Permount. Slides were left to dry for 48 hours. All tissue slices that were processed and mounted underwent quantification of BrdU+ cells. BrdU+ labeled cells were counted throughout the subgranular layer of the DG on all sections with a bright-field microscopy camera (Nikon Eclipse 80i), at 1000x magnitude with the 100x oil objective, using a modified optical fractionator approach similar to a previous study (Malberg et al., 2000). Since only a fraction of slices (1 in 5 were used) were used for counting BrdU+ labeled cells, the total number of cells for a specific slice was calculated with the following equation:

*Total estimated number of cells per slice throughout DG = [(total number of cells counted) ÷ (number of slices counted)] * 5 (section sampling fraction)*

The volume (area per point: 4000μ^2) of the granule cell layer was quantified using the 4x objective, using Cavalieri's principle (Stereologer system and software; Systems Planning and Analysis, Inc., Alexandria, VA). Section thickness was measured optically at 1000x magnification using z-axis microcator attached to the microscope stage. The total volume of the granule cell layer was calculated using the following formula:

*Total estimated granule cell layer volume= (average slice thickness) * (area [calculated using 4000 u^2 disectors]) x 5 (section sampling fraction)*

The density of BrdU+ cells in the DG granule cell layer for each animal was calculated by dividing the total number labeled cell counts by the total volume of the granule cell layer.

2.18 Statistical analysis

The body weights across treatment days were analyzed using a mixed ANOVA with day as a within subjects measure and genotype and treatment as between group factors. The total distance traveled in the locomotor activity test was summed across the entire session and analyzed with a two-way ANOVA using genotype and treatment as a between-subjects factor. The homing

test included several measures for both trial 1 and trial 2: total time spent exploring both zones, time exploring home zone, time exploring new zone, number of midline crossings, number of home zone visits, number of new zone visits, time taken to first explore home zone, time taken to first explore new zone, and % of exploration time spent in home zone. These measures were assessed separately for each trial using a two-way ANOVA with genotype and treatment as a between-subjects factor. For the immunohistochemistry analyses, total BrdU+ cell counts, total granule cell layer volume, slice thickness, number of slices, and cell density were all analyzed using a two-way ANOVA using genotype and treatment as a between-subjects factor.

CHAPTER 3. RESULTS

3.1 (Ts65Dn x B6C3F1) vs (Ts65Dn x B6C3.Dyrk1a$^{fl/fl}$) offspring

As previously mentioned, two breeding schemes of mice were used in the current study (Ts65Dn x B6C3F1) and (Ts65Dn x B6C3F1.Dyrk1a$^{fl/fl}$) to generate trisomic and euploid mice, and only results from male mice were reported in the current study. Table 1 details the background of male mice used for the Dyrk1a protein analysis in SA1. Only euploid and trisomic Dyrk1a$^{fl/+}$ male mice were used at P12, P15, and P18. At P24, P30 and P42 a mix of male offspring from both (Ts65Dn x B6C3F1) and (Ts65Dn x B6C3.Dyrk1a$^{fl/+}$) matings were used for Western blot analysis. However, the SA1 results reported here will solely focus on the Western blot analysis with euploid and trisomic Dyrk1a$^{fl/+}$ male mice. The Western blot analysis of male mice from (Ts65Dn x B6C3F1) matings are reported in the Appendix.

Table 1. The distribution of male mice from (Ts65Dn x B6C3F1) and (Ts65Dn x B6C3.Dyrk1a$^{fl/fl}$) matings used for SA1.

Background stock distribution of animals used for SA1				
Age	(Ts65Dn x B6C3F1)		(Ts65Dn x B6C3.Dyrk1a$^{fl/fl}$)	
	Euploid	Trisomic	Euploid	Trisomic
P12	0	0	7	8
P15	0	0	6	7
P18	0	0	7	8
P24	4	4	3	3
P30	1	1	5	5
P42	1	3	3	1

In SA2, males from 11 (Ts65Dn x B6C3.Dyrk1a$^{fl/fl}$) litters and 6 (Ts65Dn x B6C3F1) litters were tested. Table 2 summarizes the litter demographics from these two breeding schemes, however, the behavioral outcomes from SA2 are of male mice from (Ts65Dn x B6C3.Dyrk1a$^{fl/fl}$) litters. SA2 outcomes of male mice from (Ts65Dn x B6C3F1) litters are reported in the Appendix. There were no significant differences on the average litter size, the number of trisomic mice produced within a litter, nor were there any differences in the proportion of trisomic mice produced within a litter (see Table 2). However, there was a non-significant trend towards (Ts65Dn x B6C3.Dyrk1a$^{fl/fl}$) matings producing a significantly lower proportion of trisomic males versus (Ts65Dn x B6C3F1) matings (p=0.07).

Table 2. Demographics of offspring from (Ts65Dn.B6C3.Dyrk1a$^{fl/fl}$) and (Ts65Dn x B6C3F1) litters for SA2.
Data includes both male and females. Data are represented as mean ± SEM.

	(Ts65Dn x B6C3F1) (6 litters)			(Ts65Dn x B6C3.Dyrk1a$^{fl/fl}$)(11 litters)		
	Females	Males	Collapsed	Females	Male	Collapsed
Mice per litter	1.83±0.79	3.6±0.84	5.5±1.08	2.00±0.33	3.09±0.60	5.09±0.53
Average number of trisomic mice per litter	0.66±0.33	2.5±0.56	3.1±0.47	1.09±0.28	1.45±0.51	2.45±0.57
Average proportion (%) of trisomic mice per litter at P14	11.66±5.69	51.11±11.11	62.77±7.95	23.73±7.72	24.74±8.08	48.48±8.90

Offspring from both (Ts65Dn x B6C3F1) and (Ts65Dn x B6C3.Dyrk1a$^{fl/fl}$) matings were used in SA2. However, the majority of mice used for SA2 were euploid and trisomics from (Ts65Dn x B6C3.Dyrk1a$^{fl/fl}$) matings (see Table 3) and the primary analysis presented here will utilize only the male euploid and trisomic mice from (Ts65Dn x B6C3.Dyrk1a$^{fl/fl}$) matings.

Data from mice of both mating schemes (Ts65Dn x B6C3F1) and (Ts65Dn x B6C3.Dyrk1a$^{fl/fl}$), as well as mice from just the (Ts65Dn x B6C3F1) litters are reported in the Appendix. During SA2 we observed that the offspring of (Ts65Dn x B6C3.Dyrk1a$^{fl/fl}$) matings, particularly trisomic mice, appeared to weigh more than trisomic offspring from (Ts65Dn x B6C3F1) matings (see Figure 5). When analyzing locomotor activity in trisomic mice, weight had a significant effect on the total distance travelled in the locomotor test. The total distance traveled in the locomotor activity test was collapsed across DMSO and CX-4945 treatments and segregated into whether a mouse weighed under or over 5.4 grams at the time of testing (Figure 6). This analysis highlighted two important findings; 1) there was a greater proportion of Ts65Dn mice that weighed under 5.4 grams than Ts65Dn.Dyrk1a$^{fl/+}$ mice, and 2) of the 2 Ts65Dn.Dyrk1a$^{fl/+}$ mice that did weigh under 5.4 grams, their locomotor activity performance was not significantly altered by their low weight. In stark comparison, Ts65Dn mice that weighed under 5.4 grams had significant deficits in locomotor activity, regardless of which treatment they received.

Table 3. Distribution of male offspring from (Ts65Dn x B6C3F1) and (Ts65Dn x B6C3.Dyrk1a) litters for SA2.
The majority of animals used for SA2 were offspring from (Ts65Dn x B6C3.Dyrk1a$^{fl/fl}$) matings.

Background distribution of animals used for SA2								
	(Ts65Dn x B6C3F1)				(Ts65Dn x B6C3.Dyrk1a$^{fl/fl}$)			
	Euploid +DMSO	Euploid + CX-4945	Trisomic + DMSO	Trisomic + CX-4945	Euploid + DMSO	Euploid + CX-4945	Trisomic + DMSO	Trisomic + CX-4945
Treatment	1	3	4	11	12	7	9	7
Homing Task	1	3	4	11	11	6	8	7
Locomotor Activity	1	2	4	11	11	7	8	7
Cell Proliferation	0	2	3	2	9	5	6	7

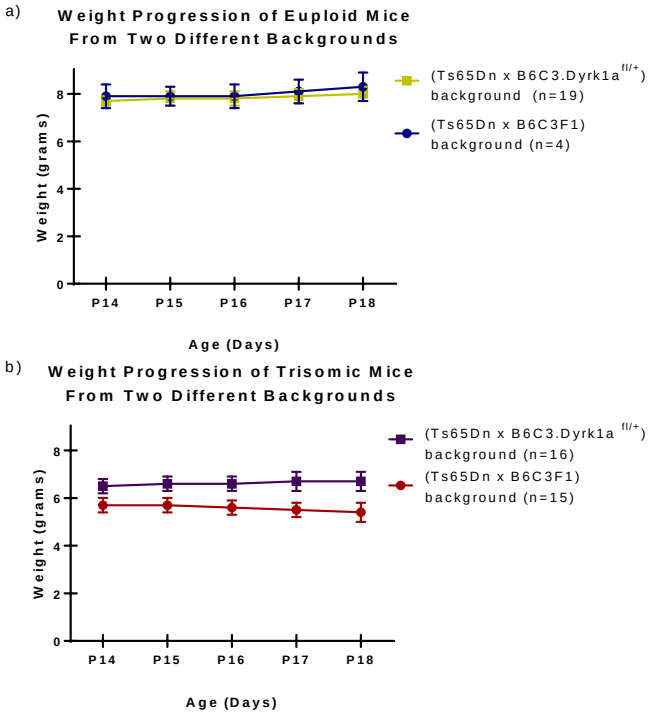

Figure 5. Weight progression of offspring from (Ts65Dn x B6C3F1) and (Ts65Dn x B6C3.Dyrk1a) matings.
5a depicts the average weight progression of eupoid mice from the two different mating schemes used in the current study. 5b depicts the progression of the trisomic mice from the two different mating schemes. Both 5a and 5b are collapsed across treatment groups. Data are represented as mean ± SEM.

These findings and the primary use of euploid and trisomic Dyrk1a$^{fl/+}$ in SA1 resulted in the current study to analyze and subsequently report euploid and trisomic Dyrk1a$^{fl/+}$ outcomes. All data from this point on represents the offspring from (Ts65Dn x B6C3.Dyrk1a$^{fl/fl}$) matings. There was not sufficient statistical power to draw meaningful statistical conclusions about offspring from a (Ts65Dn x B6C3F1) matings. The data of male mice from the (Ts65Dn x B6C3F1) matings are presented separately in the Appendix, along with analysis of data combined across mating schemes.

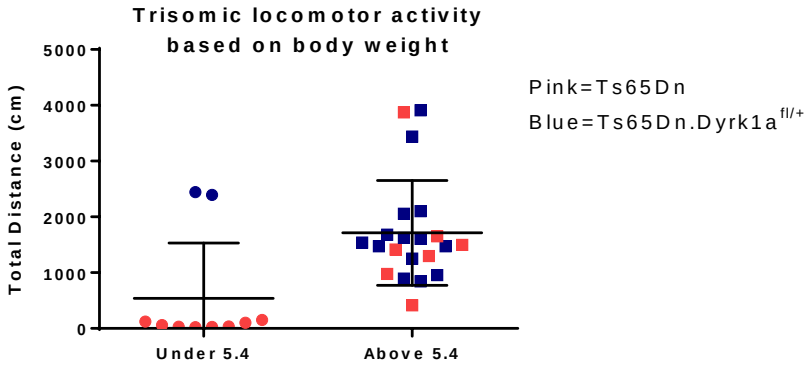

Figure 6. Locomotor activity of trisomic mice from (Ts65Dn x B6C3F1) and (Ts65Dn x B6C3.Dyrk1a$^{fl/fl}$) matings based on body weight
Male trisomic mice were grouped by their weight (under or over 5.4 grams) at the time of locomotor testing. Pink represent Ts65Dn trisomic mice, and the blue depicts Ts65Dn.Dyrk1a$^{fl/+}$ mice.

3.2 Aim 1: Dyrk1a Protein Levels at five distinct postnatal ages

3.2.1 Dyrk1a protein levels at P12

There was a trend for trisomic Ts65Dn mice exhibiting higher levels of Dyrk1a than euploid controls across all three brain regions (p=0.08). As seen in Table 4, there were no significant main or interactive effects of genotype in Dyrk1a protein levels at P12 in male Ts65Dn

mice in the cerebral cortex [t(13)= -0.855, p=0.408, d=0.44]; the cerebellum [t(13)= -1.196, p=0.253, d=0.62] or the hippocampus [t(13)= -1.658, p=0.121, d=0.82]. There were no significant correlations between Dyrk1a protein levels across brain regions.

Table 4. Protein levels at six distinct postnatal ages in euploid (Eu) and trisomic (Ts) mice from (Ts65Dn x B6C3.Dyrk1a$^{fl/fl}$) matings

Both 4a and 4b represent euploid and trisomic Dyrk1a$^{fl/+}$ mice from (Ts65Dn x B6C3.Dyrk1a$^{fl/fl}$) matings. Ts values within a brain region represent the mean Dyrk1a protein levels normalized to euploid levels. Data are represented as mean ± SEM. Ts male mice exhibited significantly elevated Dyrk1a protein levels across all tissues measured at P15, as indicated by the (*). 4a depicts perinatal and adolescent mice that underwent Western blots using the Abnova 7D10 Dyrk1a antibody and total protein load as a normalization. The respective effect size for each of the brain regions within an age are listed. Table 4b depicts the young adult and adult mice that were ran on a Western blot using the Bethyl A303-802A Dyrk1a antibody. The effect size for P30 brain regions is listed, however, at P42 there was only 1 trisomic mouse from (Ts65Dn x B6C3.Dyrk1a$^{fl/fl}$) matings so no effect sizes are reported.

a) Western Blots ran using Abnova Dyrk1a protein & normalizing to total protein load				
Age	**Group**	**Cerebellum**	**Hippocampus**	**Cerebral Cortex**
P12	**Eu (n=7)**	1.00 ± 0.05	1.00 ± 0.07	1.00 ± 0.08
	Ts (n=8)	1.19 ± 0.13	1.37 ± 0.14	1.15 ± 0.18
Effect size		*d=0.62*	*d=0.82*	*d=0.44*
P15*	**Eu (n=6)**	1.00 ± 0.11	1.00 ± 0.02	1.00 ± 0.07
	Ts (n=7)	2.01 ± 0.27*	1.53 ± 0.07*	1.63 ± 0.16*
Effect size		*d=1.90*	*d=3.99*	*d=1.90*
P18	**Eu (n=7)**	1.00 ± 0.06	1.00 ± 0.09	1.00 ± 0.05
	Ts (n=7)	1.16 ± 0.13	1.29 ± 0.16	1.31 ± 0.17
Effect size		*d=0.58*	*d=0.77*	*d=0.85*
P24	**Eu (n=3)**	1.00 ± 0.24	1.00 ± 0.32	1.00 ± 0.20
	Ts (n=3)	1.11 ± 0.34	0.94 ± 0.20	0.76 ± 0.14
Effect size		*d=0.19*	*d=0.05*	*d=1.43*

b) Western Blots ran using Bethyl Dyrk1a protein & normalizing to actin				
Age	**Group**	**Cerebellum**	**Hippocampus**	**Cerebral Cortex**
P30	**Eu (n=5)**	1.00 ± 0.13	1.00 ± 0.10	1.00 ± 0.13
	Ts (n=5)	1.08 ± 0.13	1.15 ± 0.10	0.76 ± 0.08
Effect size		*d=0.54*	*d=0.97*	*d=1.01*
P42	**Eu (n=3)**	1.00 ± 0.04	1.00 ± 0.07	1.00 ± 0.24
	Ts (n=1)	0.40	0.64	0.36

3.2.2 Dyrk1a protein levels at P15

As shown in Figure 7, Ts65Dn male mice exhibited higher levels of Dyrk1a protein across all three brain regions versus euploid controls [mixed ANOVA, main effect of genotype: $F(1,13)=35.83$, $p<0.001$] at P15. Follow up analyses showed Ts65Dn mice exhibited significantly higher levels of Dyrk1a protein versus euploid controls in the cerebellum [$t(13)= -3.82$, $p=0.002$, $d=1.90$], cerebral cortex [$t(13)= -3.764$, $p=0.002$, $d=1.90$], and hippocampus [$t(13)= -7.025$, $p<0.001$, $d=3.99$]. A Pearson's correlation of Dyrk1a protein levels was run within each genotype in order to determine if Dyrk1a protein levels were significantly correlated across brain regions. There was a trend towards a significant correlation between Dyrk1a protein levels in the cerebral cortex and hippocampus in trisomic mice, suggesting a similar regulation mechanism for Dyrk1a in these two brain regions ($r=0.751$, $p=0.052$).

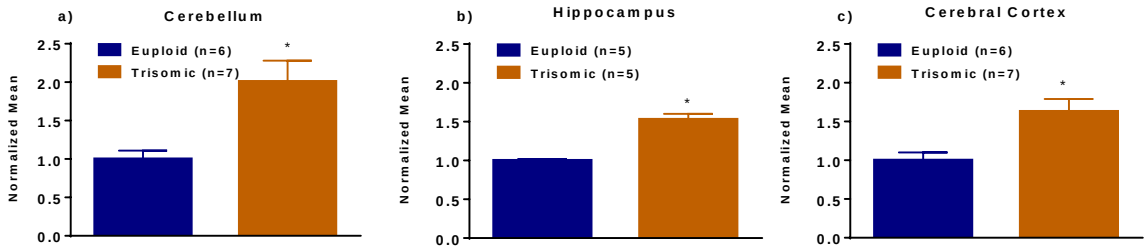

Figure 7. Dyrk1a protein levels in P15 male euploid and Ts65Dn mice from (Ts65Dn x B6C3.Dyrk1a$^{fl/fl}$) matings

The Dyrk1a protein levels in the a) cerebellum, b) hippocampus and c) cerebral cortex of P15 male euploid and Ts65Dn mice. Ts65Dn mice had significantly elevated levels versus euploid controls in each brain region, as indicated by the (*) ($p<0.05$). Data are represented as mean ± SEM. 7d depicts a representative image of a western blot ran on two euploid (Eu) and two trisomic (Ts) male mice. The values in yellow text below the green bands are the measure of Dyrk1a fluorescence. The values in white text above the green bands represent the ratio of Dyrk1a fluorescence: total protein loaded, normalized to the euploids within each brain region. Cerebellum (CB), Cerebral Cortex (CTX), Hippocampus (HP). After the fluorescent membrane in 7d was scanned, it was stained with coommasie dye, as seen in Figure 7e. The total protein load was quantified by drawing identical rectangular boxes (outlined in yellow) in each lane. The number above the lane represents the total amount of protein.

Figure 7 continued

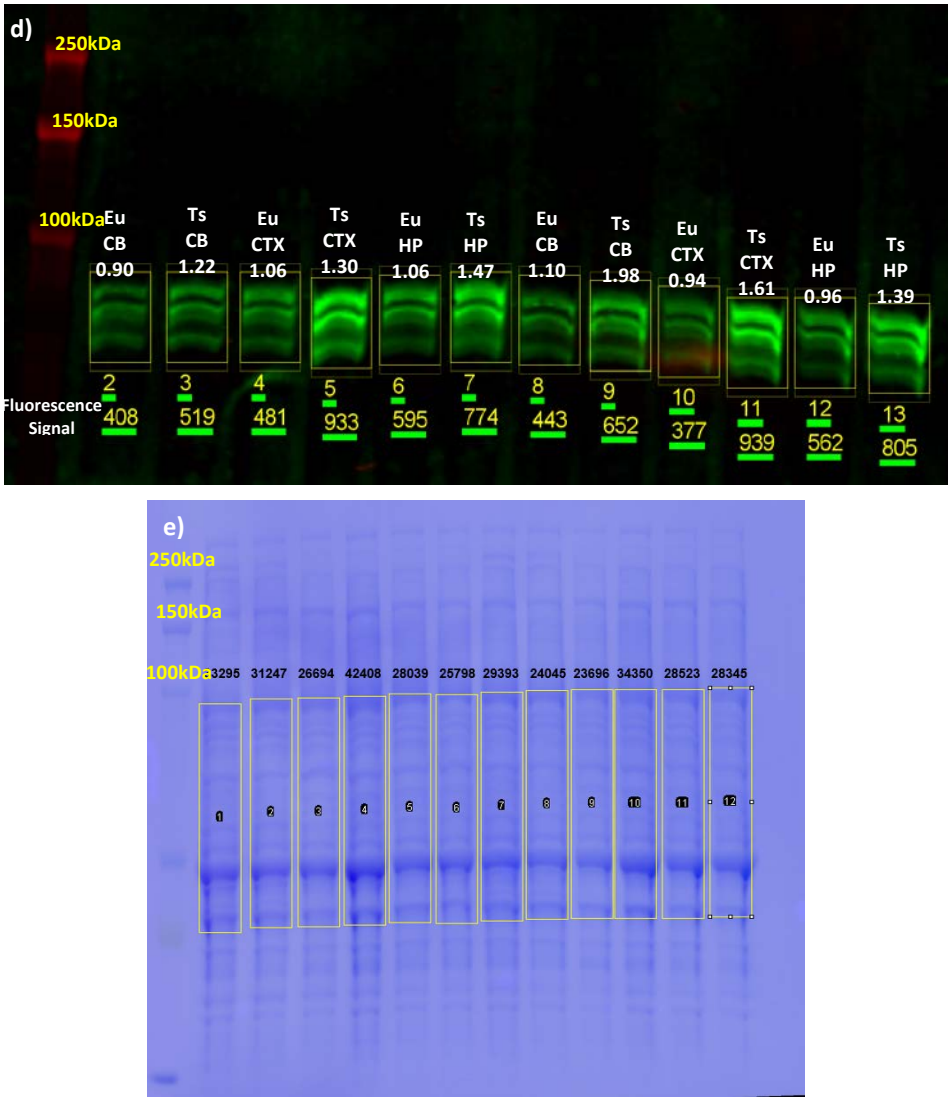

3.2.3 Dyrk1a protein levels at P18

A mixed ANOVA revealed no significant main or interactive effects of genotype in Dyrk1a protein at P18 in male Ts65Dn mice in the cerebral cortex [$t(14)= -1.731$, $p=0.105$, $d=0.85$], cerebellum [$t(14)= -1.167$, $p=0.263$, $d=0.58$], or the hippocampus [$t(14)= -1.586$, $p=0.135$,

d=0.77]. There was a strong trend for trisomic mice having elevated Dyrk1a protein levels across all brain regions (*p*=0.058) (see Table 4).

3.2.4 Dyrk1a protein levels at P24

As seen in Table 4a, there were no significant main or interactive effects of genotype on Dyrk1a protein levels at P24 in male Ts65Dn mice in the cerebral cortex [t(4)= 1.753, *p*=0.154, *d*=1.43], cerebellum [t(4)= -0.221, *p*=0.836, *d*=0.19] or the hippocampus [t(4)= 0.064, *p*=0.952, *d*=0.05].

3.2.5 Dyrk1a protein levels at P30

There were no significant main or interactive effects of genotype on Dyrk1a protein at P30 in male Ts65Dn mice in the cerebral cortex [t(8)= 1.758, *p*=0.117, *d*=1.01], cerebellum [t(8)= -0.895, *p*=0.397, *d*=0.54] or the hippocampus [t(8)= -1.584, *p*=0.152, *d*=0.97] (see Table 4b and Appendix).

3.2.6 Dyrk1a protein levels at P42

At P42, only 3 euploid and one trisomic mouse from (Ts65Dn x B6C3.Dyrk1a$^{fl/fl}$) matings underwent Western blot analysis to measure Dyrk1a protein levels. No statistical analysis was run on these animals, and the averages and single blot levels are reported in Table 4b.

3.3 Aim 2: Treatment with CX-4945 or DMSO from P14 – P18

3.3.1 Attrition and treatment group sizes

A total of 57 male mice were treated with either CX-4945 or 10% DMSO. Three male mice died while receiving treatment. Two euploid mice receiving CX-4945 treatment died on P18 and one trisomic mouse receiving 10% DMSO was found dead on P18. The primary statistical

analysis for SA2 includes only euploid and trisomic Dyrk1a$^{fl/+}$ mice; see the Appendix for additional analysis that include the mice from (Ts65Dn x B6C3F1) matings. The final treatment group sizes and the number of litters represented from (Ts65Dn x B6C3.Dyrk1a$^{fl/fl}$) matings were as follows; Eu+DMSO (n=12, 5 litters), Eu+ CX+4945 (n=7, 4 litters), Ts+DMSO (n=9, 3 litters), Ts+CX-4945 (n=7, 3 litters).

3.3.2. Body weight throughout treatment

All male mice significantly increased their weight over the five days of treatment [main effect of day, F(4,124)=4.0, p=0.004]. However, trisomic mice had significantly lower body weights compared to euploid mice [main effect of genotype, F(1,31)=9.23, p=0.005] (Figure 8).

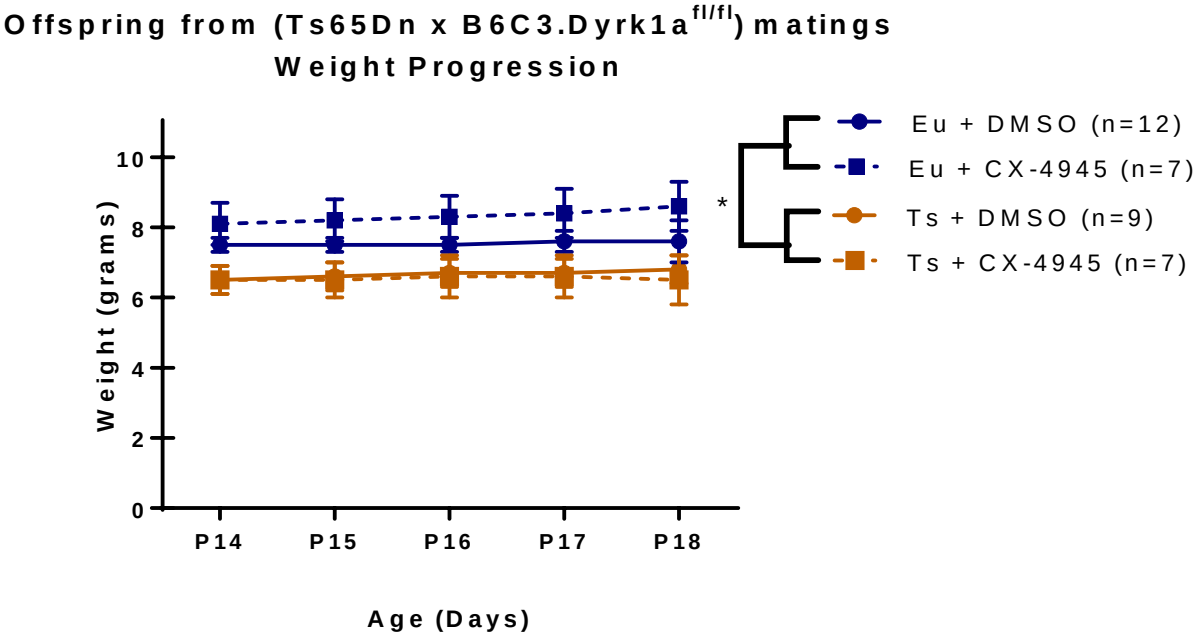

Figure 8. Body weight trajectory across P14-P18 in offspring from (Ts65Dn x B6C3.Dyrk1a$^{fl/fl}$) matings
All four treatment groups significantly increased their body weight over the course of five days of treatment, however, male trisomic mice had significantly smaller body weights compared to male euploids, as indicated by the (*). Data are represented as mean ± SEM.

3.3.3 Locomotor activity

There were no significant main or interactive effects of genotype or treatment on the total distance traveled in the locomotor task (Figure 9). The current study also had an *a priori* hypothesis that trisomic mice treated with CX-4945 would exhibit significantly improved locomotion compared to trisomic mice treated with DMSO. An independent samples t-test revealed no significant differences between these two groups [$t(14)= 1.299$, $p=0.215$, $d=0.66$]. With the current group sizes of 7 (Ts+CX-4945) and 9 (Ts+DMSO), a post hoc power analysis demonstrated that the experiment only had a 22% power to detect differences between the current group means. A power analysis was conducted (GraphPad StatMate) using effect sizes of the current experiment with power set at 0.50 and $\alpha=0.05$, two-tailed. In order for the Ts+CX-4945 and Ts+DMSO group differences to reach significance, the sample sizes would have to increase to 18 mice per treatment group. Therefore, the pattern of CX-4945 increasing trisomic locomotion activity could be due to an underpowered data set.

A Pearson's correlation was used to assess any relationship between body weight at the time of testing and total distance travelled. Collapsed across all groups, there were no significant correlations between these two variables. When run on each treatment group, only the Ts+DMSO group showed a significant positive correlation between body weight and total distance travelled ($r=0.784$, $r^2=0.614$, $n=9$, $p=0.012$).

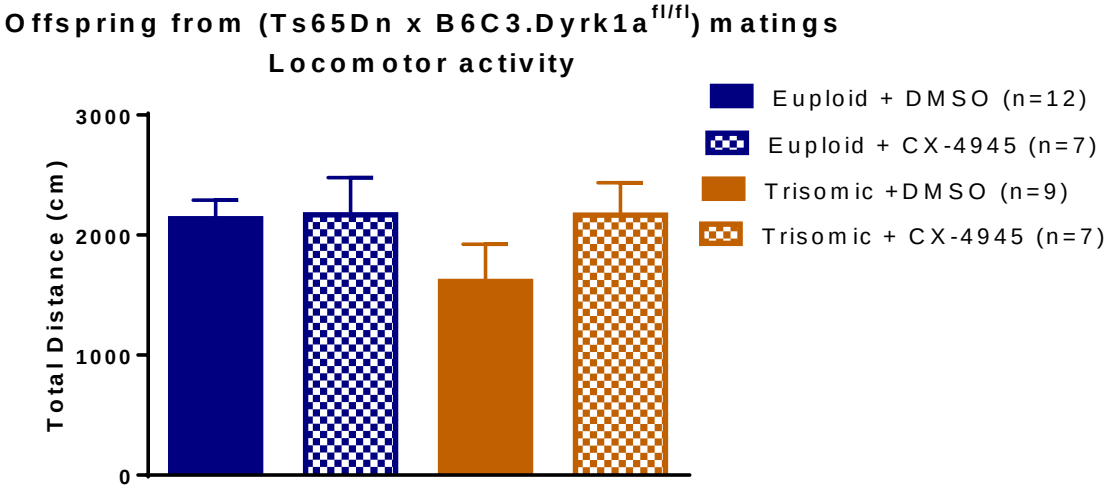

Figure 9. The total distance travelled in a 10 minute locomotor activity test in offspring from (Ts65Dn x B6C3.Dyrk1a$^{fl/fl}$) matings
There were no significant differences between the four treatment groups. Data are represented as mean ± SEM.

3.3.4 Homing task

3.3.4.1 Total time spent exploring

There were no significant main or interactive effects on the total time spent exploring both zones, although there was a strong trend towards euploid mice exhibiting significantly more exploration in trial 1 versus trisomic mice (p=0.058), as seen in Figure 10a. An independent t-test was used to test the *a priori* hypothesis that trisomic mice treated with CX-4945 would exhibit significantly improved homing task behavior compared to trisomic mice treated with DMSO. There were no significant differences in the total time spent exploring both zones in trial 1 between Ts+DMSO and Ts+CX-4945 mice [t(13)=0.816, *p*=0.429, *d*=0.42]. The current study had a power of 12% to detect a differences between the group means. A power analysis was conducted (GraphPad StatMate) using effect sizes of the current experiment with power set at 0.5 and α=0.05, two-tailed test. The current group sizes would need to increase to approximately 24 animals per

group in order to significantly detect this difference. There were no significant differences observed in trial 2. When the total time spent exploring was summed across trials (trial 1 total time spent exploring + trial 2 total time spent exploring) euploid mice showed higher levels of exploration compared to trisomic mice [main effect of genotype, $F(1,28)=4.2$, $p=0.048$], as seen in Figure 10b.

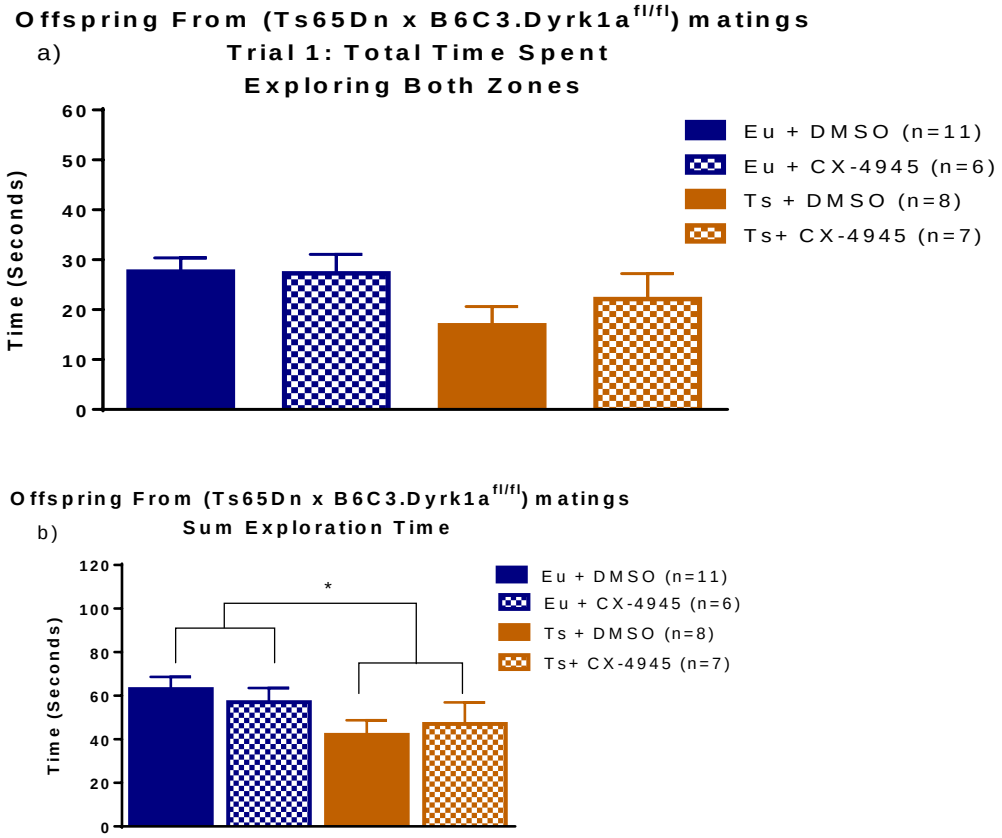

Figure 10. Total time spent exploring both zones and sum exploration time in offspring from (Ts65Dn x B6C3.Dyrk1a$^{fl/fl}$) matings

The total time spent exploring both zones across the four treatment groups during trial 1. In Figure 10a, there was a strong trend for euploid mice to spend more time exploring both the home cage and new cage bedding zone versus trisomic mice, although this did not reach significance ($p=0.058$). Figure 10b represents the total time spent exploring summed across both trials (trial 1 total exploration time + trial 2 total exploration time). When collapsed across trials, euploid mice spend significantly more time exploring than trisomic mice (as indicated by the *). Data are represented as mean ± SEM.

3.3.4.2 Total midline crossings

There were no significant differences between the groups on the number of midline crossings made in trial 1 or trial 2 (Table 5).

3.3.4.3 Total time spent exploring home zone

There was a trend for euploid mice to spend significantly more time in the home zone on trial 1 versus trisomic mice, however, this did not reach significance (p=0.08). An independent t-test was used to test the *a priori* hypothesis that trisomic mice treated with CX-4945 would exhibit significantly improved homing task behavior compared to trisomic mice treated with DMSO. There were no significant differences in the total time spent exploring the home zone in trial 1 between Ts+DMSO and Ts+CX-4945 mice [t(13)= 1.128, p=0.280, d=0.57]. The current experiment had a power of 18% to detect a differences between the group means.

A power analysis was conducted (GraphPad StatMate) using effect sizes of the current experiment with power set at 0.5 and α=0.05, two-tailed test. The current group sizes would need to increase to approximately 15 animals per group in order to detect significant differences between Ts+DMSO and Ts+CX-4945 in the time spent exploring the home zone on trial 1. There were no significant differences between euploid and trisomic mice in home zone exploration in trial 2.

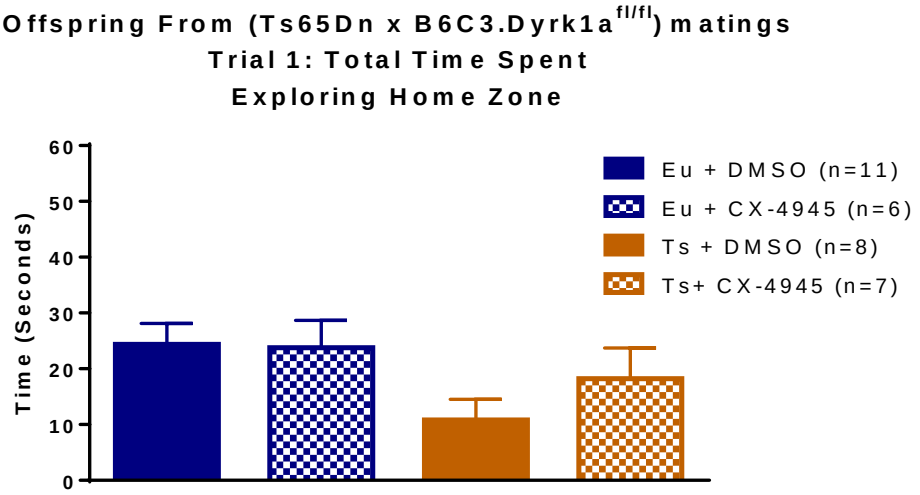

Figure 11. The total time spent exploring the home zone in trial 1 in offspring from (Ts65Dn x B6C3.Dyrk1a$^{fl/fl}$) matings
There was a trend towards euploid mice spending more time exploring the zone containing the home cage bedding versus trisomic mice, but this did not reach significance (p=0.08). An independent t-test testing an *a priori* hypothesis between the two trisomic treatment groups did not reveal any significant differences, despite a moderate effect size (*d*=0.57). The power of the group sizes in the current study (18%) is no sufficient to detect the current mean group differences. Data are represented as mean ± SEM.

3.3.4.4 Number of home zone visits

There were no significant main or interactive effects on the number of home zone visits in trial 1. However, there was a significant treatment x genotype interaction on trial 2 [F(1,28)= 6.6, p=0.015], with Ts+DMSO mice visiting the home zone significantly more than the Euploid + DMSO treatment group, as seen in Figure 12.

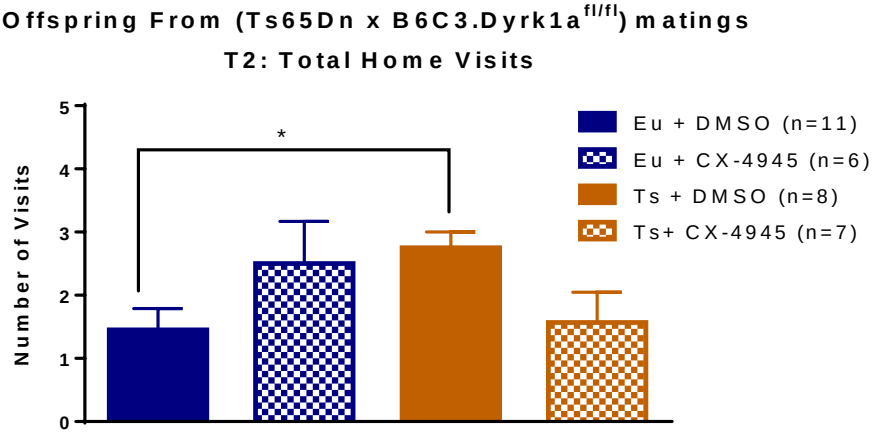

Figure 12. The total number of home visits on trial 2 in offspring from (Ts65Dn x B6C3.Dyrk1a$^{fl/fl}$) matings
The Ts+DMSO group had significantly more home zone visits than the Eu+DMSO group, as indicated by the (*). Data are represented as mean ± SEM.

3.3.4.5 Total time spent exploring new zone

There were no significant differences between groups on the total time spent exploring the new zone in trial 1. However, euploid mice spent significantly more time exploring the new zone versus trisomic mice on trial 2 [main effect of genotype, F(1,28)=8.6, *p*=0.007], as seen in Figure 13.

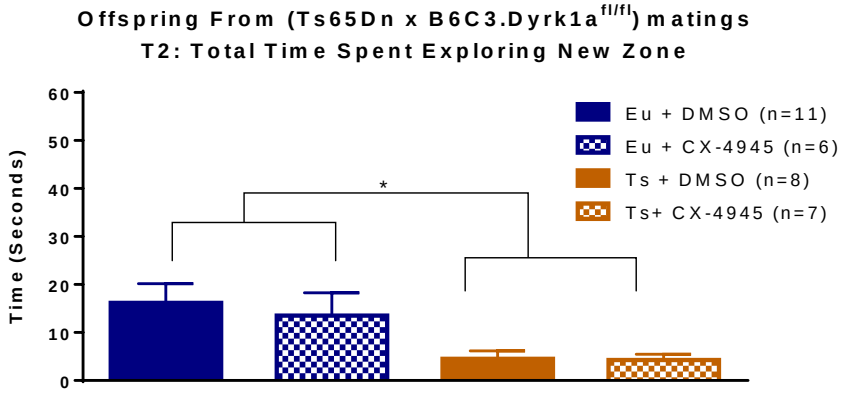

Figure 13. The total time spent exploring the new zone in trial 2 in offspring from (Ts65Dn x B6C3.Dyrk1a$^{fl/fl}$) matings
Data are represented as mean ± SEM. Both euploid groups spent significantly more time exploring the new zone versus the trisomic treatment groups, as indicated by the (*).

3.3.4.6 Number of new zone visits

There were no significant differences between groups in the number of new zone visits in trial 1 or trial 2 (Table 5).

3.3.4.7 Time taken to first explore home zone and new zone

There were no significant differences between groups on the time taken to first explore the home zone on trial 1 or trial 2. In addition, there were no significant differences between groups on the time taken to first explore the new zone on trial 1 or trial 2 (Table 5).

3.3.4.8 Home preference

A home preference score was calculated as: [total time spent exploring home zone/ total time spent exploring home zone + total time spent exploring new zone]. There were no significant differences between groups on home preference scores on trial 1 or trial 2 (Table 5).

Table 5. Non-significant homing task measures in offspring from (Ts65Dn x B6C3.Dyrk1a$^{fl/fl}$) matings

There were no significant differences between genotypes or treatments in several homing measures from either trial 1 or trial 2. Data are represented as mean ± SEM.

Trial	Homing Measure	Eu+DMSO (n=11)	Eu+ CX-4945 (n=6)	Ts+DMSO (n=8)	Ts+CX-4945 (n=7)
Trial 1	Total midline crossings	2.36 ± 0.50	1.67 ± 0.84	2.38 ± 0.65	2.86 ± 0.88
	Number of new zone visits	0.64 ± 0.24	1.17 ± 0.54	1.88 ± 0.44	0.86 ± 0.34
	Time taken to first explore home zone	19.73 ± 4.3	17.67 ± 4.21	36.88 ± 6.48	21.71 ± 5.96
	Time taken to first explore new zone	43.09 ± 6.8	36.50 ± 10.75	24.75 ± 9.46	32.29 ± 10.04
	Home exploration preference	92.2 ± 3.1	80.45 ± 11.58	84.36 ± 8.31	76.77 ± 9.76
Trial 2	Total midline crossings	2.73 ± 0.71	3.67 ± 1.14	5.00 ± 0.90	3.43 ± 0.84
	Number of new zone visits	2.55 ± 0.36	2.33 ± 0.84	1.75 ± 0.31	1.43 ± 0.36
	Time taken to first explore home zone	30.00 ± 5.94	26.67 ± 10.44	12.63 ± 2.31	21.00 ± 7.30
	Time taken to first explore new zone	9.45 ± 2.13	16.83 ± 8.77	17.50 ± 6.51	26.71 ± 9.07
	Home exploration preference	51.48 ± 9.95	59.43 ± 11.49	70.15 ± 10.72	73.00 ± 12.66

3.3.5 Immunohistochemistry

Euploid mice had significantly more BrdU-labeled cells counted throughout the dentate gyrus subventricular zone versus trisomic controls (Figure 14a) [main effect of genotype, $F(1,23)=5.2$, $p=0.032$]. Euploid mice also had a significantly larger dentate gyrus granule cell layer volume (Figure 14b) [$F(1,23)=14.04$, $p=0.001$]. However, CX-4945 treatment did not alter either of these effects.

There were no significant main or interactive effects on the total number of slices counted or cellular density (Table 6). Euploid mice treated with CX-4945 had significantly thicker slices [genotype x treatment interaction, $F(1,23)=6.1$, $p=0.021$]. This was likely due to random variation in vibratome slicing or differential shrinkage during the processing procedure. LSD post hoc

analysis showed that mice in the Eu+CX-4945 group had significantly thicker slices than the Eu+DMSO group (Table 6; p=0.021). The average slice thickness for the Eu+CX-4945 group was 20.1µ versus 19.6µ for the Eu+DMSO group, see Table 6. Group means for total volume of the dentate gyrus are also shown in Table 5. (Table 6).

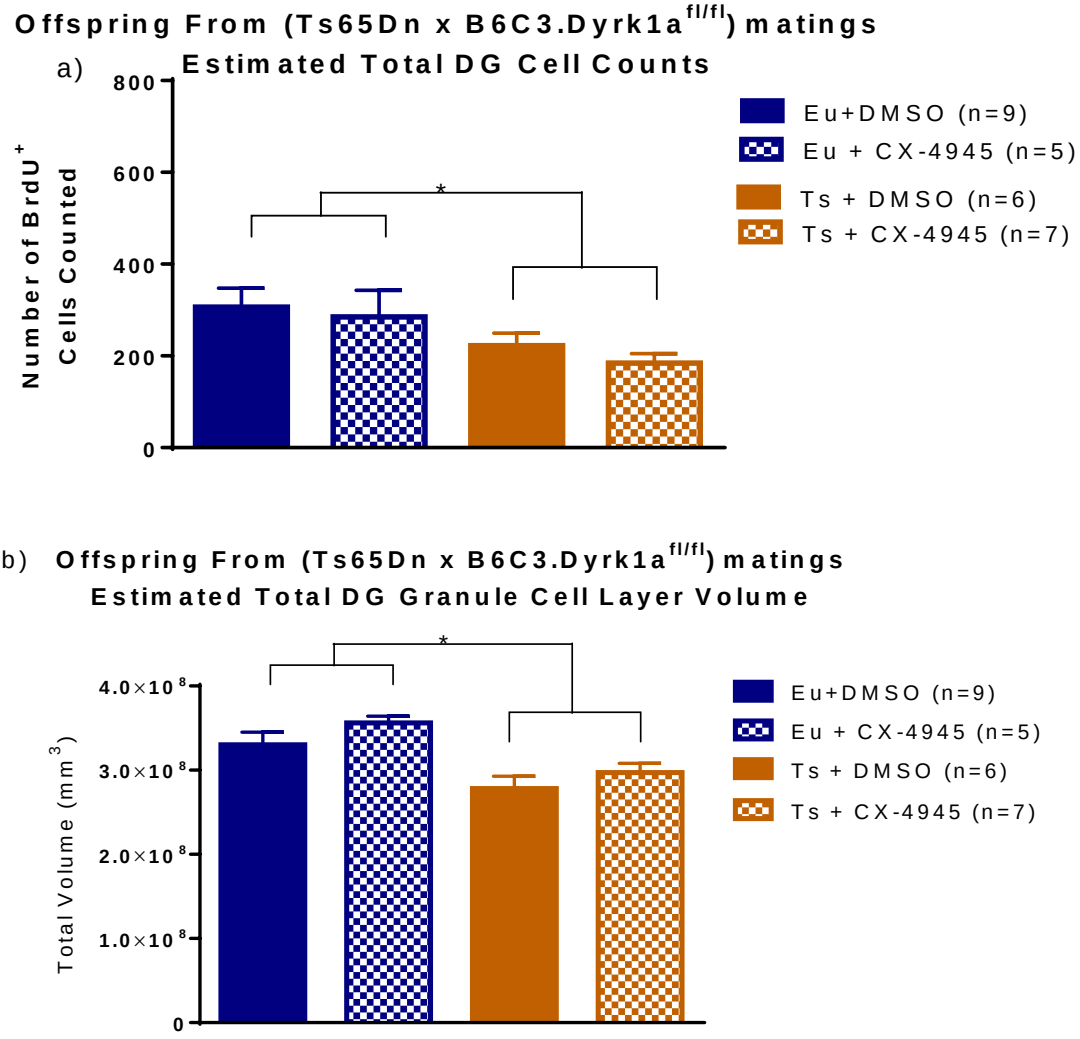

Figure 14. Total cell counts and granule cell layer volume in offspring from (Ts65Dn x B6C3.Dyrk1a$^{fl/fl}$) matings

Figure 14a depicts the total estimated number of BrdU^{+} labeled cells throughout the DG. Euploid mice had a higher number of estimated total cells counted than trisomic mice, as indicated by the (*), $p<0.05$. Figure 14b represents the estimated total DG granule cell layer volume, euploid mice had a significantly greater volume than trisomic mice, as indicated by the (*). Data are represented as mean ± SEM.

Table 6. Anatomical DG measures in offspring from (Ts65Dn x B6C3.Dyrk1a$^{fl/fl}$) matings

There were no differences between Euploid (Eu) and Trisomic (Ts) groups in the total number of slices examined or cell density. There was a significant difference in total cell counts, with Eu mice have higher cell counts than Ts mice, as well as in total dentate gyrus volume, with Eu mice displaying a significantly greater volume than trisomic mice.

Group	Slices	Thickness	Total Cell Counts (Q^-)	Estimated Total Cell Counts of DG [(Q^-)/(# of slices)] * 5	Estimated Total Volume of DG (mm^3)	Cell Density ($cells/mm^3$)
Eu+DMSO (n=9)	11 ± 0.37	19.6 ± 0.1	663.2 ± 90	306.3 ± 41.3	3.30^8 ± $0.15x10^8$	$10.0x10^{-6}$ ± $1.26x10^{-6}$
Eu+CX-4945 (n=5)	11.2 ± 0.4	20.1 ± 0.1	650.0 ± 136	285.1 ± 58.0	$3.56x10^8$ ± $0.08x10^8$	$9.1x10^{-6}$ ± $1.90x10^{-6}$
Ts+DMSO (n=6)	10.8 ± 0.3	19.9 ± 0.1	479 ± 60	222.1±27.6	$2.7x10^8$ ± $0.14x10^8$	$8.6x10^{-6}$ ± $0.99x10^{-6}$
Ts+CX-4945 (n=7)	11.6 ± 0.2	19.5 ± 0.1	424 ± 42	184.6±20.1	$2.9x10^8$ ± $0.11x10^8$	$7.0x10^{-6}$ ± $0.64x10^{-6}$

CHAPTER 4. DISCUSSION

4.1 Two significant considerations for data interpretation

There are two important findings that emerged from the current study that should be addressed. First, the background of trisomic mice should be carefully monitored. In the current study, trisomic mice from two slightly different backgrounds were used for two main reasons. The laboratory was currently generating Ts65Dn mice that carried a floxed allele of Dyrk1a for use in a future study (Ts65Dn.Dyrk1a$^{fl/+}$). These mice had very similar backgrounds to the traditional Ts65Dn mice that have been extensively used in our laboratory (Stringer et al., 2015; Stringer et al., 2017). Presumably, the only significant difference between Ts65Dn.Dyrk1a$^{fl/+}$ and Ts65Dn mice was the presence of a single floxed Dyrk1a allele. This floxed allele was not functionally active and it was assumed that the utilization of both breeding schemes would yield identical outcomes. A second reason for utilizing these mice is that Ts65Dn are difficult to breed (Roper et al., 2006) and it was hypothesized that the use of Ts65Dn.Dyrk1a$^{fl/+}$ mice would allow for an adequate production of mice. However, it became obvious near the end of SA2 that there were differences between the two breeding schemes.

As mentioned in the results, there was not enough statistical power to draw significant conclusions about any differences between the two different breeding schemes of mice. It was observed that (Ts65Dn x B6C3.Dyrk1a$^{fl/fl}$) F6-F8 matings generally resulted in larger litter sizes. However, there were no significant differences between the two breeding schemes in the size of the litters or the percent of trisomic mice produced within a litter. Both breeding schemes averaged ~50% trisomic mouse production within a given litter, which is higher than previously reported (Roper et al., 2006). The current study only analzyed 6 (Ts65Dn x B6C3F1) and 11 (Ts65Dn x

B6C3.Dyrk1a$^{fl/fl}$) litters, so additional litters will need to be assessed in order to determine if there are any significant differences in litter demographics (litter size, % of trisomic mice within a litter). The offspring from the (Ts65Dn x B6C3.Dyrk1a$^{fl/fl}$) F6-F8 matings also appeared to weigh significantly more than those from the (Ts65Dn x B6C3F1) matings, especially between Ts65Dn.Dyrk1a$^{fl/+}$ and Ts65Dn mice. There are a few factors that could be contributing to these apparent differences. First, there could be specific genes that are fixed in the Ts65Dn.Dyrk1a$^{fl/+}$and euploid.Dyrk1a$^{fl/+}$ mice. The B6C3.Dyrk1a$^{fl/fl}$ mice were used for mating after ~7-9 generations of inbreeding. At this stage, approximately ~70% of the genome is fixed and one piece of evidence supporting this is that B6C3.Dyrk1a$^{fl/fl}$ mice all had a black coat color whereas B6C3F1 mice have an agouti coat color (Silver, 1995). One possibility is that a gene involved in development or vitality could also be fixed, resulting in the trend towards significantly heavier mice. This could suggest that offspring from (Ts65Dn x B6C3F1.Dyrk1a$^{fl/fl}$) matings exhibit significantly higher hybrid vigor compared to offspring from (Ts65Dn x B6C3F1) matings. One of the main differences between the Ts65Dn.Dyrk1a$^{fl/+}$ and Ts65Dn mice is the presence of a floxed Dyrk1a allele. It is possible that the floxed allele could be "leaky", altering Dyrk1a expression even without Cre-recombinase. However, Ts65Dn.Dyrk1a$^{fl/+}$ mice exhibited significantly elevated Dyrk1a protein levels versus euploid.Dyrk1a$^{fl/+}$ mice, so this possibility is unlikely. Nevertheless, future studies should monitor the genetic background of trisomic mice in order to ensure consistencies within a laboratory and across the DS research field.

There was a lack of significant behavioral improvements after CX-4945 treatment from P14-P18. However, this could be due to the lack of power observed in the current study. After differences between the two breeding schemes of mice were observed, it was determined to solely analyze and report results on offspring from the (Ts65Dn x B6C3.Dyrk1a$^{fl/fl}$) matings. This was

the most appropriate approach as the elevation of Dyrk1a protein at P15 (which was the basis for the timing of the CX-4945 treatment) was composed solely of male mice from the (Ts65Dn x B6C3F1.Dyrk1a$^{fl/fl}$) matings. A consequence of this decision was a reduction in sample sizes, especially in both of the trisomic treatment groups. When analyzing the locomotor activity and homing test measures, there was no reported significant effects, but there appeared to be a pattern of improved phenotypes in trisomic mice treated with CX-4945. To probe this pattern further, the effect sizes were calculated and many of the behavioral outcomes that lack statistical significance showed modest effect sizes, ranging from 0.42 – 0.67. A subsequent power analysis on this data showed that the majority of the outcomes measured in the current study were significantly underpowered to detect the observable group differences. This was also seen in SA1, as there were strong trends towards trisomic mice exhibiting significantly elevated Dyrk1a protein levels across all three brain regions at P12 and P18. The following discussion section takes these findings into consideration while discussing the implications of the outcomes of the current study.

4.2 Peak elevations of Dyrk1a protein levels occur at P15 in Ts65Dn mice

This study was the first to systematically assess perinatal and adolescent levels of Dyrk1a protein in the cerebellum, cerebral cortex and hippocampus of Ts65Dn male mice. Ts65Dn mice displayed significant elevated levels of Dyrk1a protein with a large effect size at P15 in the cerebellum, cerebral cortex and hippocampus, with non-significant trends towards elevation on P12($p=0.08$) and P18 ($p=0.058$). These non-significant trends showed strong effect sizes (see Table 4), which could mean that Dyrk1a is in fact elevated in trisomic mice at these ages, however, the current study was underpowered and was unable to detect a significant elevation. Though Dyrk1a tended to be higher in trisomic mice compared to euploid controls, the effects were largest at P15 and never reached significance at the other ages (P24, P30, P42).

Currently, there is only one other study that has examined Dyrk1a protein levels in the Ts65Dn mouse between E11.5 and 6 weeks of age. Yin et al. examined Dyrk1a protein levels in the forebrain at P5, P10, P15, P20, P25, P30 and P35 in Ts65Dn mice (sex not specified) (Yin et al., 2017). They reported that trisomic mice had significantly elevated levels of Dyrk1a protein at all seven ages. However, there are several differences between the current study and Yin et al. (Yin et al., 2017).

First, the current study assessed Dyrk1a protein levels in the cerebellum, cerebral cortex and hippocampus, whereas the Yin et al. examined Dyrk1a protein levels in the forebrain (unknown whether the entire forebrain was extracted). Differences in Dyrk1a protein levels between these brain regions is not surprising, considering the growing evidence that the regulation and expression of Dyrk1a protein is likely temporally and spatially tissue specific. The current study also utilized a different quantification method for Dyrk1a protein, using total protein staining as a loading control. In contrast, Yin et al. used the traditionally used housekeeping protein actin as a loading control. Recent evidence suggests that total protein may be a superior control, as β-actin levels can be affected by neurological diseases and alterations in cellular processes (Eaton et al., 2013; Aldridge et al., 2008). Alterations in β-actin levels in Ts65Dn mice have not been published, but differences in β-actin levels across brain regions has been observed in our laboratory. Yin et al. did not report on any differences in β-actin levels, but their small group sizes (3-5) may be insignificant to detect differences. Interestingly, they did report that Dyrk1a protein levels did decrease with age in both the euploid and trisomic mice, but it is unknown whether β-actin levels changed as well. In addition, it is unknown if males and/or females were used for Western blot analysis, as sexual dimorphisms may impact Dyrk1a protein levels (Yin et al., 2017). Stringer et al. (2017) reported that P42 Ts65Dn mice exhibited significantly lower levels of Dyrk1a

in the cerebellum versus euploid controls, but found no differences in Dyrk1a protein levels in the cerebral cortex or hippocampus. In contrast, the majority of studies examining adult Ts65Dn mice (>3.5 months of age) have reported significant elevations in Dyrk1a protein levels (Stringer et al., 2017). However, many of these studies either examined the entire brain (brain homogenate) or examined a single brain region. It is crucial that future studies try and determine Dyrk1a protein levels across multiple brain regions, as this will be a necessary step towards understanding the expression landscape of Dyrk1a in Ts65Dn mice.

4.2 What is known about Dyrk1a expression and its connection to brain deficits?

Dyrk1a expression studies conducted in normally developing mice could help hypothesize which tissues to target and analyze for expression in Ts65Dn mice. *Dyrk1a* expression is observed at E8 in the telencephalon and prospective spinal cord, then gradually migrates caudo-laterally (E8.5-9.5) and dorso-medially (E10). This direction of expression follows the typical neurogenesis path, supporting its role in this process (Hämmerle et al., 2008). *Dyrk1a* was observed outside of these developing nervous tissues, such as in migrating neural crest cells and the branchial arch. E11, E17 and adult mice displayed *Mnb/Dyrk1a* expression in the olfactory bulb, cerebellum, cortex, piriform cortex, hippocampus, hypothalamus, spinal cord and retina (Guimerâ et al., 1996; Song et al., 1996; Rahmani et al., 1998). This pattern of expression in multiple CNS regions parallels the influential role of *Dyrk1a* in several developmental processes (Duchon et al., 2016).

At the protein level, Dyrk1a is expressed at several embryonic stages (E14.5, E16.5) throughout the cortical layers, including co-localizing with TUJ1 (Neuron-specific Class III β-tubulin) and NeuN (neuronal specific nuclear protein) in forebrain neurons, and is observed in the nucleus of cells from the ventricular zone in ICR mice (Hämmerle et al., 2008). At P5, Dyrk1a is localized in the Purkinje cell nucleus in cerebellar cells, and a high co-localization with MAP2 and

Dynamin 1 (microtubule-associated proteins) at P8 was observed (Hämmerle et al., 2008). At P14, significant Dyrk1a expression was detected in the external granular, molecular layer and internal granule cell layer of the cerebral cortex (mouse model unknown) (Martí et al., 2003). In adult ICR mice, Dyrk1a protein was localized in the soma and dendrites, as well as the nucleus of cerebral cortex pyramidal neurons (Hämmerle et al., 2008). A fractionation-based Western blot on frontal cortex tissue extracted from adult and aged Ts65Dn mice revealed that Dyrk1a was primarily located in the cytoskeleton. This cytoskeleton fraction also contained synaptic proteins (synapsin 1), suggesting that Dyrk1a could primarily localized in cytoskeleton within a synapse. Dyrk1a was also observed in the nucleus and cytosol (Kaczmarski et al., 2014). In contrast, Dyrk1a was primarily localized within the nucleus of DG granule cells of adult ICR mice (Hämmerle et al., 2008). The high level of Dyrk1a expression throughout these brain regions suggest that its overexpression influences phenotypes associated with those regions.

In the current study, strong trends for trisomic mice exhibiting elevated Dyrk1a protein levels at P12 (p=0.08) and P18 (p=0.058) were observed, suggesting that Dyrk1a is highly expressed during Ts65Dn perinatal development. Dyrk1a expression studies have not been extensively conducted in Ts65Dn mice, but Ts65Dn mice do exhibit deficient phenotypes in these brain regions during neonatal and perinatal ages. For example, Ts65Dn mice exhibit deficits in embryonic corticogenesis such as decreases in neocortical layer thickness, reductions in cellular density, and a slower cell cycle in neocortical progenitors (Chakrabarti et al., 2007). At postnatal ages, P22 Ts65Dn mice exhibit dendritic and synaptic abnormalities in the hippocampus (Belichenko et al., 2004). Ts65Dn mice exhibit deficits in perinatal hippocampal neurogenesis including a reduction in BrdU-labeled DG cell proliferation, cell survival, the number of DG granule cells and the number of neural precursors (Bianchi et al., 2010; Stagni et al., 2016).

Decreased cell proliferation is also seen in fetuses (~17-20 week) with DS (Contestabile et al., 2007). In the cerebellum, Ts65Dn mice exhibit numerous structural deficits including a smaller cerebellar volume and a reduction in granule cell number (Baxter et al., 2000; Roper et al., 2006). At P14, Ts65Dn mice exhibit a significant reduction in internal granular layer (IGL) thickness, which could be attributed to the reduction in granule cell precursor (GCP) mitosis observed beginning at P0 (Roper et al., 2006). Many of these histological deficits are thought to be the cause of cell cycle dysfunction, to which Dyrk1a overexpression has been strongly linked. For example, an overexpression of Dyrk1a (observed in the current study) is hypothesized to cause cell cycle dysregulation in mouse models of DS (Haydar et al., 2012). Of particular interest is the G_1/S phase, a crucial time when cells will either leave the cell cycle in order to differentiate, or pass through the G_1 checkpoint and commit to entering the cell cycle to undergo another round of cell division (Ohnuma et al., 2003). Studies using neural cell lines have demonstrated that expression of MNB/DYRK1A or Dyrk1a induces neuronal differentiation (Yang et al., 2001; Kelly et al., 2005); however, its stable overexpression appears to impair normal neuronal differentiation (Park et al., 2007). Thus, the transient expression of Dyrk1a could promote cell cycle exit, and its subsequent down regulation allows cells to undergo neuronal differentiation (Hämmerle et al., 2008; Tejedor and Hämmerle, 2011). This mechanism of action could be attributed to the ability of Dyrk1a to phosphorylate and possibly regulate two major cell cycle proteins; Cyclin D1 and p27 (Najas et al., 2015; Tejedor and Hämmerle, 2011). Cyclin D1 promotes G_1-to-S phase transition and is required for cell proliferation. The protein p27 is crucial for neuronal differentiation, and promotes cell cycle exit (Hindley et al., 2012; Frank et al., 2009). The regulation of these two key cell cycle components is necessary for an appropriate “speed” at which

the cell cycle phases occur, resulting in a balance between the number of progenitor cells and the production of differentiated neurons (Salomoni et al., 2010).

Overexpression of DYRK1A/Dyrk1a both *in vivo* and *in vitro* results in the nuclear export of Cyclin D1, resulting in reductions in Cyclin D1 protein levels at multiple developmental ages in TgDyrk1a mice (E11.5 & E14.5) (Yabut et al., 2010; Park et al., 2010; Soppa et al., 2014; Najas et al., 2015). In addition, DYRK1A/Dyrk1a overexpression results in more cells in the G_1/0 phase versus S or G_2/M phase, resulting in a cell proliferation deficits, premature cell exit and differentiation, and the nuclear export of Cyclin D1 (Soppa et al., 2014; Najas et al., 2015). In Ts65Dn, E11.5, embryos contain 1.5 fold more Dyrk1a protein, and display significant decreases in Cyclin D1 levels. Normalization of Dyrk1a copy number restored levels of Cyclin D1, the number of intermediate progenitors, as well as the production of neurons at multiple developmental time points (Najas et al., 2015).

Although the deficits in cortical, hippocampal and cerebellar formation in Ts65Dn mice are well established, a connection between these deficits and an observable behavioral phenotype at a specific age is not well understood. The current study discovered that Dyrk1a protein is significantly elevated at P15, which could be directly affecting the observed hippocampal neurogenesis deficit via hyperphoshporylation of cell cycle proteins (i.e. Cyclin D1). However, future studies will need to determine in what cell types (i.e. pyramidal cells, neurons, Purkinje cells) and where Dyrk1a localizes (nucleus, cytosol) in order to pursue hypotheses concerning which specific substrates and intracellular processes Dyrk1a could be regulating. Dyrk1a phosphorylation regulates substrates located in both the nucleus and cytosol, and this regulation is likely to be tissue and time-specific (Martí et al., 2003; Kaczmarski et al., 2014; de Graaf et al., 2004; Woods et al., 2001; Arron et al., 2006; Chen-Hwang et al., 2002). While Dyrk1a may be

mediating proliferation deficits through Cyclin D1 phosphorylation during embryonic ages, this has not yet been established for perinatal Ts65Dn mice. Assessing protein levels in a brain region is a fundamental first step towards understanding the influence of Dyrk1a on phenotypes. To strengthen the current study's findings, research should look to analyze Dyrk1a expression on a cellular level in order to develop a comprehensive understanding of Dyrk1a expression in a specific brain region at a specific age.

4.3 Behavioral and histological phenotypes in perinatal euploid and Ts65Dn mice

4.3.1 Locomotor activity

There were no significant differences in locomotor activity between euploid and trisomic mice, although trisomic mice did exhibit a non-significant trend towards hypoactive behavior. In addition, the administration of CX-4945 alter locomotion in any of the treatment groups. As previously mentioned, there was a moderate effect size observed (d=0.66) despite the non-significant p value. A power analysis revealed that the current sample sizes were too low to detect the group differences of the effect size indicated by the current data. The group sizes would need to increase to 11 mice per group in order to detect these differences. Therefore, while the improvements in locomotion in mice treated with CX-4945 did not reach statistical significance, the moderate effect sizes and low group numbers warrant a further investigation of the effects of CX-4945 on locomotion.

Trisomic mice who weighed below 5.4 grams at the time of locomotor testing had severe deficits in locomotor activity, as many exhibited a complete lack of movement during the trial. Trisomic mice who weighed over 5.4 grams still exhibited hypo-locomotion as compared to euploid mice. Thus, weighing under 5.4 grams could be below a threshold stage of developmental maturation needed for to attain ambulatory activity typical for normally developing euploid mice

in this specific task. With weight significantly influencing locomotor performance in the trisomic mice, this raises the possibility that the age at which the mice were tested or the type of task used here may not be appropriate to evaluate locomotor activity in perinatal Ts65Dn mice. For example, Ts65Dn exhibit hyperactive behavior at P21 but the mice tested in the current study were younger (P16 or P17). The developmental delays in the younger Ts65Dn mice may be more pronounced than at P21, which could explain the deficits in locomotion that were observed. The apparatus used to measure locomotor activity at P21 in Ts65Dn mice was smaller than the chamber used here, and there was a "stimulus" object placed in the center of the apparatus (Holtzman et al., 1996). The smaller apparatus, combined with an object in the activity space might be a more motivating environment for the trisomic mice to explore. The lack of trisomic locomotion in the current study appears to be task-dependent, as there were no differences between the euploid and trisomic groups in the number of midline crossings in the homing task. In addition, the experimenter observed smaller mice that were placed in the chamber to move towards a corner and remain stationary throughout the task. Future studies should take into careful consideration the developmental maturity (correlated with weight) of the animals being tested, and adjust the activity chamber settings as needed.

This perinatal phenotype is especially interesting considering that at older ages, while trisomic mice still weigh less than euploid controls (Roper et al., 2006), they generally display a hyperactive phenotype (Stringer et al., 2015; Reeves et al., 1995) However, this phenotype is variable depending on the age at which mice were tested (Martínez-Cué et al., 2002), whether an open field task or 24-hour home cage locomotion was utilized (Rueda et al., 2008; Stewart et al., 2007), as well as the length and lighting conditions of the task (Coussons-Read et al., 1996; Escorihuela et al., 1995; Llorens-Martin et al., 2010; Sago et al., 2000). These varying outcomes

highlight the method-dependent variability of activity phenotypes observed in Ts65Dn mice, and suggest that factors, such as the age of the mice and the length of the activity test, should be taken into consideration by future studies. Linking locomotor defects to a specific gene, such as *Dyrk1a*, has been difficult for the DS research field. Transgenic mice overexpressing *Dyrk1a* have also yielded contrasting findings for hyperactive behavior (Branchi et al., 2004; Ortiz-Abalia et al., 2008). When *Dyrk1a* is normalized via the delivery of a short hairpin RNA (shRNA) to the striatum, hyperactive behavior was normalized in 2-3 month old TgDyrk1a mice (Ortiz-Abalia et al., 2008). However, when *Dyrk1a* expression was normalized from conception, Ts65Dn mice still exhibited a hyperactive phenotype in the open field task at approximately 5-6 months of age (García-Cerro et al., 2014). Thus, there are likely multiple genetic influences on the activity phenotype that are both spatially and temporally dependent.

4.3.2 Homing task

The modified homing task used here showed that euploid mice spent more time exploring both zones across the two trials, indicative of an exploration deficit in trisomic mice. In addition, euploid mice spent significantly more time exploring the new zone on trial 2. There were no significant differences in the number of midline crossings, suggesting that the exploration deficit observed in trisomic mice was not due to motor deficits. Similar to the locomotor task, the administration of CX-4945 did not significantly alter any of the homing task measures in either the euploid or trisomic groups. Although the outcomes did not reach statistical significance, moderate effect sizes were still observed (0.42-0.57) and many of the homing measures were underpowered, ($1-\beta = 0.12-0.18$) limiting the ability to detect the observable group differences. Additional mice in each treatment group will need to be added in order to more conclusively state the effect of CX-4945 on homing task behavior.

The homing task as used in this study may be best considered an assessment of pre-weaning exploratory behavior, in addition to utilizing olfaction, as eye opening had already occurred in all mice at the time of testing. The utilization of a second trial in the current homing task methodology was to determine if mice had a persistent preference for the zone containing the home cage bedding, regardless of which zone (zone 1 or zone 2) it was located in. The switching of the stimuli location from trial 1 to trial 2 controlled for any spatial preference that may have been present from trial 1. The starting location of the two types of bedding was counterbalanced across animals, however it is difficult to ensure balanced starting locations of each bedding when also blind to genotypes. Thus, future studies should take this into consideration in order to optimize this task and reduce any unnecessary biases.

To date, there are only a few studies assessing homing behavior in Ts65Dn and other mouse models of DS. These studies all used the same homing task methodology by placing home cage bedding across 1/3 of a new, empty cage. The mice were placed up against the wall (opposite the home cage bedding) and the time to enter the home cage bedding was recorded. Ts65Dn mice are significantly slower to reach home cage bedding than euploid controls at P12 (Holtzman et al., 1996), with similar deficits reported at P14 in a transgenic *Dyrk1a* mouse model (Altafaj et al., 2001) and at P12 in the Ts1Cje mouse model of DS (Guedj et al., 2015). In these studies, olfaction significantly contributed to performance, as the homing task was administered before eye opening. *Dyrk1a* expression in the olfactory bulb in young mouse models of DS is not known, but it is highly expressed in adult mice (strain unknown). If this patterning is similar in young mouse models of DS, conducting the homing task so that it relies on olfaction may be a step towards linking *Dyrk1a* to an olfactory-based homing task deficit.

4.3.3 Cell proliferation

This study found that at P18, euploid mice had significantly more BrdU-labeled cells and a greater DG granule cell layer volume compared to trisomic mice. However, CX-4945 did not significantly alter the number of BrdU+ cells in either group, indicating it did not change proliferation of neuroprogenitor cells in the DG. In addition, there were no significant differences between groups in the number of slices counted or cell density. However, the current study only had 11% power to detect the current group differences. In accordance with a *a priori* hypothesis, an independent t-test between Eu+DMSO and Ts+DMSO groups on cell density revealed no significant differences, but a moderate effect size [$t(13)= 0.768$, $p=0.456$, $d=0.41$]. Consistent with our findings, 18-day-old Ts65Dn mice are reported to have deficits in proliferating BrdU+ labeled cells in the DG, although this study did not report any cell density or volume measures (Contestabile et al., 2007). Another study examined Ts65Dn mice at P15 and found that trisomic mice exhibited reduced proliferation as indicated by a reduced number of BrdU+ cells in the DG, as well as reduced granule cell layer volume and granule cell density (Bianchi et al., 2010). That study agrees with our finding of a cell proliferation DG granule cell layer volume deficit at P18, however, differences in granule cell density did not reach significance in our study.. When comparing across these three studies, the methods were very similar, with mice given a BrdU injection (100-150mg/kg) and sacrificed 2 hours later. The other two studies did have fewer animals per group (3-6 versus 7-9 for the current study) but the high methodological similarities between these three studies confirms a strong cell proliferation deficit in Ts65Dn mice between P15 and P18. A deficit in cell proliferation could lead to a significant decrease in the number of new neurons in the DG, which has been strongly linked to learning in animal models (Leuner et

al., 2006). Thus, the proliferation deficit observed in Ts65Dn mice could significantly contribute to the learning and memory deficits that are also observed in these mice.

4.4 What are the best behavioral tasks to use in perinatal euploid and Ts65Dn mice?

With a push for therapeutics to occur earlier in Ts65Dn development, it is important to establish a consistent battery of behavioral and developmental assessments to determine the safety and efficacy of potential therapeutics (Guedj et al., 2014; Stagni et al., 2015). Neonatal and perinatal developmental milestones are typically observed P0 and P18, and ideally are measured over multiple days (Hill et al., 2008; Fox, 1965). The ability of the homing task to be modified to assess general locomotor activity and exploratory behavior in a single trial/day is a powerful tool for assessing perinatal behavior. Since there are few developmental milestones that have not been reached by P18, the homing task could serve as a useful assessment during that specific developmental period. The locomotor test used here may not be sensitive to detect locomotor deficits in Ts65Dn mice. Ts65Dn mice exhibit hyperactive behavior starting at P21, but it is possible that at earlier ages the mice are hypoactive due to developmental delay. If this is true, the testing conditions used here (large chambers; 10-minute sessions; room temperature) may have suppressed activity in the Ts65Dn mice, considering that their significantly lower body weight likely correlates with general developmental delay relative to euploid controls. Alternate locomotor testing (i.e. smaller box, shorter test, warmer environment) may help determine if this hypoactive phenotype is persistent across different behavioral paradigms. Reduced DG cell proliferation and granule cell neurogenesis is a consistently reported phenotype in perinatal Ts65Dn mice. Linking this cellular deficit to a specific cognitive or behavioral phenotype is a challenge. Many studies that administer perinatal treatments in DS mouse models either look at histological phenotypes immediately after the cessation of treatment, such as cell proliferation in

the DG, or the mice are allowed to age and phenotypes during adolescence and early adulthood are assessed (Bianchi et al., 2010; Stagni et al., 2016; Roper et al., 2006; Stagni et al., 2013). One example of this was the administration of 50mg/kg/day [0.4mg/mL] of EGCG to Ts65Dn mice starting at P22-P97 (Stringer, *unpublished results*). Starting on P75, the mice were trained on a pattern separation radial arm maze, which is thought to rely on the function of newly generated granule cells in the DG. The mice received treatment throughout the testing, and cell proliferation in the DG was assessed on P97. While EGCG treatment did not significantly improve Ts65Dn performance on the task or DG cell proliferation, the study adds to the growing number of studies administering therapeutics to perinatal/young adolescent Ts65Dn mice. As previously mentioned, the behavioral phenotypes of Ts65Dn mice from P14- weaning are not as well established as neonatal or adolescent/adult phenotypes. If perinatal age is a therapeutic target, additional studies will be needed to establish the trajectory of various cognitive and behavioral phenotypes during this time.

Many of the behavioral outcomes reported here were underpowered, despite moderate effect sizes. It will be important for future studies to use fully-powered designs and select behavioral tasks and measurable outcomes that are sensitive to CX-4945 treatment. For example, the current utilization of the locomotor chambers may be too aversive of an environment to detect differences in perinatal euploid and trisomic mice. Despite this, there was still strong effect sizes observed between Ts+DMSO and Ts+CX-4945 groups. If adequate numbers of subjects were included or a more sensitive locomotion task was used (smaller apparatus, stimulus object), the effect of CX-4945 on this behavior may be more conclusive.

4.5 Lack of phenotypic improvements with 75mg/kg CX-4945 from P14-P18 in Ts65Dn mice

A single injection of 75mg/kg/day of CX-4945 was used in the current study and there was a lack of statistically significant improvements across multiple phenotypes. It is reiterated, however, that moderate effect sizes were observed and a pattern of improved locomotor behavior and homing task performance was observed in the Ts+CX-4945 treatment group. In addition to evaluating the potential effect of CX-4945 treatment parameters on the reported outcomes, the possibility of underpowered group sizes could also be driving the lack of phenotypic improvement.

The current study's dose of 75mg/kg/day was largely based on a recent study that administered 75mg/kg to transgenic *Dyrk1a* mice via oral gavage (Kim et al., 2016). That study reported that 30 minutes after a single dose of CX-4945, transgenic *Dyrk1a* mice had a significant reduction in phosphorylated tau levels in the hippocampus versus transgenic *Dyrk1a* mice given DMSO (Kim et al., 2016). With this evidence, 75mg/kg a day was chosen as a starting dose for perinatal Ts65Dn mice. While the previously mentioned study used oral gavage, this would be difficult to administer and stressful to pre-weaning animals, so it was decided that a SC injection would be a less aversive option for route of administration. The significant effects observed with 75mg/kg in adult mice suggested that this dose would be sufficient to observe significant improvements in perinatal mouse phenotypes. Studies using CX-4945 commonly administered CX-4945 twice a day, however, disturbing the pre-weaning animals twice a day could be a significant stressor. One possibility is that the current dose of CX-4945 is too high. No adverse phenotypes were observed in euploid mice (2 copies of Dyrk1a) receiving CX-4945. If CX-4945 was inhibiting Dyrk1a below a normal threshold level, we might see negative outcomes in the euploid mice.

Another possibility is that 75mg/kg a day is not a high enough dose. Studies have used significantly higher doses in mouse models of cancer, but there are several factors to consider. First, different routes of administration (ROA) of the same CX-4945 dose could produce different outcomes. The breakdown and metabolism of CX-4945 is not known and depending on the solvent used to mix CX-4945 (current study used DMSO), there may be variations in its pharmacokinetic properties. It will be important for future studies to assess if there is an optimal ROA for CX-4945 treatment. In addition, DMSO was used to suspend CX-4945 in solution (25mM CX-4945 dissolved with 90% PBS and 10% DMSO). This equated to a 10g mouse receiving ~10µL of DMSO, or ~1µl/g dose of DMSO. DMSO is commonly used as solvent for water-insoluble compounds (Santos et al., 2003; Broadwell et al., 1982). However, adverse side effects after *in vivo* administration of DMSO have been reported. For example, Swiss albino mice (~20-30 grams) given an IP injection of DMSO solutions greater than 25% exhibited significantly altered mortality rates (Worthley et al., 1969). An IP injection of 1µL/g or 0.5µL/g [90% Saline & 10% DMSO or 95% saline & 5% DMSO] to 6-8 week old CD-1 mice did not alter rotarod performance. However, adverse side effects have been reported at 1µL/g and lower doses. Eight hours after a single 0.3µL/g dose in P7 mice, there was a significant increase in the rate of apoptosis throughout the cerebrum (Hanslick et al., 2009). This dose of DMSO is approximately half of what the mice in the current study received. The study also reported significant increases in apoptosis in P7 mice after single doses of 1.25, 3 and 10µL/g. In addition to P7 mice, P17 mice were also treated with a single 10µL/g DMSO injection, where significant white matter degeneration and high levels of cell apoptosis in the DG were observed. There were no other doses examined in the P17 animals, and while a 10µL/g injection DMSO is significantly more than the current study administered, the adverse apoptotic findings at P7 with 0.3µL/g DMSO suggest that there could be adverse cellular

effects with the administration of 1µL/g DMSO (Hanslick et al., 2009). Differences in neurogenesis between animals receiving a daily saline or DMSO IP injection (0.3µL/g) from P16-P28 have been reported, although these two groups were not statistically compared (George et al., 2013).

If the current study doubled the dose (maintaining a 25mM concentration) to 150mg/kg, a 10g mouse would receive ~17 µL of DMSO. Not only would this be a significant volume amount to inject (~170µL), but this amount of DMSO has produced aversive side effects (Hanslick et al., 2009). It may be necessary to administer twice daily injections of CX, however, the amount of DMSO that a mouse would receive over the course of the day would remain the same as a single injection of the same dose. It is important to note that the majority of studies injecting treatments in neonatal or perinatal mouse models of DS use saline as a vehicle for the drug (Bianchi et al., 2010; Stagni et al., 2016). Thus, the use of DMSO as a CX-4945 vehicle in the current study makes it difficult to ascertain if the dose itself or the presence of DMSO led to null results. However, publications on Dyrk1a inhibitors administered to mouse models of DS, ALGERNON (unknown amount of DMSO), L41 (10% DMSO) and F-DANDY (unknown amount of DMSO), also used DMSO as a solvent (Nakano-Kobayashi et al., 2017; Naert et al., 2015). Thus, alternate solvents to dissolve CX-4945 in should be explored, such as polyethylene glycol, or NaH_2PO_4 buffer. Future studies administering CX-4945 (or any Dyrk1a inhibitor dissolved in DMSO) could be strengthened by assessing any independent effects of DMSO on behavioral and cognitive effects by including a vehicle (i.e. saline) control.

4.6 Limitations

There are several limitations that future studies should be taken into consideration, such as potential stress effects of a treatment injection. Stressful experiences during development and

throughout the lifespan can significantly alter the production of granule cells in the hippocampus (Gould et al., 1999). For example, a single exposure of rat pups to a predator odor significantly decreased the production of granule cells in the DG 24 hours later (Tanapat et al., 1998). Neonatal and adolescent stress in mice can alter the expression of genes involved in stress responses and impair performance on neurobehavioral tests (Juul et al., 2011; Yohn et al., 2017). The current study did not include a non-injected control group, so it is unknown whether the stress of the injections themselves altered any of the observed phenotypes. However, injections have been reported to cause a stress response in mice, so it will be important to establish any effects of injection stress in pre-weaning mice (Wokke, 2017; Meijer et al., 2006). One approach could be to first analyze the phenotypes of non-injected euploid and trisomic mice. If there are significant differences, this would establish the baseline phenotypes for each group, without any injection or treatment confounds.

One of the biggest obstacles in the field is the lack of a Dyrk1a-specific kinase activity assay. HPLC- and radioactive-based assays have been used in multiple studies to try and determine Dyrk1a kinase activity (Stringer et al., 2017; Stringer et al., 2015; Papadopoulos, 2011). However, these methods report high variability within the assay, and the independent contribution of Dyrk1a activity cannot be accurately quantified. Thus, these methods are more representative of general kinase activity within a given tissue. While a more reliable Dyrk1a kinase activity assay is being developed, measuring the levels of known Dyrk1a substrates in order to obtain a semi-quantitative measure of Dyrk1a inhibition after treatment may be necessary. For example, an elevation in Dyrk1a protein and a significant decrease in Cyclin D1 protein was observed in E11.5 Ts65Dn embryos, prompting a further investigation to elucidate the mechanism of Dyrk1a-mediate Cyclin D1 phosphorylation. This relationship may not be present at all ages in Ts65Dn mice, therefore,

it will be important for future studies to assess the spatial and temporal specificity of specific Dyrk1a substrates in relation to Dyrk1a expression.

If the focus is on targeting and inhibiting Dyrk1a, a more effective approach could be to target Dyrk1a at the onset of its overexpression and through its period of greatest overexpression for stronger conclusions to be drawn between the therapeutic administration and the measured phenotype. Studies taking this approach would have to consider the translation of prenatal development between mice and humans. Brain development in a P15 mouse is approximately equivalent to the a human newborn (Clancy et al., 2001). Screening for DS in humans can occur as early as ~10-12 weeks of gestation by examining cell free DNA (cFDNA) (Norton et al., 2015). This gestational age translates to approximately E14-E15 in mice (Clancy et al., 2001; Clancy et al., 2007). Although elevations in Dyrk1a protein levels have been detected at E11.5 in Ts65Dn embryos (Najas et al., 2015), E14-E15 may represent the earliest age at which therapeutics administered in mice could transition to a clinical setting.

4.7 Conclusions

The current study was the first to administer CX-4945 to Ts65Dn with the goal of improving phenotypes via Dyrk1a inhibition. However, there are still several considerations regarding the efficacy of this therapeutic in Ts65Dn mice. These CX-4945 considerations are similar to another therapeutic that is of interest in DS, EGCG. A recent review by Stringer et al. (2017) highlights several factors that are contributing to the heterogeneity in studies administering EGCG to improve DS-related deficits. Similar to this recent review on EGCG, factors such as the age of the mice, the amount of DMSO used to dissolve CX-4945, the length of treatment, the treatment group sizes and the route of administration are just a few factors that will need to be considered in future investigations testing CX-4945 in Ts65Dn mice.

This study demonstrated that level of Dyrk1a protein levels in Ts65Dn mice are both spatially and temporally dependent throughout perinatal and adolescent development. These results showcase the importance of identifying specific time points to guide targeted therapeutics to inhibit Dyrk1a kinase activity. This study also administered the novel Dyrk1a inhibitor, CX-4945 at a time when Dyrk1a protein was elevated in Ts65Dn mice (P15-P18). After 5 consecutive days of CX-4945 treatment, there were no significant improvements in locomotion, homing ability, or cell proliferation in the hippocampus. However, these studies had moderate effect sizes and were found to be significantly underpowered. This study has laid the groundwork for future studies to further explore the efficacy of CX-4945 treatment to Ts65Dn mice. In addition, this study highlighted the importance of assessing the outcomes of trisomic mice produced from two different mating schemes (Ts65Dn x B6C3F1) and (Ts65Dn x B6C3.Dyrk1a$^{fl/fl}$). This study will help advance the DS research field in its efforts to optimize Dyrk1a-targeted therapeutic administration and administer behavioral assessments that are appropriate for determining treatment efficacy.

REFERENCES

ÁBRAHÁM, H., VINCZE, A., VESZPRÉMI, B., KRAVJÁK, A., GÖMÖRI, É., KOVÁCS, G. G. & SERESS, L. 2012. Impaired myelination of the human hippocampal formation in Down syndrome. *International Journal of Developmental Neuroscience,* 30**,** 147-158.

ADAYEV, T., WEGIEL, J. & HWANG, Y.-W. 2011. Harmine is an ATP-competitive inhibitor for dual-specificity tyrosine phosphorylation-regulated kinase 1A (Dyrk1A). *Archives of biochemistry and biophysics,* 507**,** 212-218.

AHMED, M. M., DHANASEKARAN, A. R., BLOCK, A., TONG, S., COSTA, A. C., STASKO, M. & GARDINER, K. J. 2015. Protein dynamics associated with failed and rescued learning in the Ts65Dn mouse model of Down syndrome. *PloS one,* 10**,** e0119491.

ALDRIDGE, G. M., PODREBARAC, D. M., GREENOUGH, W. T. & WEILER, I. J. 2008. The use of total protein stains as loading controls: an alternative to high-abundance single-protein controls in semi-quantitative immunoblotting. *Journal of neuroscience methods,* 172**,** 250-254.

ALLEN, E. G., FREEMAN, S. B., DRUSCHEL, C., HOBBS, C. A., O'LEARY, L. A., ROMITTI, P. A., ROYLE, M. H., TORFS, C. P. & SHERMAN, S. L. 2009. Maternal age and risk for trisomy 21 assessed by the origin of chromosome nondisjunction: a report from the Atlanta and National Down Syndrome Projects. *Human genetics,* 125**,** 41-52.

ALTAFAJ, X., DIERSSEN, M., BAAMONDE, C., MARTÍ, E., VISA, J., GUIMERÀ, J., OSET, M., GONZÁLEZ, J. R., FLÓREZ, J. & FILLAT, C. 2001. Neurodevelopmental delay, motor abnormalities and cognitive deficits in transgenic mice overexpressing Dyrk1A (minibrain), a murine model of Down's syndrome. *Human Molecular Genetics,* 10**,** 1915-1923.

ALTMAN, J. & SUDARSHAN, K. 1975. Postnatal development of locomotion in the laboratory rat. *Animal behaviour,* 23**,** 896-920.

ALVAREZ, M., ALTAFAJ, X., ARANDA, S. & DE LA LUNA, S. 2007. DYRK1A autophosphorylation on serine residue 520 modulates its kinase activity via 14-3-3 binding. *Molecular biology of the cell,* 18**,** 1167-1178.

ALVAREZ, M., ESTIVILL, X. & DE LA LUNA, S. 2003. DYRK1A accumulates in splicing speckles through a novel targeting signal and induces speckle disassembly. *J Cell Sci,* 116**,** 3099-107.

ANTONARAKIS, S. E., LYLE, R., DERMITZAKIS, E. T., REYMOND, A. & DEUTSCH, S. 2004. Chromosome 21 and down syndrome: from genomics to pathophysiology. *Nature reviews genetics,* 5**,** 725.

ARANDA, S., LAGUNA, A. & DE LA LUNA, S. 2011. DYRK family of protein kinases: evolutionary relationships, biochemical properties, and functional roles. *The FASEB Journal,* 25**,** 449-462.

ARRON, J. R., WINSLOW, M. M., POLLERI, A., CHANG, C.-P., WU, H., GAO, X., NEILSON, J. R., CHEN, L., HEIT, J. J. & KIM, S. K. 2006. NFAT dysregulation by increased dosage of DSCR1 and DYRK1A on chromosome 21. *Nature,* 441**,** 595-600.

ARTIOLI, T. O., WITSMISZYN, E., FERREIRA, A. B. & PINTO, C. F. 2017. Assessing Down syndrome BMI and body composition. *International Medical Review on Down Syndrome,* 21**,** 23-26.

BAXTER, L. L., MORAN, T. H., RICHTSMEIER, J. T., TRONCOSO, J. & REEVES, R. H. 2000. Discovery and genetic localization of Down syndrome cerebellar phenotypes using the Ts65Dn mouse. *Human Molecular Genetics,* 9**,** 195-202.

BECKER, W. & JOOST, H.-G. 1998. Structural and functional characteristics of Dyrk, a novel subfamily of protein kinases with dual specificity. *Progress in nucleic acid research and molecular biology,* 62**,** 1-17.

BECKER, W. & JOOST, H. G. 1999. Structural and functional characteristics of Dyrk, a novel subfamily of protein kinases with dual specificity. *Prog Nucleic Acid Res Mol Biol,* 62**,** 1-17.

BECKER, W. & SIPPL, W. 2011. Activation, regulation, and inhibition of DYRK1A. *FEBS journal,* 278**,** 246-256.

BECKER, W. & SIPPL, W. 2011. Activation, regulation, and inhibition of DYRK1A. *The FEBS journal,* 278**,** 246-256.

BECKER, W., SOPPA, U. & J TEJEDOR, F. 2014. DYRK1A: a potential drug target for multiple Down syndrome neuropathologies. *CNS & Neurological Disorders-Drug Targets (Formerly Current Drug Targets-CNS & Neurological Disorders),* 13**,** 26-33.

BELICHENKO, P. V., MASLIAH, E., KLESCHEVNIKOV, A. M., VILLAR, A. J., EPSTEIN, C. J., SALEHI, A. & MOBLEY, W. C. 2004. Synaptic structural abnormalities in the Ts65Dn mouse model of Down Syndrome. *Journal of Comparative Neurology,* 480**,** 281-298.

BIANCHI, P., CIANI, E., CONTESTABILE, A., GUIDI, S. & BARTESAGHI, R. 2010. Lithium restores neurogenesis in the subventricular zone of the Ts65Dn mouse, a model for Down syndrome. *Brain Pathology,* 20**,** 106-118.

BIANCHI, P., CIANI, E., GUIDI, S., TRAZZI, S., FELICE, D., GROSSI, G., FERNANDEZ, M., GIULIANI, A., CALZA, L. & BARTESAGHI, R. 2010. Early pharmacotherapy restores neurogenesis and cognitive performance in the Ts65Dn mouse model for Down syndrome. *Journal of Neuroscience,* 30**,** 8769-8779.

BON, B. W. M. V. & HOISCHEN, A. 2011. Intragenic deletion in DYRK1A leads to mental retardation and primary microcephaly. *Clinical* ….

BRADFORD, M. M. 1976. A rapid and sensitive method for the quantitation of microgram quantities of protein utilizing the principle of protein-dye binding. *Analytical biochemistry,* 72**,** 248-254.

BRANCHI, I., BICHLER, Z., MINGHETTI, L., DELABAR, J. M., MALCHIODI-ALBEDI, F., GONZALEZ, M.-C., CHETTOUH, Z., NICOLINI, A., CHABERT, C. & SMITH, D. J. 2004. Transgenic mouse in vivo library of human Down syndrome critical region 1: association between DYRK1A overexpression, brain development abnormalities, and cell cycle protein alteration. *Journal of Neuropathology & Experimental Neurology,* 63**,** 429-440.

BROADBENT, N. J., SQUIRE, L. R. & CLARK, R. E. 2004. Spatial memory, recognition memory, and the hippocampus. *Proceedings of the National Academy of Sciences of the United States of America,* 101**,** 14515-14520.

BROADWELL, R. D., SALCMAN, M. & KAPLAN, R. S. 1982. Morphologic effect of dimethyl sulfoxide on the blood-brain barrier. *Science,* 217**,** 164-166.

BULL, M. J. 2011. Health supervision for children with Down syndrome. *Pediatrics,* 128**,** 393-406.

CARLESIMO, G. A., MAROTTA, L. & VICARI, S. 1997. Long-term memory in mental retardation: evidence for a specific impairment in subjects with Down's syndrome. *Neuropsychologia,* 35**,** 71-9.

CARLESIMO, G. A., MAROTTA, L. & VICARI, S. 1997. Long-term memory in mental retardation: evidence for a specific impairment in subjects with Down's syndrome. *Neuropsychologia,* 35**,** 71-79.

CARR, J. & COLLINS, S. 2018. 50 years with Down syndrome: A longitudinal study. *Journal of Applied Research in Intellectual Disabilities*.

CENTER, J., BEANGE, H. & MCELDUFF, A. 1998. People with mental retardation have an increased prevalence of osteoporosis: a population study. *American Journal on Mental Retardation,* 103**,** 19-28.

CHAKRABARTI, L., GALDZICKI, Z. & HAYDAR, T. F. 2007. Defects in embryonic neurogenesis and initial synapse formation in the forebrain of the Ts65Dn mouse model of Down syndrome. *The Journal of neuroscience,* 27**,** 11483-11495.

CHEN-HWANG, M.-C., CHEN, H.-R., ELZINGA, M. & HWANG, Y.-W. 2002. Dynamin is a minibrain kinase/dual specificity Yak1-related kinase 1A substrate. *Journal of Biological Chemistry,* 277**,** 17597-17604.

CHEN, C.-K., SYMMONS, O., USLU, V. V., TSUJIMURA, T., RUF, S., SMEDLEY, D. & SPITZ, F. 2013. TRACER: a resource to study the regulatory architecture of the mouse genome. *BMC genomics,* 14**,** 215.

CHEN, L., LEE, M.-J., LI, H. & YANG, C. S. 1997. Absorption, distribution, and elimination of tea polyphenols in rats. *Drug Metabolism and Disposition,* 25**,** 1045-1050.

CHEON, M., KIM, S., OVOD, V., JERALA, N. K., MORGAN, J., HATEFI, Y., IJUIN, T., TAKENAWA, T. & LUBEC, G. 2003. Protein levels of genes encoded on chromosome 21 in fetal Down syndrome brain: challenging the gene dosage effect hypothesis (Part III). *Amino acids,* 24**,** 127-134.

CHOONG, X. Y., TOSH, J. L., PULFORD, L. J. & FISHER, E. 2015. Dissecting Alzheimer disease in Down syndrome using mouse models. *Frontiers in behavioral neuroscience,* 9**,** 268.

CHOW, H. S., CAI, Y., ALBERTS, D. S., HAKIM, I., DORR, R., SHAHI, F., CROWELL, J. A., YANG, C. S. & HARA, Y. 2001. Phase I pharmacokinetic study of tea polyphenols following single-dose administration of epigallocatechin gallate and polyphenon E. *Cancer Epidemiology Biomarkers & Prevention,* 10**,** 53-58.

CHOW, H. S., CAI, Y., HAKIM, I. A., CROWELL, J. A., SHAHI, F., BROOKS, C. A., DORR, R. T., HARA, Y. & ALBERTS, D. S. 2003. Pharmacokinetics and safety of green tea polyphenols after multiple-dose administration of epigallocatechin gallate and polyphenon E in healthy individuals. *Clinical Cancer Research,* 9**,** 3312-3319.

CLANCY, B., DARLINGTON, R. & FINLAY, B. 2001. Translating developmental time across mammalian species. *Neuroscience,* 105**,** 7-17.

CLANCY, B., FINLAY, B. L., DARLINGTON, R. B. & ANAND, K. 2007. Extrapolating brain development from experimental species to humans. *Neurotoxicology,* 28**,** 931-937.

CONTESTABILE, A., FILA, T., CECCARELLI, C., BONASONI, P., BONAPACE, L., SANTINI, D., BARTESAGHI, R. & CIANI, E. 2007. Cell cycle alteration and decreased cell proliferation in the hippocampal dentate gyrus and in the neocortical germinal matrix of fetuses with Down syndrome and in Ts65Dn mice. *Hippocampus,* 17**,** 665-678.

COOPER, J. D., SALEHI, A., DELCROIX, J.-D., HOWE, C. L., BELICHENKO, P. V., CHUA-COUZENS, J., KILBRIDGE, J. F., CARLSON, E. J., EPSTEIN, C. J. & MOBLEY, W. C. 2001. Failed retrograde transport of NGF in a mouse model of Down's syndrome: reversal of cholinergic neurodegenerative phenotypes following NGF infusion. *Proceedings of the National Academy of Sciences,* 98**,** 10439-10444.

COSTA, A. C. & SCOTT-MCKEAN, J. J. 2013. Prospects for improving brain function in individuals with Down syndrome. *CNS drugs,* 27**,** 679-702.

COURCET, J.-B., FAIVRE, L., MALZAC, P., MASUREL-PAULET, A., LOPEZ, E., CALLIER, P., LAMBERT, L., LEMESLE, M., THEVENON, J., GIGOT, N., DUPLOMB, L., RAGON, C., MARLE, N., MOSCA-BOIDRON, A.-L., HUET, F., PHILIPPE, C., MONCLA, A. & THAUVIN-ROBINET, C. 2012. The DYRK1A gene is a cause of syndromic intellectual disability with severe microcephaly and epilepsy. *Journal of medical genetics,* 49**,** 731-6.

COUSSONS-READ, M. E. & CRNIC, L. S. 1996. Behavioral assessment of the Ts65Dn mouse, a model for Down syndrome: altered behavior in the elevated plus maze and open field. *Behavior genetics,* 26**,** 7-13.

DAS, I., PARK, J.-M., SHIN, J. H., JEON, S. K., LORENZI, H., LINDEN, D. J., WORLEY, P. F. & REEVES, R. H. 2013. Hedgehog agonist therapy corrects structural and cognitive deficits in a Down syndrome mouse model. *Science translational medicine,* 5**,** 201ra120-201ra120.

DAVISSON, M., SCHMIDT, C., REEVES, R. H., IRVING, N., AKESON, E., HARRIS, B. & BRONSON, R. T. 1993. Segmental trisomy as a mouse model for Down syndrome. *Progress in clinical and biological research,* 384**,** 117-133.

DAVISSON, M. T., SCHMIDT, C. & AKESON, E. C. 1990. Segmental trisomy of murine chromosome 16: a new model system for studying Down syndrome. *Progress in clinical and biological research,* 360**,** 263.

DE GRAAF, K., HEKERMAN, P., SPELTEN, O., HERRMANN, A., PACKMAN, L. C., BÜSSOW, K., MÜLLER-NEWEN, G. & BECKER, W. 2004. Characterization of Cyclin L2, a Novel Cyclin with an Arginine/Serine-rich Domain PHOSPHORYLATION BY DYRK1A AND COLOCALIZATION WITH SPLICING FACTORS. *Journal of Biological Chemistry,* 279**,** 4612-4624.

DEBDAB, M., CARREAUX, F., RENAULT, S., SOUNDARARAJAN, M., FEDEROV, O., LOZACH, O., BABAULT, L., BARATTE, B., OGAWA, Y. & HAGIWARA, M. 2011. Design, synthesis and biological evaluation of leucettines, a class of potent CLK and DYRK kinases inhibitors derived from the marine sponge leucettamine B. Modulation of alternative RNA splicing. *J Med Chem,* 54**,** 4172-4186.

DEBDAB, M., CARREAUX, F., RENAULT, S., SOUNDARARAJAN, M., FEDOROV, O., FILIPPAKOPOULOS, P., LOZACH, O., BABAULT, L., TAHTOUH, T. & BARATTE, B. 2011. Leucettines, a class of potent inhibitors of cdc2-like kinases and dual specificity, tyrosine phosphorylation regulated kinases derived from the marine sponge leucettamine B: modulation of alternative pre-RNA splicing. *Journal of medicinal chemistry,* 54**,** 4172-4186.

DUCHON, A. & HERAULT, Y. 2016. DYRK1A, a Dosage-Sensitive Gene Involved in Neurodevelopmental Disorders, Is a Target for Drug Development in Down Syndrome. *Frontiers in Behavioral Neuroscience,* 10**,** 104.

DUCHON, A., RAVEAU, M., CHEVALIER, C., NALESSO, V., SHARP, A. J. & HERAULT, Y. 2011. Identification of the translocation breakpoints in the Ts65Dn and Ts1Cje mouse lines: relevance for modeling Down syndrome. *Mammalian Genome,* 22**,** 674-684.

EATON, S. L., ROCHE, S. L., HURTADO, M. L., OLDKNOW, K. J., FARQUHARSON, C., GILLINGWATER, T. H. & WISHART, T. M. 2013. Total protein analysis as a reliable loading control for quantitative fluorescent Western blotting. *PloS one,* 8**,** e72457.

EDGIN, J. O., ANAND, P., ROSSER, T., PIERPONT, E. I., FIGUEROA, C., HAMILTON, D., HUDDLESTON, L., MASON, G., SPANÒ, G. & TOOLE, L. 2017. The Arizona Cognitive Test Battery for Down Syndrome: Test-Retest Reliability and Practice Effects. *American journal on intellectual and developmental disabilities,* 122**,** 215-234.

EDGIN, J. O., CLARK, C. A., MASSAND, E. & KARMILOFF-SMITH, A. 2015. Building an adaptive brain across development: targets for neurorehabilitation must begin in infancy. *Frontiers in behavioral neuroscience,* 9.

EDGIN, J. O., MASON, G. M., ALLMAN, M. J., CAPONE, G. T., DELEON, I., MASLEN, C., REEVES, R. H., SHERMAN, S. L. & NADEL, L. 2010. Development and validation of the Arizona Cognitive Test Battery for Down syndrome. *Journal of neurodevelopmental disorders,* 2**,** 149.

EPSTEIN, C. 2001. *The metabolic & molecular bases of inherited disease,* New York; Montreal: McGraw-Hill.

EPSTEIN, C. J., COX, D. R. & EPSTEIN, L. B. 1985. Mouse trisomy 16: an animal model of human trisomy 21 (Down syndrome). *Annals of the New York Academy of Sciences,* 450**,** 157-168.

ESBENSEN, A. J., HOOPER, S. R., FIDLER, D., HARTLEY, S. L., EDGIN, J., D'ARDHUY, X. L., CAPONE, G., CONNERS, F. A., MERVIS, C. B. & ABBEDUTO, L. 2017. Outcome measures for clinical trials in Down syndrome. *American journal on intellectual and developmental disabilities,* 122**,** 247-281.

ESCORIHUELA, R. M., FERNÁNDEZ-TERUEL, A., VALLINA, I. F., BAAMONDE, C., LUMBRERAS, M. A., DIERSSEN, M., TOBEÑA, A. & FLÓREZ, J. 1995. A behavioral assessment of Ts65Dn mice: a putative Down syndrome model. *Neuroscience letters,* 199**,** 143-146.

FERGUSON, A. D., SHETH, P. R., BASSO, A. D., PALIWAL, S., GRAY, K., FISCHMANN, T. O. & LE, H. V. 2011. Structural basis of CX-4945 binding to human protein kinase CK2. *FEBS letters,* 585**,** 104-110.

FOX, W. 1965. Reflex-ontogeny and behavioural development of the mouse. *Animal behaviour,* 13**,** 234-IN5.

FRANK, C. L. & TSAI, L.-H. 2009. Alternative functions of core cell cycle regulators in neuronal migration, neuronal maturation, and synaptic plasticity. *Neuron,* 62**,** 312-326.

FREEMAN, S. B., BEAN, L. H., ALLEN, E. G., TINKER, S. W., LOCKE, A. E., DRUSCHEL, C., HOBBS, C. A., ROMITTI, P. A., ROYLE, M. H., TORFS, C. P., DOOLEY, K. J. & SHERMAN, S. L. 2008. Ethnicity, sex, and the incidence of congenital heart defects: a report from the National Down Syndrome Project. *Genetics in medicine : official journal of the American College of Medical Genetics,* 10**,** 173-80.

FREEMAN, S. B., TAFT, L. F., DOOLEY, K. J., ALLRAN, K., SHERMAN, S. L., HASSOLD, T. J., KHOURY, M. J. & SAKER, D. M. 1998. Population-based study of congenital heart defects in Down syndrome. *American journal of medical genetics,* 80**,** 213-7.

GARCÍA-CERRO, S., MARTÍNEZ, P., VIDAL, V., CORRALES, A., FLÓREZ, J., VIDAL, R., RUEDA, N., ARBONÉS, M. L. & MARTÍNEZ-CUÉ, C. 2014. Overexpression of Dyrk1A is implicated in several cognitive, electrophysiological and neuromorphological alterations found in a mouse model of Down syndrome. *PloS one,* 9**,** e106572.

GARDINER, K., HERAULT, Y., LOTT, I. T., ANTONARAKIS, S. E., REEVES, R. H. & DIERSSEN, M. 2010. Down syndrome: from understanding the neurobiology to therapy. *Journal of Neuroscience,* 30**,** 14943-14945.

GARDINER, K. J. 2015. Pharmacological approaches to improving cognitive function in Down syndrome: current status and considerations. *Drug design, development and therapy,* 9**,** 103.

GEORGE, S., KADAM, S. D., IRVING, N. D., MARKOWITZ, G. J., RAJA, S., KWAN, A., TU, Y., CHEN, H., ROHDE, C. & SMITH, D. R. 2013. Impact of trichostatin A and sodium valproate treatment on post-stroke neurogenesis and behavioral outcomes in immature mice. *Frontiers in cellular neuroscience,* 7**,** 123.

GODFREY, M. & LEE, N. R. 2018. Memory profiles in Down syndrome across development: a review of memory abilities through the lifespan. *Journal of neurodevelopmental disorders,* 10**,** 5.

GOODRICH-HUNSAKER, N. J., LIVINGSTONE, S. A., SKELTON, R. W. & HOPKINS, R. O. 2010. Spatial deficits in a virtual water maze in amnesic participants with hippocampal damage. *Hippocampus,* 20**,** 481-491.

GOULD, E. & TANAPAT, P. 1999. Stress and hippocampal neurogenesis. *Biological psychiatry,* 46**,** 1472-1479.

GRIBBLE, S. M., WISEMAN, F. K., CLAYTON, S., PRIGMORE, E., LANGLEY, E., YANG, F., MAGUIRE, S., FU, B., RAJAN, D. & SHEPPARD, O. 2013. Massively parallel sequencing reveals the complex structure of an irradiated human chromosome on a mouse background in the Tc1 model of Down syndrome. *PLoS One,* 8**,** e60482.

GUEDJ, F., BIANCHI, D. W. & DELABAR, J.-M. 2014. Prenatal treatment of Down syndrome: a reality? *Current Opinion in Obstetrics and Gynecology,* 26**,** 92-103.

GUEDJ, F., PENNINGS, J. L., FERRES, M. A., GRAHAM, L. C., WICK, H. C., MICZEK, K. A., SLONIM, D. K. & BIANCHI, D. W. 2015. The fetal brain transcriptome and neonatal behavioral phenotype in the Ts1Cje mouse model of Down syndrome. *American Journal of Medical Genetics Part A,* 167**,** 1993-2008.

GUIDI, S., BONASONI, P., CECCARELLI, C., SANTINI, D., GUALTIERI, F., CIANI, E. & BARTESAGHI, R. 2008. Neurogenesis impairment and increased cell death reduce total neuron number in the hippocampal region of fetuses with Down syndrome. *Brain Pathology,* 18**,** 180-197.

GUIDI, S., STAGNI, F., BIANCHI, P., CIANI, E., RAGAZZI, E., TRAZZI, S., GROSSI, G., MANGANO, C., CALZÀ, L. & BARTESAGHI, R. 2013. Early pharmacotherapy with fluoxetine rescues dendritic pathology in the Ts65Dn mouse model of Down syndrome. *Brain Pathology,* 23**,** 129-143.

GUIJARRO, M., VALERO, C., PAULE, B., GONZALEZ-MACIAS, J. & RIANCHO, J. 2008. Bone mass in young adults with Down syndrome. *Journal of Intellectual Disability Research,* 52**,** 182-189.

GUIMERÂ, J., CASAS, C., PUCHARCÔS, C., SOLANS, A., DOMÈNECH, A., PLANAS, A. M., ASHLEY, J., LOVETT, M., ESTIVILL, X. & PRITCHARD, M. A. 1996. A human homologue of Drosophila minibrain (MNB) is expressed in the neuronal regions affected in Down syndrome and maps to the critical region. *Human molecular genetics,* 5**,** 1305-1310.

GUPTA, M., DHANASEKARAN, A. R. & GARDINER, K. J. 2016. Mouse models of Down syndrome: gene content and consequences. *Mammalian Genome,* 27**,** 538-555.

GUTIERREZ-CASTELLANOS, N., WINKELMAN, B. H., TOLOSA-RODRIGUEZ, L., DEVENNEY, B., REEVES, R. H. & DE ZEEUW, C. I. 2013. Size does not always matter: Ts65Dn Down syndrome mice show cerebellum-dependent motor learning deficits that cannot be rescued by postnatal SAG treatment. *Journal of Neuroscience,* 33**,** 15408-15413.

HÄMMERLE, B., ELIZALDE, C. & TEJEDOR, F. J. 2008. The spatio-temporal and subcellular expression of the candidate Down syndrome gene Mnb/Dyrk1A in the developing mouse brain suggests distinct sequential roles in neuronal development. *European Journal of Neuroscience,* 27**,** 1061-1074.

HANSLICK, J. L., LAU, K., NOGUCHI, K. K., OLNEY, J. W., ZORUMSKI, C. F., MENNERICK, S. & FARBER, N. B. 2009. Dimethyl sulfoxide (DMSO) produces widespread apoptosis in the developing central nervous system. *Neurobiology of disease,* 34**,** 1-10.

HARTLEY, D., BLUMENTHAL, T., CARRILLO, M., DIPAOLO, G., ESRALEW, L., GARDINER, K., GRANHOLM, A.-C., IQBAL, K., KRAMS, M. & LEMERE, C. 2015. Down syndrome and Alzheimer's disease: Common pathways, common goals. *Alzheimer's & dementia: the journal of the Alzheimer's Association,* 11**,** 700-709.

HATTORI, M., FUJIYAMA, A., TAYLOR, T., WATANABE, H., YADA, T., PARK, H.-S., TOYODA, A., ISHII, K., TOTOKI, Y. & CHOI, D.-K. 2000. The DNA sequence of human chromosome 21. *Nature,* 405**,** 311-319.

HAYDAR, T. F. & REEVES, R. H. 2012. Trisomy 21 and early brain development. *Trends in neurosciences,* 35**,** 81-91.

HERAULT, Y., DELABAR, J. M., FISHER, E. M., TYBULEWICZ, V. L., YU, E. & BRAULT, V. 2017. Rodent models in Down syndrome research: impact and future opportunities. *Disease models & mechanisms,* 10**,** 1165-1186.

HILL, J. M., LIM, M. A. & STONE, M. M. 2008. Developmental milestones in the newborn mouse. *Neuropeptide Techniques***,** 131-149.

HIMPEL, S., PANZER, P., EIRMBTER, K., CZAJKOWSKA, H., SAYED, M., PACKMAN, L. C., BLUNDELL, T., KENTRUP, H., GRÖTZINGER, J. & JOOST, H.-G. 2001. Identification of the autophosphorylation sites and characterization of their effects in the protein kinase DYRK1A. *Biochemical Journal,* 359**,** 497-505.

HINDLEY, C. & PHILPOTT, A. 2012. Co-ordination of cell cycle and differentiation in the developing nervous system. *Biochemical Journal,* 444**,** 375-382.

HOF, P. R., BOURAS, C., PERL, D. P., SPARKS, D. L., MEHTA, N. & MORRISON, J. H. 1995. Age-related distribution of neuropathologic changes in the cerebral cortex of patients with Down's syndrome: quantitative regional analysis and comparison with Alzheimer's disease. *Archives of neurology,* 52**,** 379-391.

HOLTZMAN, D. M., SANTUCCI, D., KILBRIDGE, J., CHUA-COUZENS, J., FONTANA, D. J., DANIELS, S. E., JOHNSON, R. M., CHEN, K., SUN, Y. & CARLSON, E. 1996. Developmental abnormalities and age-related neurodegeneration in a mouse model of Down syndrome. *Proceedings of the National Academy of Sciences,* 93**,** 13333-13338.

HUNSAKER, M. R., SMITH, G. K. & KESNER, R. P. 2016. Adaptation of the Arizona Cognitive Task Battery for use with the Ts65Dn Mouse Model of Down Syndrome. *bioRxiv***,** 061754.

JARROLD, C. & BADDELEY, A. D. 1997. Short-term Memory for Verbal and Visuospatial Information in Down's Syndrome. *Cogn Neuropsychiatry,* 2**,** 101-22.

JARROLD, C., BADDELEY, A. D. & PHILLIPS, C. E. 2002. Verbal short-term memory in Down syndrome: A problem of memory, audition, or speech? *Journal of Speech, Language, and Hearing Research,* 45**,** 531-544.

JARROLD, C., BADDELEY, A. D. & PHILLIPS, C. E. 2002. Verbal short-term memory in Down syndrome: a problem of memory, audition, or speech? *Journal of speech, language, and hearing research : JSLHR,* 45**,** 531-44.

JERNIGAN, T. L., BELLUGI, U., SOWELL, E., DOHERTY, S. & HESSELINK, J. R. 1993. Cerebral Morphologic Distinctions Between Williams and Down Syndromes. *Archives of Neurology,* 50**,** 186-191.

JUUL, S. E., BEYER, R. P., BAMMLER, T. K., FARIN, F. M. & GLEASON, C. A. 2011. Effects of neonatal stress and morphine on murine hippocampal gene expression. *Pediatric research,* 69**,** 285.

KACZMARSKI, W., BARUA, M., MAZUR-KOLECKA, B., FRACKOWIAK, J., DOWJAT, W., MEHTA, P., BOLTON, D., HWANG, Y. W., RABE, A. & ALBERTINI, G. 2014. Intracellular distribution of differentially phosphorylated dual-specificity tyrosine phosphorylation-regulated kinase 1A (DYRK1A). *Journal of neuroscience research,* 92**,** 162-173.

KÄLLÉN, B., MASTROIACOVO, P. & ROBERT, E. 1996. Major congenital malformations in Down syndrome. *American journal of medical genetics,* 65**,** 160-6.

KELLY, P. A. & RAHMANI, Z. 2005. DYRK1A enhances the mitogen-activated protein kinase cascade in PC12 cells by forming a complex with Ras, B-Raf, and MEK1. *Molecular biology of the cell,* 16**,** 3562-3573.

KENTRUP, H., BECKER, W., HEUKELBACH, J., WILMES, A., SCHÜRMANN, A., HUPPERTZ, C., KAINULAINEN, H. & JOOST, H.-G. 1996. Dyrk, a dual specificity protein kinase with unique structural features whose activity is dependent on tyrosine residues between subdomains VII and VIII. *Journal of Biological Chemistry,* 271**,** 3488-3495.

KII, I., SUMIDA, Y., GOTO, T., SONAMOTO, R., OKUNO, Y., YOSHIDA, S., KATO-SUMIDA, T., KOIKE, Y., ABE, M. & NONAKA, Y. 2016. Selective inhibition of the kinase DYRK1A by targeting its folding process. *Nature communications,* 7.

KIM, LEE, K.-S., KIM, A.-K., CHOI, M., CHOI, K., KANG, M., CHI, S.-W., LEE, M.-S., LEE, J.-S. & LEE, S.-Y. 2016. A chemical with proven clinical safety rescues Down-syndrome-related phenotypes in through DYRK1A inhibition. *Disease Models & Mechanisms,* 9**,** 839-848.

KIM, H., LEE, K.-S., KIM, A.-K., CHOI, M., CHOI, K., KANG, M., CHI, S.-W., LEE, M.-S., LEE, J.-S. & LEE, S.-Y. 2016. A chemical with proven clinical safety rescues Down-syndrome-related phenotypes in through DYRK1A inhibition. *Disease models & mechanisms,* 9**,** 839-848.

KIM, H., SABLIN, S. O. & RAMSAY, R. R. 1997. Inhibition of monoamine oxidase A by β-carboline derivatives. *Archives of Biochemistry and Biophysics,* 337**,** 137-142.

KOEHLER, S., BLACK, S., SINDEN, M., KIDRON, D., SZEKELY, C., PARKER, J., FOSTER, J., MOSCOVITCH, M., WINOCUR, G. & SZALAI, J. 1998. Memory impairments in relation to hippocampal and parahippocampal atrophy in Alzheimer's disease: An MR volumetry study. *Neuropsychologia,* 36**,** 101-14.

KORBEL, J. O., TIROSH-WAGNER, T., URBAN, A. E., CHEN, X.-N., KASOWSKI, M., DAI, L., GRUBERT, F., ERDMAN, C., GAO, M. C. & LANGE, K. 2009. The genetic architecture of Down syndrome phenotypes revealed by high-resolution analysis of human segmental trisomies. *Proceedings of the National Academy of Sciences,* 106**,** 12031-12036.

KURABAYASHI, N. & SANADA, K. 2013. Increased dosage of DYRK1A and DSCR1 delays neuronal differentiation in neocortical progenitor cells. *Genes & development,* 27**,** 2708-2721.

LARSEN, K. B., LAURSEN, H., GRAEM, N., SAMUELSEN, G. B., BOGDANOVIC, N. & PAKKENBERG, B. 2008. Reduced cell number in the neocortical part of the human fetal brain in Down syndrome. *Ann Anat,* 190**,** 421-7.

LAVENEX, P. B., BOSTELMANN, M., BRANDNER, C., COSTANZO, F., FRAGNIÈRE, E., KLENCKLEN, G., LAVENEX, P., MENGHINI, D. & VICARI, S. 2015. Allocentric spatial learning and memory deficits in Down syndrome. *Frontiers in psychology,* 6**,** 62.

LAWS, G. 2002. Working memory in children and adolescents with Down syndrome: evidence from a colour memory experiment. *J Child Psychol Psychiatry,* 43**,** 353-64.

LEE, M.-J., MALIAKAL, P., CHEN, L., MENG, X., BONDOC, F. Y., PRABHU, S., LAMBERT, G., MOHR, S. & YANG, C. S. 2002. Pharmacokinetics of tea catechins after ingestion of green tea and (−)-epigallocatechin-3-gallate by humans formation of different metabolites and individual variability. *Cancer Epidemiology Biomarkers & Prevention,* 11**,** 1025-1032.

LEJEUNE, J., GAUTIER, M. & TURPIN, R. 1959. Study of somatic chromosomes from 9 mongoloid children. *Comptes rendus hebdomadaires des seances de l'Academie des sciences,* 248**,** 1721.

LEUNER, B., GOULD, E. & SHORS, T. J. 2006. Is there a link between adult neurogenesis and learning? *Hippocampus,* 16**,** 216-224.

LEVERENZ, J. B. & RASKIND, M. A. 1998. Early amyloid deposition in the medial temporal lobe of young Down syndrome patients: a regional quantitative analysis. *Experimental neurology,* 150**,** 296-304.

LIM, M. A., STACK, C. M., CUASAY, K., STONE, M. M., MCFARLANE, H. G., WASCHEK, J. A. & HILL, J. M. 2008. Regardless of genotype, offspring of VIP-deficient female mice exhibit developmental delays and deficits in social behavior. *International Journal of Developmental Neuroscience,* 26**,** 423-434.

LLORENS-MARTIN, M., RUEDA, N., TEJEDA, G. S., FLOREZ, J., TREJO, J. L. & MARTÍNEZ-CUÉ, C. 2010. Effects of voluntary physical exercise on adult hippocampal neurogenesis and behavior of Ts65Dn mice, a model of Down syndrome. *Neuroscience,* 171**,** 1228-1240.

LYLE, R., BÉNA, F., GAGOS, S., GEHRIG, C., LOPEZ, G., SCHINZEL, A., LESPINASSE, J., BOTTANI, A., DAHOUN, S. & TAINE, L. 2009. Genotype–phenotype correlations in Down syndrome identified by array CGH in 30 cases of partial trisomy and partial monosomy chromosome 21. *European Journal of Human Genetics,* 17**,** 454-466.

LYLE, R., BÉNA, F., GAGOS, S., GEHRIG, C., LOPEZ, G., SCHINZEL, A., LESPINASSE, J., BOTTANI, A., DAHOUN, S. & TAINE, L. 2009. Genotype–phenotype correlations in Down syndrome identified by array CGH in 30 cases of partial trisomy and partial monosomy chromosome 21. *European Journal of Human Genetics,* 17**,** 454.

MALBERG, J. E., EISCH, A. J., NESTLER, E. J. & DUMAN, R. S. 2000. Chronic antidepressant treatment increases neurogenesis in adult rat hippocampus. *Journal of Neuroscience,* 20**,** 9104-9110.

MANGAN, P. A. 1992. Spatial memory abilities and abnormal development of the hippocampal formation in Down syndrome.

MARCUS, C. L., KEENS, T. G., BAUTISTA, D. B., VON PECHMANN, W. S. & WARD, S. L. 1991. Obstructive sleep apnea in children with Down syndrome. *Pediatrics,* 88**,** 132-9.

MARSCHKE, R., BORAD, M., MCFARLAND, R., ALVAREZ, R., LIM, J., PADGETT, C., VON HOFF, D., O'BRIEN, S. & NORTHFELT, D. 2011. Findings from the phase I clinical trials of CX-4945, an orally available inhibitor of CK2. *Journal of Clinical Oncology,* 29**,** 3087-3087.

MARTí, E., ALTAFAJ, X., DIERSSEN, M., DE LA LUNA, S., FOTAKI, V., ALVAREZ, M., PÉREZ-RIBA, M., FERRER, I. & ESTIVILL, X. 2003. Dyrk1A expression pattern supports specific roles of this kinase in the adult central nervous system. *Brain research,* 964**,** 250-263.

MARTíNEZ-CUÉ, C., BAAMONDE, C., LUMBRERAS, M., PAZ, J., DAVISSON, M. T., SCHMIDT, C., DIERSSEN, M. & FLÓREZ, J. 2002. Differential effects of environmental enrichment on behavior and learning of male and female Ts65Dn mice, a model for Down syndrome. *Behavioural brain research,* 134**,** 185-200.

MCFARLANE, L., TRUONG, V., PALMER, J. & WILHELM, D. 2013. Novel PCR assay for determining the genetic sex of mice. *Sexual Development,* 7**,** 207-211.

MEIJER, M., SPRUIJT, B., VAN ZUTPHEN, L. & BAUMANS, V. 2006. Effect of restraint and injection methods on heart rate and body temperature in mice. *Laboratory animals,* 40**,** 382-391.

MIKULECKÁ, A., SUBRT, M., STUCHLIK, A. & KUBOVÁ, H. 2014. Consequences of early postnatal benzodiazepines exposure in rats. I. Cognitive-like behavior. *Frontiers in behavioral neuroscience,* 8**,** 101.

MILOJEVICH, H. & LUKOWSKI, A. 2016. Recall memory in children with Down syndrome and typically developing peers matched on developmental age. *Journal of Intellectual Disability Research,* 60**,** 89-100.

MIRANDA, S. B. & FANTZ, R. L. 1974. Recognition memory in Down's syndrome and normal infants. *Child Development***,** 651-660.

MØLLER, R. S., KÜBART, S. & HOELTZENBEIN, M. 2008. Truncation of the Down syndrome candidate gene DYRK1A in two unrelated patients with microcephaly. *The American Journal of …*.

MOTTE, J. & WILLIAMS, R. S. 1989. Age-related changes in the density and morphology of plaques and neurofibrillary tangles in Down syndrome brain. *Acta Neuropathologica,* 77**,** 535-546.

MUNIR, F., CORNISH, K. M. & WILDING, J. 2000. A neuropsychological profile of attention deficits in young males with fragile X syndrome. *Neuropsychologia,* 38**,** 1261-1270.

NAERT, G., FERRÉ, V., MEUNIER, J., KELLER, E., MALMSTRÖM, S., GIVALOIS, L., CARREAUX, F., BAZUREAU, J.-P. & MAURICE, T. 2015. Leucettine L41, a DYRK1A-preferential DYRKs/CLKs inhibitor, prevents memory impairments and neurotoxicity induced by oligomeric Aβ25–35 peptide administration in mice. *European Neuropsychopharmacology,* 25**,** 2170-2182.

NAJAS, S., ARRANZ, J., LOCHHEAD, P. A., ASHFORD, A. L., OXLEY, D., DELABAR, J. M., COOK, S. J., BARALLOBRE, M. J. & ARBONÉS, M. L. 2015. DYRK1A-mediated cyclin D1 degradation in neural stem cells contributes to the neurogenic cortical defects in down syndrome. *EBioMedicine,* 2**,** 120-134.

NAKANO-KOBAYASHI, A., AWAYA, T., KII, I., SUMIDA, Y., OKUNO, Y., YOSHIDA, S., SUMIDA, T., INOUE, H., HOSOYA, T. & HAGIWARA, M. 2017. Prenatal neurogenesis induction therapy normalizes brain structure and function in Down syndrome mice. *Proceedings of the National Academy of Sciences,* 114**,** 10268-10273.

NETZER, W. J., POWELL, C., NONG, Y., BLUNDELL, J., WONG, L., DUFF, K., FLAJOLET, M. & GREENGARD, P. 2010. Lowering beta-amyloid levels rescues learning and memory in a Down syndrome mouse model. *PloS one,* 5**,** e10943-e10943.

NEUMANN, F., GOURDAIN, S., ALBAC, C., DEKKER, A. D., BUI, L. C., DAIROU, J., SCHMITZ-AFONSO, I., HUE, N., RODRIGUES-LIMA, F. & DELABAR, J. M. 2018. DYRK1A inhibition and cognitive rescue in a Down syndrome mouse model are induced by new fluoro-DANDY derivatives. *Scientific reports,* 8**,** 2859.

NGUYEN, T. L., FRUIT, C., HÉRAULT, Y., MEIJER, L. & BESSON, T. 2017. Dual-specificity tyrosine phosphorylation-regulated kinase 1A (DYRK1A) inhibitors: A survey of recent patent literature. *Expert opinion on therapeutic patents,* 27**,** 1183-1199.

NOBLE, M. E., ENDICOTT, J. A. & JOHNSON, L. N. 2004. Protein kinase inhibitors: insights into drug design from structure. *Science,* 303**,** 1800-1805.

NORTON, M. E., JACOBSSON, B., SWAMY, G. K., LAURENT, L. C., RANZINI, A. C., BRAR, H., TOMLINSON, M. W., PEREIRA, L., SPITZ, J. L. & HOLLEMON, D. 2015. Cell-free DNA analysis for noninvasive examination of trisomy. *New England Journal of Medicine,* 372**,** 1589-1597.

NUMMINEN, H., SERVICE, E., AHONEN, T. & RUOPPILA, I. 2001. Working memory and everyday cognition in adults with Down's syndrome. *J Intellect Disabil Res,* 45**,** 157-68.

NYGAARD, E., LUDVIG REICHELT, K. & FAGAN, J. 2001. The relation between the psychological functioning of children with Down syndrome and their urine peptide levels and levels of serum antibodies to food proteins. *Down Syndrome Research and Practice,* 6**,** 139-145.

O'DOHERTY, A., RUF, S., MULLIGAN, C., HILDRETH, V., ERRINGTON, M. L., COOKE, S., SESAY, A., MODINO, S., VANES, L. & HERNANDEZ, D. 2005. An aneuploid mouse strain carrying human chromosome 21 with Down syndrome phenotypes. *Science,* 309**,** 2033-2037.

OGAWA, Y., NONAKA, Y., GOTO, T., OHNISHI, E., HIRAMATSU, T., KII, I., YOSHIDA, M., IKURA, T., ONOGI, H. & SHIBUYA, H. 2010. Development of a novel selective inhibitor of the Down syndrome-related kinase Dyrk1A. *Nature communications,* 1**,** 86.

OHNUMA, S.-I. & HARRIS, W. A. 2003. Neurogenesis and the cell cycle. *Neuron,* 40**,** 199-208.

OLMOS-SERRANO, J. L., KANG, H. J., TYLER, W. A., SILBEREIS, J. C., CHENG, F., ZHU, Y., PLETIKOS, M., JANKOVIC-RAPAN, L., CRAMER, N. P. & GALDZICKI, Z. 2016. Down syndrome developmental brain transcriptome reveals defective oligodendrocyte differentiation and myelination. *Neuron,* 89**,** 1208-1222.

ORTIZ-ABALIA, J., SAHÚN, I., ALTAFAJ, X., ANDREU, N., ESTIVILL, X., DIERSSEN, M. & FILLAT, C. 2008. Targeting Dyrk1A with AAVshRNA attenuates motor alterations in TgDyrk1A, a mouse model of Down syndrome. *The American Journal of Human Genetics,* 83**,** 479-488.

PAGANO, M. A., BAIN, J., KAZIMIERCZUK, Z., SARNO, S., RUZZENE, M., DI MAIRA, G., ELLIOTT, M., ORZESZKO, A., COZZA, G. & MEGGIO, F. 2008. The selectivity of inhibitors of protein kinase CK2: an update. *Biochemical Journal,* 415**,** 353-365.

PAPADOPOULOS, C. 2011. Identification and characterization of a new splice variant of the protein kinase DYRK4 and the role of DYRK1A during mitotic exit. Institut für Pharmakologie und Toxikologie.

PARK, J., OH, Y., YOO, L., JUNG, M.-S., SONG, W.-J., LEE, S.-H., SEO, H. & CHUNG, K. C. 2010. Dyrk1A phosphorylates p53 and inhibits proliferation of embryonic neuronal cells. *Journal of Biological Chemistry,* 285**,** 31895-31906.

PARK, J., SONG, W.-J. & CHUNG, K. C. 2009. Function and regulation of Dyrk1A: towards understanding Down syndrome. *Cellular and molecular life sciences,* 66**,** 3235-3240.

PARK, J., YANG, E. J., YOON, J. H. & CHUNG, K. C. 2007. Dyrk1A overexpression in immortalized hippocampal cells produces the neuropathological features of Down syndrome. *Molecular and Cellular Neuroscience,* 36**,** 270-279.

PARKER, S. E., MAI, C. T., CANFIELD, M. A., RICKARD, R., WANG, Y., MEYER, R. E., ANDERSON, P., MASON, C. A., COLLINS, J. S. & KIRBY, R. S. 2010. Updated national birth prevalence estimates for selected birth defects in the United States, 2004–2006. *Birth Defects Research Part A: Clinical and Molecular Teratology,* 88**,** 1008-1016.

PENNINGTON, B. F., MOON, J., EDGIN, J., STEDRON, J. & NADEL, L. 2003. The neuropsychology of Down syndrome: evidence for hippocampal dysfunction. *Child development,* 74**,** 75-93.

PIERRE, F., CHUA, P. C., O'BRIEN, S. E., SIDDIQUI-JAIN, A., BOURBON, P., HADDACH, M., MICHAUX, J., NAGASAWA, J., SCHWAEBE, M. K., STEFAN, E., VIALETTES, A., WHITTEN, J. P., CHEN, T. K., DARJANIA, L., STANSFIELD, R., ANDERES, K., BLIESATH, J., DRYGIN, D., HO, C., OMORI, M., PROFFITT, C., STREINER, N., TRENT, K., RICE, W. G. & RYCKMAN, D. M. 2011. Discovery and SAR of 5-(3-chlorophenylamino)benzo[c][2,6]naphthyridine-8-carboxylic acid (CX-4945), the first clinical stage inhibitor of protein kinase CK2 for the treatment of cancer. *J Med Chem,* 54**,** 635-54.

PIERRE, F., CHUA, P. C., O'BRIEN, S. E., SIDDIQUI-JAIN, A., BOURBON, P., HADDACH, M., MICHAUX, J., NAGASAWA, J., SCHWAEBE, M. K. & STEFAN, E. 2011. Pre-clinical characterization of CX-4945, a potent and selective small molecule inhibitor of CK2 for the treatment of cancer. *Molecular and cellular biochemistry,* 356**,** 37.

PINTER, J. D., BROWN, W. E., ELIEZ, S., SCHMITT, J. E., CAPONE, G. T. & REISS, A. L. 2001. Amygdala and hippocampal volumes in children with Down syndrome: a high-resolution MRI study. *Neurology,* 56**,** 972-4.

PINTER, J. D., ELIEZ, S., SCHMITT, J. E., CAPONE, G. T. & REISS, A. L. 2001. Neuroanatomy of Down's syndrome: a high-resolution MRI study. *The American journal of psychiatry,* 158**,** 1659-65.

PLETCHER, M. T., WILTSHIRE, T., CABIN, D. E., VILLANUEVA, M. & REEVES, R. H. 2001. Use of comparative physical and sequence mapping to annotate mouse chromosome 16 and human chromosome 21. *Genomics,* 74**,** 45-54.

POMETLOVÁ, M., HRUBÁ, L., ŠLAMBEROVÁ, R. & ROKYTA, R. 2009. Cross-fostering effect on postnatal development of rat pups exposed to methamphetamine during gestation and preweaning periods. *International Journal of Developmental Neuroscience,* 27**,** 149-155.

RAHMANI, Z., LOPES, C., RACHIDI, M. & DELABAR, J.-M. 1998. Expression of the mnb (dyrk) protein in adult and embryonic mouse tissues. *Biochemical and biophysical research communications,* 253**,** 514-518.

REEVES, R. H., IRVING, N. G., MORAN, T. H., WOHN, A., KITT, C., SISODIA, S. S., SCHMIDT, C., BRONSON, R. T. & DAVISSON, M. T. 1995. A mouse model for Down syndrome exhibits learning and behaviour. *Nature genetics,* 11.

REINHOLDT, L. G., DING, Y., GILBERT, G. T., CZECHANSKI, A., SOLZAK, J. P., ROPER, R. J., JOHNSON, M. T., DONAHUE, L. R., LUTZ, C. & DAVISSON, M. T. 2011. Molecular characterization of the translocation breakpoints in the Down syndrome mouse model Ts65Dn. *Mammalian genome,* 22**,** 685-691.

RIBEIRO, S. T., TESIO, M., RIBOT, J. C., MACINTYRE, E., BARATA, J. T. & SILVA-SANTOS, B. 2017. Casein kinase 2 controls the survival of normal thymic and leukemic γδ T cells via promotion of AKT signaling. *Leukemia,* 31**,** 1603.

RICHTSMEIER, J. T., BAXTER, L. L. & REEVES, R. H. 2000. Parallels of craniofacial maldevelopment in Down syndrome and Ts65Dn mice. *Developmental Dynamics,* 217**,** 137-145.

ROBERTS, L. V. & RICHMOND, J. L. 2015. Preschoolers with Down syndrome do not yet show the learning and memory impairments seen in adults with Down syndrome. *Developmental science,* 18**,** 404-419.

ROPER, R. J., BAXTER, L. L., SARAN, N. G., KLINEDINST, D. K., BEACHY, P. A. & REEVES, R. H. 2006. Defective cerebellar response to mitogenic Hedgehog signaling in Down's syndrome mice. *Proceedings of the National Academy of Sciences of the United States of America,* 103**,** 1452-1456.

ROPER, R. J., JOHN, H. K. S., PHILIP, J., LAWLER, A. & REEVES, R. H. 2006. Perinatal loss of Ts65Dn Down syndrome mice. *Genetics,* 172**,** 437-443.

ROPER, R. J. & REEVES, R. H. 2006. Understanding the basis for Down syndrome phenotypes. *PLoS genetics,* 2**,** e50.

ROSSI, M., DE AZUA, I. R., BARELLA, L. F., SAKAMOTO, W., ZHU, L., CUI, Y., LU, H., REBHOLZ, H., MATSCHINSKY, F. M. & DOLIBA, N. M. 2015. CK2 acts as a potent negative regulator of receptor-mediated insulin release in vitro and in vivo. *Proceedings of the National Academy of Sciences,* 112**,** E6818-E6824.

ROUBERTOUX, P. L. & KERDELHUÉ, B. 2006. Trisomy 21: from chromosomes to mental retardation. *Behavior genetics,* 36**,** 346-354.

RUEDA, N., FLOREZ, J. & MARTINEZ-CUE, C. 2008. Chronic pentylenetetrazole but not donepezil treatment rescues spatial cognition in Ts65Dn mice, a model for Down syndrome. *Neuroscience letters,* 433**,** 22-27.

RUEDA, N., FLÓREZ, J. & MARTÍNEZ-CUÉ, C. 2012. Mouse models of Down syndrome as a tool to unravel the causes of mental disabilities. *Neural plasticity,* 2012.

RUZZENE, M. & PINNA, L. A. 2010. Addiction to protein kinase CK2: a common denominator of diverse cancer cells? *Biochimica et Biophysica Acta (BBA)-Proteins and Proteomics,* 1804**,** 499-504.

RYOO, S.-R., JEONG, H. K., RADNAABAZAR, C., YOO, J.-J., CHO, H.-J., LEE, H.-W., KIM, I.-S., CHEON, Y.-H., AHN, Y. S. & CHUNG, S.-H. 2007. DYRK1A-mediated hyperphosphorylation of Tau A functional link between Down syndrome and Alzheimer disease. *Journal of Biological Chemistry,* 282**,** 34850-34857.

SAGO, H., CARLSON, E. J., SMITH, D. J., RUBIN, E. M., CRNIC, L. S., HUANG, T.-T. & EPSTEIN, C. J. 2000. Genetic dissection of region associated with behavioral abnormalities in mouse models for Down syndrome. *Pediatric research,* 48**,** 606-613.

SALOMONI, P. & CALEGARI, F. 2010. Cell cycle control of mammalian neural stem cells: putting a speed limit on G1. *Trends in cell biology,* 20**,** 233-243.

SANTOS, N. C., FIGUEIRA-COELHO, J., MARTINS-SILVA, J. & SALDANHA, C. 2003. Multidisciplinary utilization of dimethyl sulfoxide: pharmacological, cellular, and molecular aspects. *Biochemical pharmacology,* 65**,** 1035-1041.

SCHMIDT-SIDOR, B., WISNIEWSKI, K., SHEPARD, T. & SERSEN, E. 1990. Brain growth in Down syndrome subjects 15 to 22 weeks of gestational age and birth to 60 months. *Clinical neuropathology,* 9**,** 181-190.

SHINDOH, N., KUDOH, J., MAEDA, H., YAMAKI, A., MINOSHIMA, S., SHIMIZU, Y. & SHIMIZU, N. 1996. Cloning of a Human Homolog of theDrosophila Minibrain/Rat Dyrk Gene from “the Down Syndrome Critical Region” of Chromosome 21. *Biochemical and biophysical research communications,* 225**,** 92-99.

SHOTT, S. R., JOSEPH, A. & HEITHAUS, D. 2001. Hearing loss in children with Down syndrome. *International journal of pediatric otorhinolaryngology,* 61**,** 199-205.

SIDDIQUI-JAIN, A., DRYGIN, D., STREINER, N., CHUA, P., PIERRE, F., O'BRIEN, S. E., BLIESATH, J., OMORI, M., HUSER, N. & HO, C. 2010. CX-4945, an orally bioavailable selective inhibitor of protein kinase CK2, inhibits prosurvival and angiogenic signaling and exhibits antitumor efficacy. *Cancer research,* 70**,** 10288-10298.

SIDDIQUI-JAIN, A., DRYGIN, D., STREINER, N., CHUA, P., PIERRE, F., O'BRIEN, S. E., BLIESATH, J., OMORI, M., HUSER, N., HO, C., PROFFITT, C., SCHWAEBE, M. K., RYCKMAN, D. M., RICE, W. G. & ANDERES, K. 2010. CX-4945, an orally bioavailable selective inhibitor of protein kinase CK2, inhibits prosurvival and angiogenic signaling and exhibits antitumor efficacy. *Cancer Res,* 70**,** 10288-98.

SILVER, L. M. 1995. *Mouse genetics: concepts and applications,* Oxford University Press.

SILVERMAN, W. 2007. Down syndrome: cognitive phenotype. *Developmental Disabilities Research Reviews,* 13**,** 228-236.

SMITH, B., MEDDA, F., GOKHALE, V., DUNCKLEY, T. & HULME, C. 2012. Recent advances in the design, synthesis, and biological evaluation of selective DYRK1A inhibitors: a new avenue for a disease modifying treatment of Alzheimer's? *ACS chemical neuroscience,* 3**,** 857-872.

SON, Y. H., SONG, J. S., KIM, S. H. & KIM, J. 2013. Pharmacokinetic characterization of CK2 inhibitor CX-4945. *Archives of pharmacal research,* 36**,** 840-845.

SONG, W.-J., STERNBERG, L. R., KASTEN-SPORTÈS, C., VAN KEUREN, M. L., CHUNG, S.-H., SLACK, A. C., MILLER, D. E., GLOVER, T. W., CHIANG, P.-W. & LOU, L. 1996. Isolation of Human and Murine Homologues of theDrosophilaMinibrain Gene: Human Homologue Maps to 21q22. 2 in the Down Syndrome "Critical Region". *Genomics,* 38**,** 331-339.

SOPPA, U., SCHUMACHER, J., FLORENCIO ORTIZ, V., PASQUALON, T., TEJEDOR, F. & BECKER, W. 2014. The Down syndrome-related protein kinase DYRK1A phosphorylates p27Kip1 and Cyclin D1 and induces cell cycle exit and neuronal differentiation. *Cell Cycle,* 13**,** 2084-2100.

STAGNI, F., GIACOMINI, A., EMILI, M., TRAZZI, S., GUIDI, S., SASSI, M., CIANI, E., RIMONDINI, R. & BARTESAGHI, R. 2016. Short-and long-term effects of neonatal pharmacotherapy with epigallocatechin-3-gallate on hippocampal development in the Ts65dn mouse model of Down syndrome. *Neuroscience,* 333**,** 277-301.

STAGNI, F., GIACOMINI, A., GUIDI, S., CIANI, E. & BARTESAGHI, R. 2015. Timing of therapies for Down syndrome: the sooner, the better. *Frontiers in behavioral neuroscience,* 9**,** 265.

STAGNI, F., GIACOMINI, A., GUIDI, S., CIANI, E. & BARTESAGHI, R. 2015. Timing of therapies for Down syndrome: the sooner, the better. *Frontiers in behavioral neuroscience,* 9.

STAGNI, F., MAGISTRETTI, J., GUIDI, S., CIANI, E., MANGANO, C., CALZÀ, L. & BARTESAGHI, R. 2013. Pharmacotherapy with fluoxetine restores functional connectivity from the dentate gyrus to field CA3 in the Ts65Dn mouse model of down syndrome. *PloS one,* 8**,** e61689.

STEWART, L. S., PERSINGER, M. A., CORTEZ, M. A. & SNEAD, O. C. 2007. Chronobiometry of behavioral activity in the Ts65Dn model of Down syndrome. *Behavior genetics,* 37**,** 388-398.

STRINGER, M., ABEYSEKERA, I., DRIA, K. J., ROPER, R. J. & GOODLETT, C. R. 2015. Low dose EGCG treatment beginning in adolescence does not improve cognitive impairment in a Down syndrome mouse model. *Pharmacology Biochemistry and Behavior,* 138**,** 70-79.

STRINGER, M., ABEYSEKERA, I., THOMAS, J., LACOMBE, J., STANCOMBE, K., STEWART, R. J., DRIA, K. J., WALLACE, J. M., GOODLETT, C. R. & ROPER, R. J. 2017. Epigallocatechin-3-gallate (EGCG) consumption in the Ts65Dn model of Down syndrome fails to improve behavioral deficits and is detrimental to skeletal phenotypes. *Physiology & Behavior,* 177**,** 230-241.

STRINGER, M., GOODLETT, C. R. & ROPER, R. J. 2017. Targeting trisomic treatments: optimizing Dyrk1a inhibition to improve Down syndrome deficits. *Molecular genetics & genomic medicine,* 5**,** 451-465.

SYLVESTER, P. 1983. The hippocampus in Down's syndrome. *Journal of Intellectual Disability Research,* 27**,** 227-236.

TAHTOUH, T., ELKINS, J. M., FILIPPAKOPOULOS, P., SOUNDARARAJAN, M., BURGY, G., DURIEU, E., COCHET, C., SCHMID, R. S., LO, D. C. & DELHOMMEL, F. 2012. Selectivity, cocrystal structures, and neuroprotective properties of leucettines, a family of protein kinase inhibitors derived from the marine sponge alkaloid leucettamine B. *Journal of medicinal chemistry,* 55**,** 9312-9330.

TANAPAT, P., GALEA, L. A. & GOULD, E. 1998. Stress inhibits the proliferation of granule cell precursors in the developing dentate gyrus. *International Journal of Developmental Neuroscience,* 16**,** 235-239.

TEIPEL, S. J., SCHAPIRO, M. B., ALEXANDER, G. E., KRASUSKI, J. S., HORWITZ, B., HOEHNE, C., MÖLLER, H.-J., RAPOPORT, S. I. & HAMPEL, H. 2003. Relation of corpus callosum and hippocampal size to age in nondemented adults with Down's syndrome. *The American journal of psychiatry,* 160**,** 1870-8.

TEIPEL, S. J., SCHAPIRO, M. B., ALEXANDER, G. E., KRASUSKI, J. S., HORWITZ, B., HOEHNE, C., MÖLLER, H.-J., RAPOPORT, S. I. & HAMPEL, H. 2003. Relation of corpus callosum and hippocampal size to age in nondemented adults with Down’s syndrome. *American Journal of Psychiatry,* 160**,** 1870-1878.

TEJEDOR, F., ZHU, X., KALTENBACH, E., ACKERMANN, A., BAUMANN, A., CANAL, I., HEISENBERG, M., FISCHBACH, K. & PONGS, O. 1995. minibrain: a new protein kinase family involved in postembryonic neurogenesis in Drosophila. *Neuron,* 14**,** 287-301.

TEJEDOR, F. J. & HÄMMERLE, B. 2011. MNB/DYRK1A as a multiple regulator of neuronal development. *FEBS journal,* 278**,** 223-235.

THOMPSON, B. J., BHANSALI, R., DIEBOLD, L., COOK, D. E., STOLZENBURG, L., CASAGRANDE, A.-S., BESSON, T., LEBLOND, B., DÉSIRÉ, L. & MALINGE, S. 2015. DYRK1A controls the transition from proliferation to quiescence during lymphoid development by destabilizing Cyclin D3. *Journal of Experimental Medicine,* 212**,** 953-970.

TONKISS, J., HARRISON, R. & GALLER, J. 1996. Differential effects of prenatal protein malnutrition and prenatal cocaine on a test of homing behavior in rat pups. *Physiology & behavior,* 60**,** 1013-1018.

TREMBLEY, J. H., CHEN, Z., UNGER, G., SLATON, J., KREN, B. T., VAN WAES, C. & AHMED, K. 2010. Emergence of protein kinase CK2 as a key target in cancer therapy. *Biofactors,* 36**,** 187-195.

TUBMAN, T. R., SHIELDS, M. D., CRAIG, B. G., MULHOLLAND, H. C. & NEVIN, N. C. 1991. Congenital heart disease in Down's syndrome: two year prospective early screening study. *BMJ (Clinical research ed.),* 302**,** 1425-7.

VICARI, S., BELLUCCI, S. & CARLESIMO, G. A. 2005. Visual and spatial long-term memory: differential pattern of impairments in Williams and Down syndromes. *Developmental Medicine & Child Neurology,* 47**,** 305-311.

VICARI, S., CARLESIMO, A. & CALTAGIRONE, C. 1995. Short-term memory in persons with intellectual disabilities and Down's syndrome. *J Intellect Disabil Res,* 39 (Pt 6)**,** 532-7.

WISEMAN, F. K., ALFORD, K. A., TYBULEWICZ, V. L. & FISHER, E. M. 2009. Down syndrome—recent progress and future prospects. *Human molecular genetics,* 18**,** R75-R83.

WISNIEWSKI, K. E. S.-S., B. 1989. Postnatal delay of myelin formation in brains from Down syndrome infants and children. *Clinical neuropathology,* 8**,** 55-62.

WOKKE, E. 2017. *Refinement: Evaluating stress and accuracy of different intraperitoneal techniques in mice.*

WOODS, Y. L., GRAHAM, R., MORRICE, N., BARTHEL, A., BECKER, W., SHAODONG, G., UNTERMAN, T. G. & COHEN, P. 2001. The kinase DYRK1A phosphorylates the transcription factor FKHR at Ser329 in vitro, a novel in vivo phosphorylation site. *Biochemical Journal,* 355**,** 597-607.

WORTHLEY, E. G. & SCHOTT, C. D. 1969. The toxicity of four concentrations of DMSO. *Toxicology and applied pharmacology,* 15**,** 275-281.

YABUT, O., DOMOGAUER, J. & D'ARCANGELO, G. 2010. Dyrk1A overexpression inhibits proliferation and induces premature neuronal differentiation of neural progenitor cells. *The Journal of neuroscience,* 30**,** 4004-4014.

YANG, E. J., AHN, Y. S. & CHUNG, K. C. 2001. Protein kinase Dyrk1 activates cAMP response element-binding protein during neuronal differentiation in hippocampal progenitor cells. *Journal of Biological Chemistry,* 276**,** 39819-39824.

YIN, X., JIN, N., SHI, J., ZHANG, Y., WU, Y., GONG, C.-X., IQBAL, K. & LIU, F. 2017. Dyrk1A overexpression leads to increase of 3R-tau expression and cognitive deficits in Ts65Dn Down syndrome mice. *Scientific reports,* 7**,** 619.

YOHN, N. L. & BLENDY, J. A. 2017. Adolescent chronic unpredictable stress exposure is a sensitive window for long-term changes in adult behavior in mice. *Neuropsychopharmacology,* 42**,** 1670.

YOON, P. W., FREEMAN, S. B., SHERMAN, S. L., TAFT, L. F., GU, Y., PETTAY, D., FLANDERS, W. D., KHOURY, M. J. & HASSOLD, T. J. 1996. Advanced maternal age and the risk of Down syndrome characterized by the meiotic stage of chromosomal error: a population-based study. *American journal of human genetics,* 58**,** 628.

YU, T., LI, Z., JIA, Z., CLAPCOTE, S. J., LIU, C., LI, S., ASRAR, S., PAO, A., CHEN, R. & FAN, N. 2010. A mouse model of Down syndrome trisomic for all human chromosome 21 syntenic regions. *Human molecular genetics,* 19**,** 2780-2791.

ZIGMAN, W. B. 2013. Atypical aging in Down syndrome. *Developmental disabilities research reviews,* 18**,** 51-67.

ZIGMAN, W. B. & LOTT, I. T. 2007. Alzheimer's disease in Down syndrome: neurobiology and risk. *Developmental Disabilities Research Reviews,* 13**,** 237-246.

ZIGMAN, W. B. & LOTT, I. T. 2007. Alzheimer's disease in Down syndrome: neurobiology and risk. *Mental retardation and developmental disabilities research reviews,* 13**,** 237-246.

APPENDIX

For all graphs, panel “a” contains data that includes male mice from both (Ts65Dn x B6C3F1) and (Ts65Dn x B6C3.Dyrk1a$^{fl/fl}$) matings. Panel “b” contains male offspring from (Ts65Dn x B6C3F1) matings. The current study focused on reporting analysis from male euploid and trisomic Dyrk1a$^{fl/+}$ mice in the results section. There was not sufficient statistical power to draw meaningful statistical conclusions about mice from a Ts65Dn background, however, this data is presented here to highlight potential differences in these mice versus male trisomic and euploid Dyrk1a$^{fl/+}$ mice.

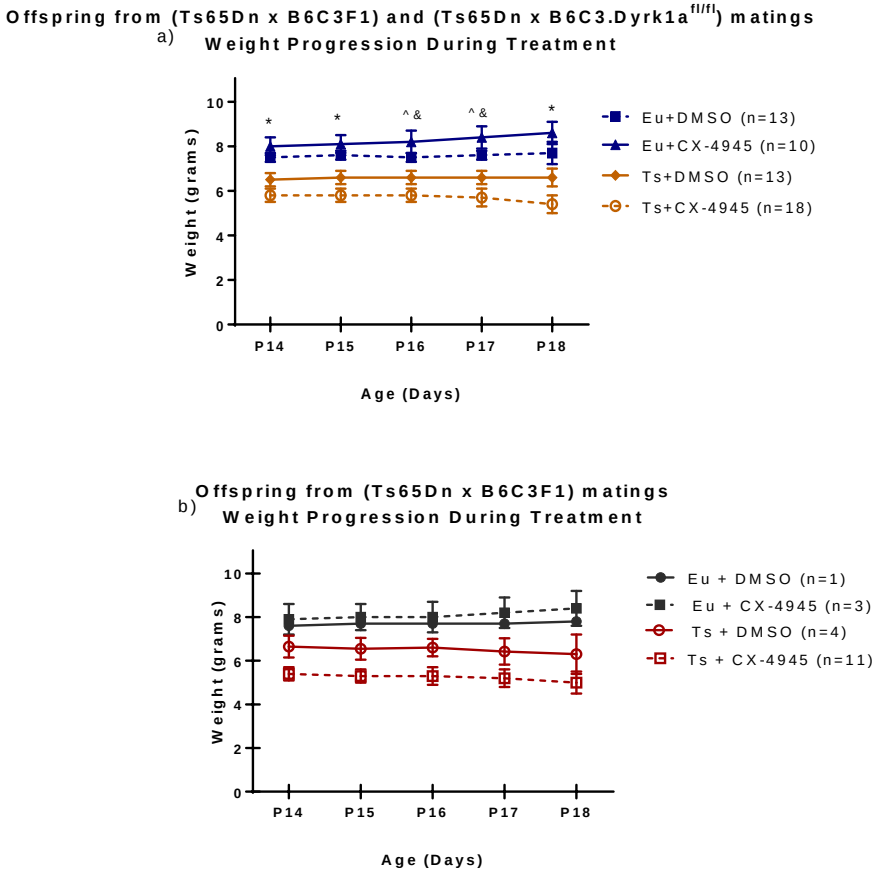

Figure 15. The trajectory of bodyweights across P15-P18 in offspring from (Ts65Dn x B6C3F1) matings and collapsed across mating schemes.

In Figure 15a, male Ts65Dn mice had significantly lower body weights and a slower growth rate over the five days of treatment compared to male euploid mice [main effect of genotype, $F(1,50)=23.96$, $p<0.001$; day x genotype interaction, $F(4,200)=4.35$, $p=0.002$]. In addition, trisomic mice receiving CX-4945 had significantly lower body weights across all five treatment days [genotype x treatment interaction, ($F(1,50)=4.87$, $p=0.0032$)]. Both euploid groups weighed significantly more than both trisomic groups on P14, P15 and P18 ($p<0.05$, as indicated by *). Mice in the Eu+CX-4945 group continued to weigh significantly more than both trisomic groups at P16 and P17 ($p<0.05$, as indicated by ^), mice in the Eu+DMSO group were only significantly heavier than the Ts+CX-4945 groups on P16 and P17 ($p<0.05$, as indicated by &). Figure 15b depicts the trajectory of male mice with a Ts65Dn background. Data are represented as mean ± SEM.

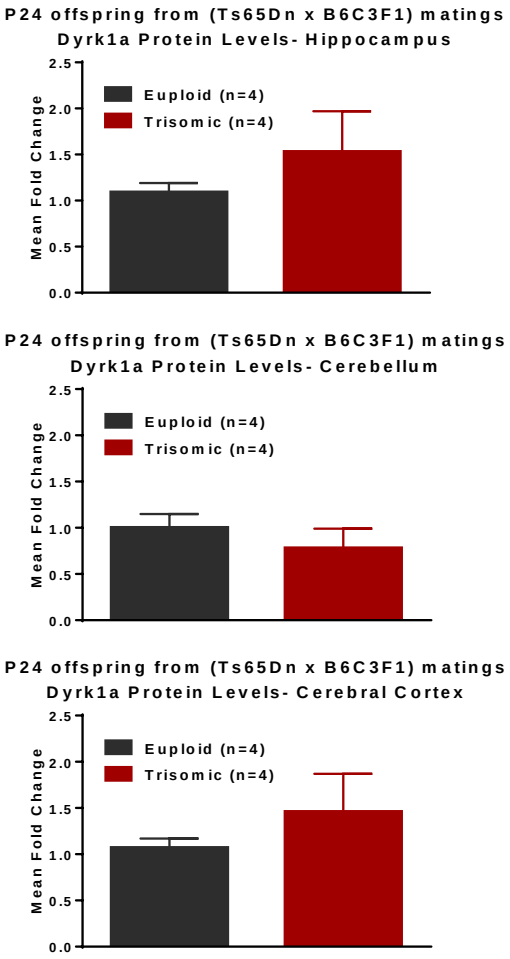

Figure 16. Dyrk1a protein levels of male P24 euploid and Ts65Dn mice from (Ts65Dn x B6C3F1) matings

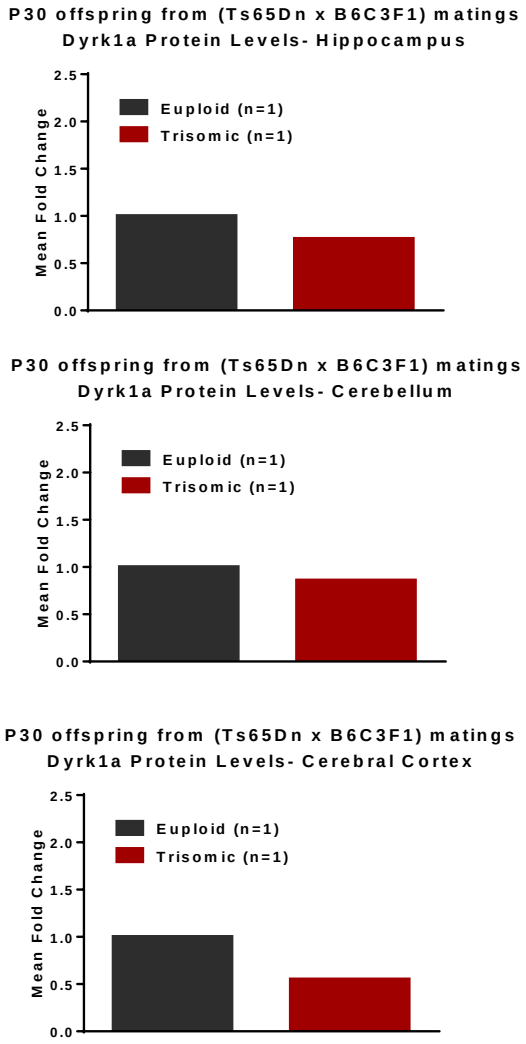

Figure 17. Dyrk1a protein levels of male P30 euploid and Ts65Dn from (Ts65Dn x B6C3F1) matings

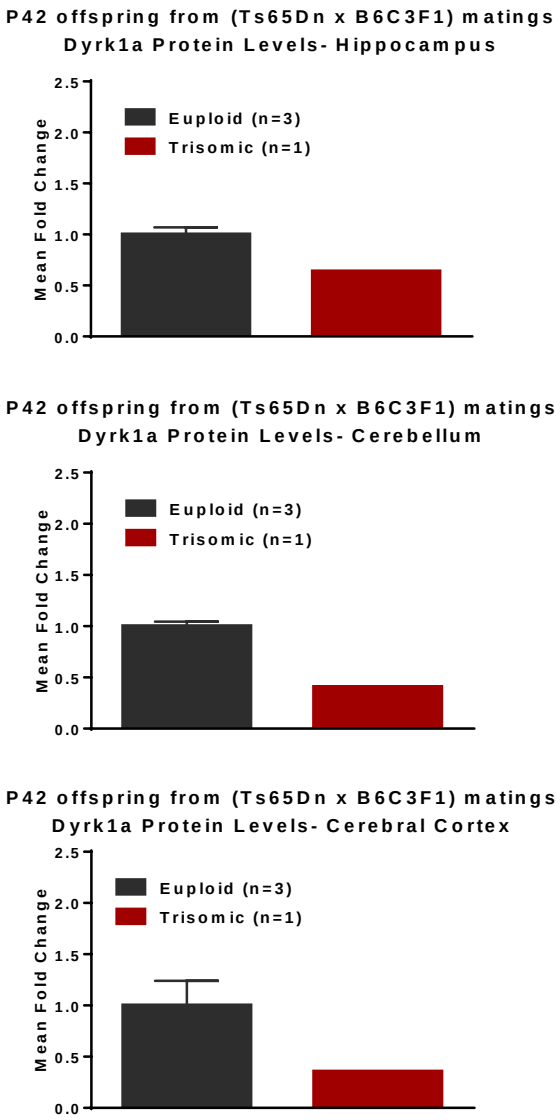

Figure 18. Dyrk1a protein levels of male P42 euploid and Ts65Dn offspring from (Ts65Dn x B6C3F1) matings

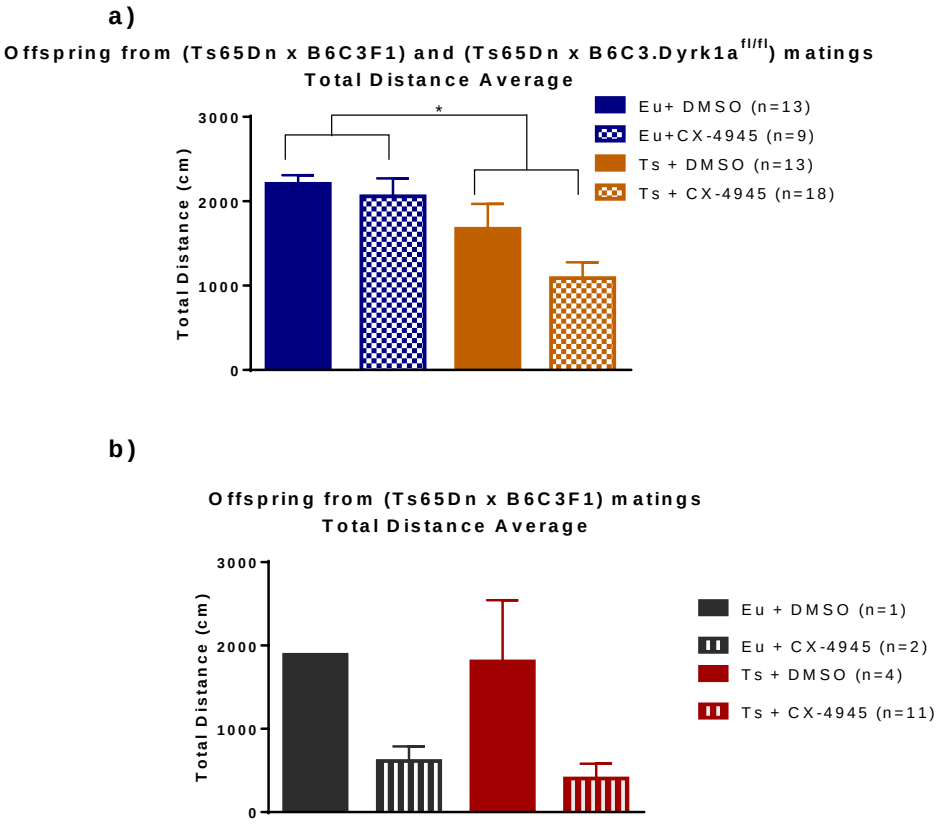

Figure 19. Locomotor task-total distance travelled in offspring from (Ts65Dn x B6C3F1) matings and collapsed across both breeding schemes

The average total distance travelled in the four treatment groups. In Figure 19a, male euploid mice travelled significantly farther in the 10 minute task than the euploid groups, as indicated by the * [main effect of genotype, $F(1,49)=4.77$, $p=0.034$]. Figure 19b depicts the locomotor activity of male offspring from (Ts65Dn x B6C3F1) matings. Data are represented as mean ± SEM.

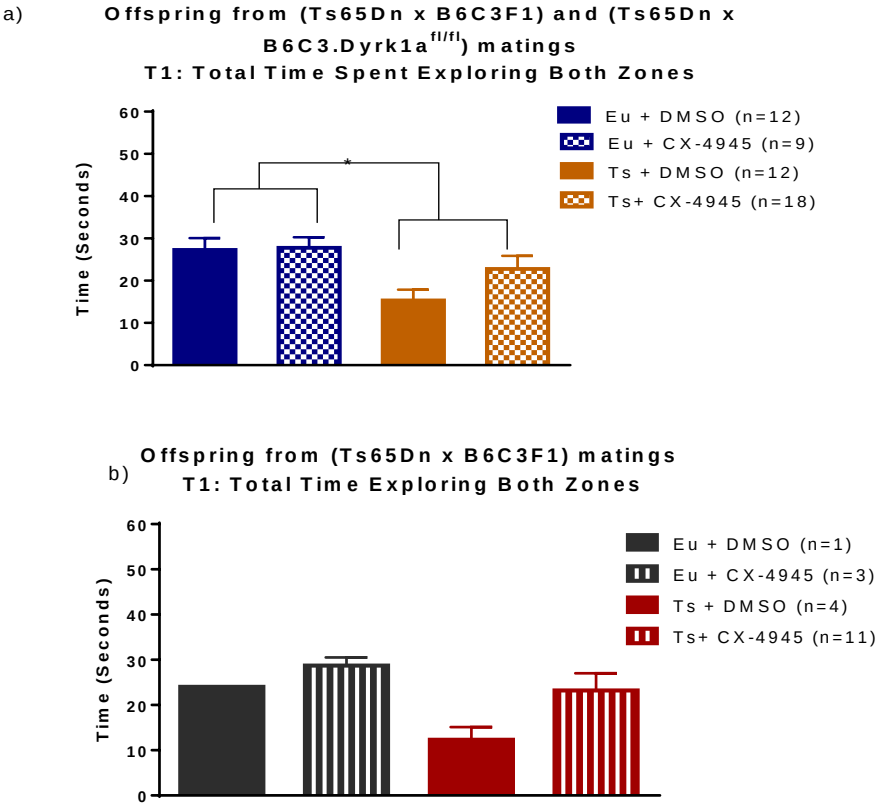

Figure 20. The total time spent exploring both zones in offspring from (Ts65Dn x B6C3F1) matings and collapsed across backgrounds

In Figure 20a, male euploid mice spent more time exploring both the home cage and new cage bedding zone versus trisomic mice, as indicated by the (*). There were no significant differences between the groups on their preference to explore the home cage zone on trial 1 or trial 2. Figure 20b depicts male mice from a Ts65Dn background. Data are represented as mean ± SEM.

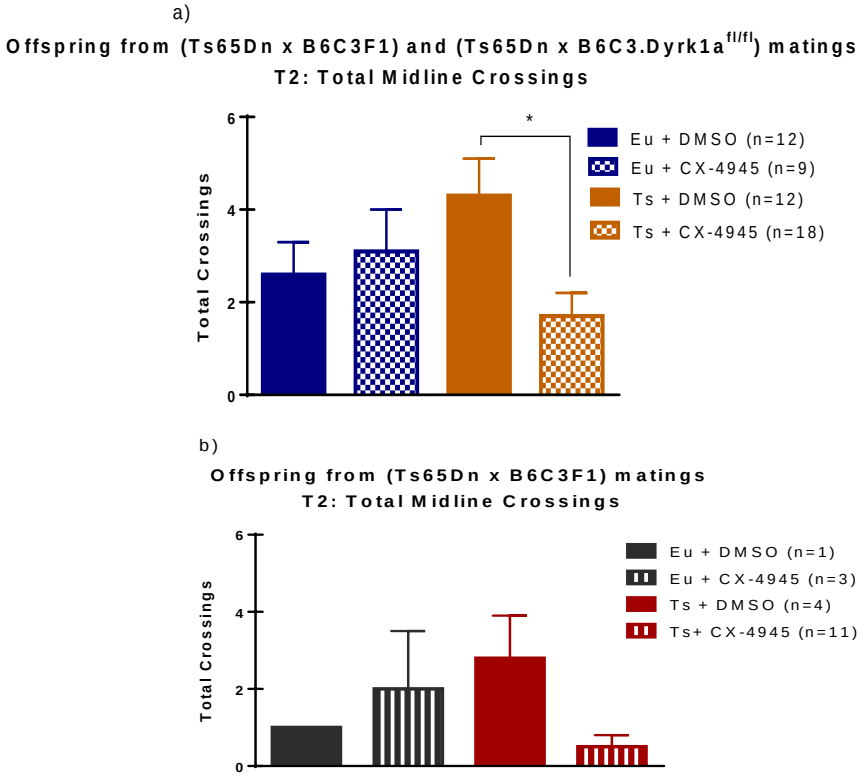

Figure 21. The number of midline crossings in offspring from (Ts65Dn x B6C3F1) matings and collapsed across both breeding schemes

There were no significant differences between groups in the number of midline crossings in trial 1. However, trisomic mice given DMSO had significantly more midline crossings in trial 2 than mice treated with CX-4945 [genotype x treatment interaction ($1,50=70.91$, $p=0.029$)], as indicated by the (*) in 21a. Figure 21b depicts the number of total midline crossings in trial 2 in male offspring from (Ts65Dn x B6C3F1) matings. Data are represented as mean ± SEM.

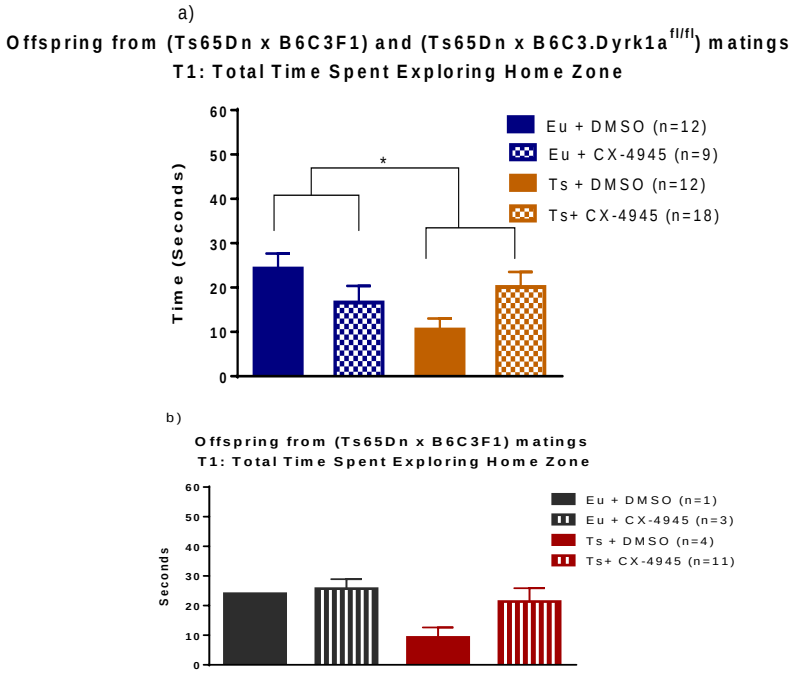

Figure 22. Trial 1: total time spent exploring home zone in offspring from (Ts65Dn x B6C3F1) matings and collapsed across both breeding schemes

In Figure 22a, on trial 1 euploid mice (collapsed across both breeding schemes) spent more time exploring the home zone versus trisomic mice, as indicated by the (*) [main effect of genotype, $F(1,47)=5.4$, $p=0.024$]. However, there were no significant main effects observed on the total time spent exploring the home zone in trial 2. Figure 22b depicts the total time spent exploring the home zone in trial 1 in offspring from (Ts65Dn x B6C3F1) matings. Data are represented as mean ± SEM.

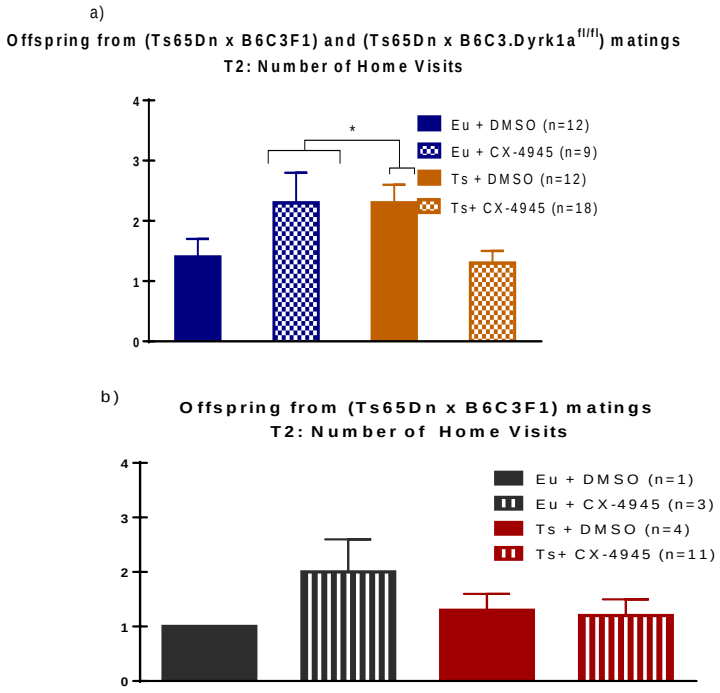

Figure 23. Trial 2: number of home visits in offspring from (Ts65Dn x B6C3F1) matings and collapsed across breeding schemes

There were no significant effects on the number of home zone or new zone visits on trial 1 in male mice collapsed across both breeding schemes. Figure 23a depicts the number of home zone visits in trial 2, where both Eu+CX-4945 and Ts+DMSO treatment groups had significantly more visits to the home zone than the Ts+CX-4945 group [genotype x treatment interaction, $F(1,47)=8.29$, $p=0.006$]. Post hoc comparisons <0.05, as indicated by the (*). Figure 23b depicts the number of home zone visits on trial 2 in male offspring from (Ts65Dn x B6C3F1). Data are represented as mean ± SEM.

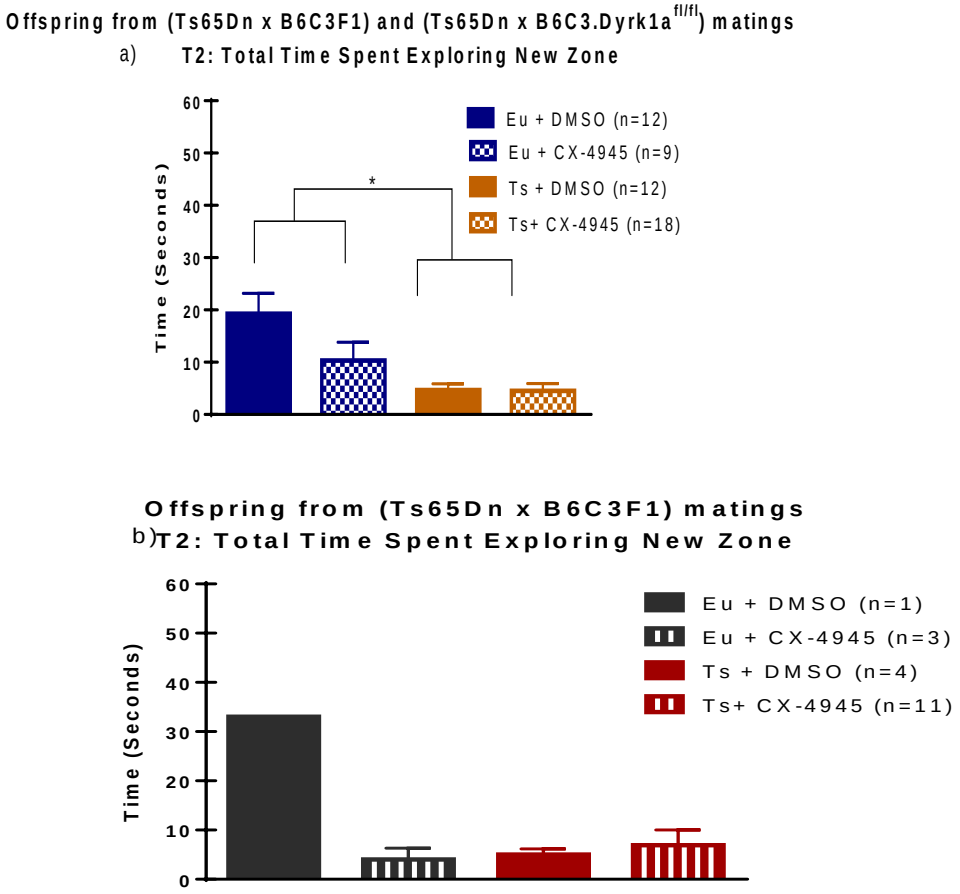

Figure 24. T2: Total time spent exploring new zone in offspring from (Ts65Dn x B6C3F1) matings and collapsed across breeding schemes

There were no significant differences on the total time spent exploring the new zone in trial 1. However, as seen in Figure 24a, male euploid mice collapsed across both breeding schemes spent significantly more time exploring the new zone in trial 2 than trisomic mice, as indicated by the (*) [main effect of genotype, ($F(1,47)=9.89$, $p=0.003$)]. Figure 24b depicts the total time spent exploring the new zone in trial 2 from male offspring from (Ts65Dn x B6C3F1) matings. Data is represented as mean ± SEM.

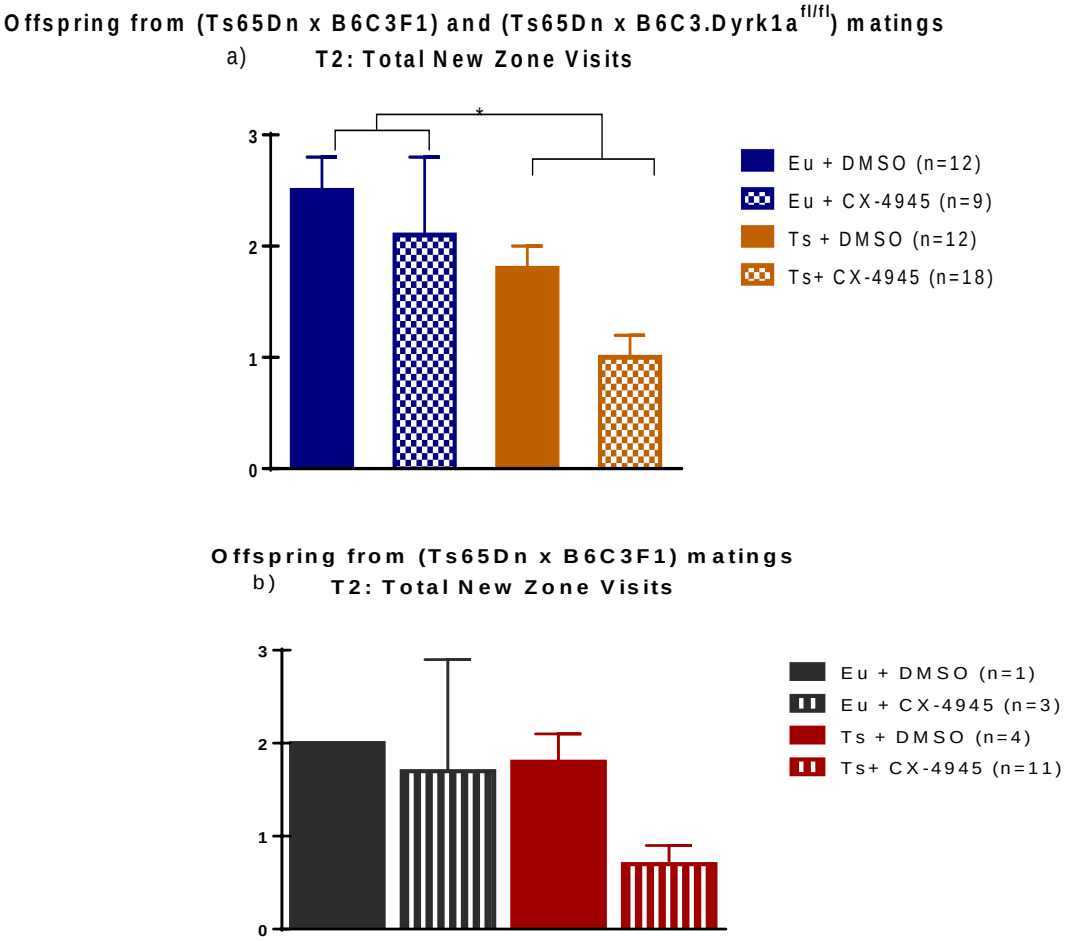

Figure 25. Trial 2: Total new zone visits in offspring from (Ts65Dn x B6C3F1) matings and collapsed across breeding schemes

Figure 25a depicts the number of new zone visits in trial 2 (male mice collapsed across breeding schemes). Euploid mice visited the new zone significantly more than trisomic mice, as indicated by the (*), [main effect of genotype, $F(1,47)=7.38$, $p=0.009$]. Figure 25b depicts the number of new zone visits in trial 2 in male offspring from (Ts65Dn x B6C3F1) matings. Data are represented as mean ± SEM.

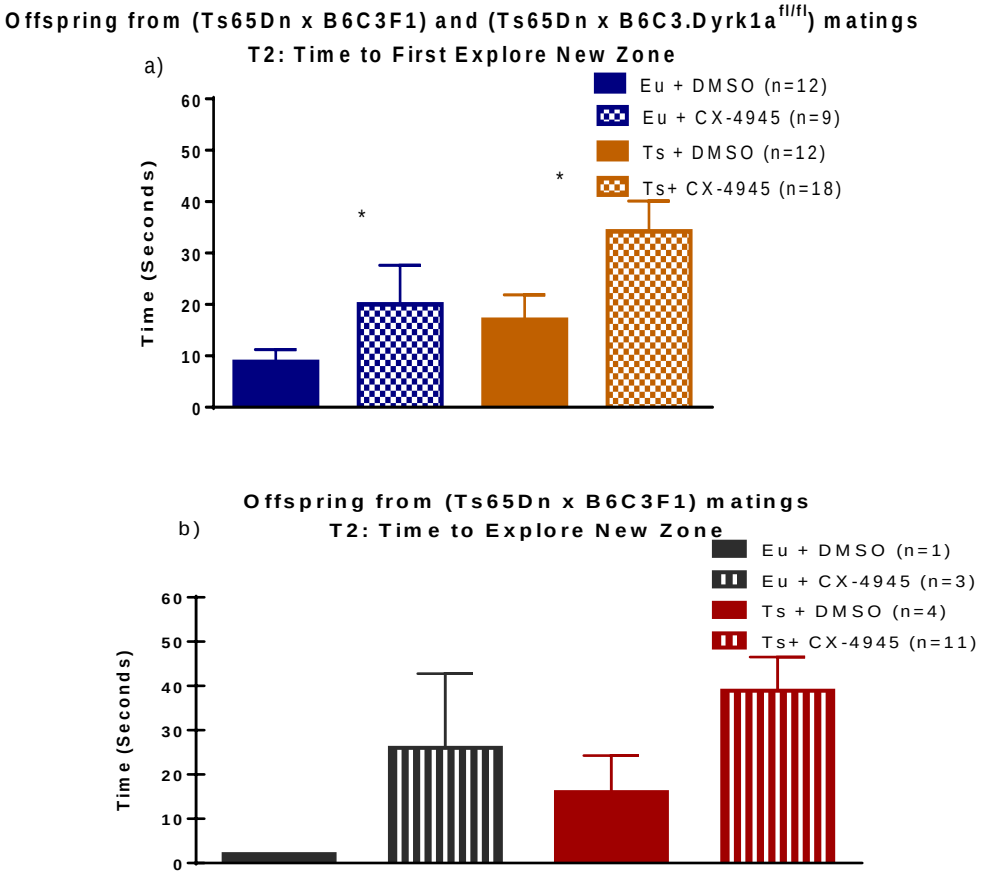

Figure 26. Time to first explore new zone in offspring from (Ts65Dn x B6C3F1) matings and collapsed across breeding schemes

There were no significant effects between groups on the time to first enter the home zone or new zone on trial 1, nor were there any differences in the time taken to first enter the home zone on trial 2. However, as seen in Figure 26a, male mice (collapsed across breeding schemes) treated with CX-4945 took significantly longer to enter the new zone on trial 2 versus mice treated with DMSO, as indicated by the (*), [main effect of treatment, $F(1,47)=6.12$, $p=0.017$)]. Figure 26b depicts the time to first explore the new zone in trial 2 by male offspring from (Ts65Dn x B6C3F1) matings. Data are represented as mean ± SEM.

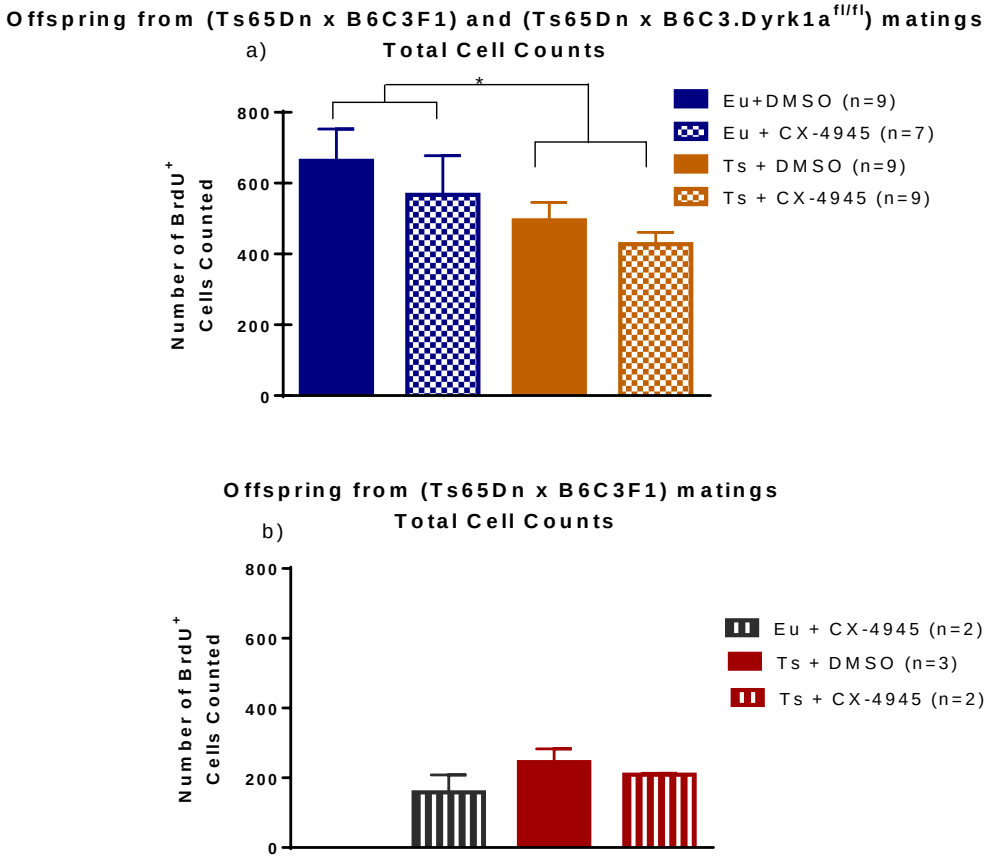

Figure 27. Total cell counts in offspring from (Ts65Dn x B6C3F1) matings and collapsed across breeding schemes

In Figure 27a, collapsed across both breeding schemes, male euploid mice had significantly higher number of BrdU-labeled cells counted throughout the dentate gyrus versus trisomic controls (Figure 24a) [main effect of genotype, $F(1,30)=4.2$, $p=0.049$]. Euploid mice also had a significantly greater dentate gyrus volume than trisomics [main effect of genotype, $F(1,30)=22.37$, $p<0.001$]. Mice treated with CX-4945 also had significantly greater dentate gyrus volume than those treated with DMSO [main effect of treatment, $F(1,30)=5.50$, $p=0.026$)]. There were no significant main or interactive effects on the total number of slices counted. Euploid mice treated with CX-4945 had significantly thicker slices [genotype x treatment interaction, $F(1,33)=8.9$, $p=0.006$]. LSD post hoc analysis showed that mice in the Eu+CX-4945 group had significantly thicker slices than the Eu+DMSO group ($p=0.025$). There was a trend for mice treated with CX-4945 displaying lower cell density than mice treated with DMSO ($p=0.07$). Figure 27b depicts the total cell counts in male offspring from (Ts65Dn x B6C3F1) matings. Data are represented as mean ± SEM.